

**POLITECNICO DI MILANO**  
Scuola di Ingegneria Industriale e dell'Informazione  
Master of Science in Energy Engineering



**POLITECNICO**  
MILANO 1863



**NTNU – Trondheim**  
Norwegian University of  
Science and Technology

**Master Thesis**

**BOIL OFF GAS HANDLING ON LNG  
FUELLED VESSELS WITH HIGH PRESSURE  
GAS INJECTED ENGINES**

**Supervisors:**

**Prof. Paolo CHIESA**

**Prof. Petter NEKSÅ**

**Candidate:**

**Arrigo Battistelli**

**Student ID number 801593**

**Academic year 2014/2015**

# Contents

<b>1</b>	<b>Introduction</b>	<b>3</b>
<b>2</b>	<b>Background</b>	<b>5</b>
2.1	LNG as ship fuel . . . . .	5
2.1.1	Motivations for LNG as a ship fuel . . . . .	5
2.1.2	Ship propulsion alternatives . . . . .	7
2.1.3	LNG fuelled ships . . . . .	9
2.2	Tank types . . . . .	11
2.3	BOG handling . . . . .	13
2.3.1	BOG reliquefaction on LNG Carriers . . . . .	14
2.4	Systems for 2-Stroke Low Speed Engine Propulsion . . . . .	20
2.4.1	ME-GI engines . . . . .	21
2.4.2	High Pressure BOG compression . . . . .	22
2.4.3	High Pressure LNG Fuel Gas Supply Systems . . . . .	23
<b>3</b>	<b>Heat pump process</b>	<b>29</b>
3.1	Heat pump process layout (HeP) . . . . .	31
3.1.1	Heat pump with dedicated Tank Reflux pump layout . . . . .	33
3.1.2	Heat pump with BOG fed Auxiliary engine layout (HeP-AUX)	34
3.2	Alternatives to the Heat Pump process . . . . .	36
3.3	Selection of a reference case . . . . .	38
3.3.1	Main engine . . . . .	39
3.3.2	Auxiliary engines . . . . .	40

3.3.3	Heat leak calculations . . . . .	41
3.4	Refrigerant . . . . .	43
4	Computer simulations . . . . .	45
4.1	Heat Pump Model flowsheet . . . . .	46
4.1.1	LNG fuel tank model . . . . .	48
4.2	Heat pump model structure . . . . .	50
4.3	Inputs to the Heat Pump Model . . . . .	53
4.4	Inputs to other models . . . . .	56
4.5	Heat Pump Model Simulation Results (HeP) . . . . .	56
4.5.1	Normal operation scenario: HeP - 100% NCR . . . . .	58
4.5.2	Sensitivity Analysis on the normal operation scenario: HeP - 100% NCR . . . . .	63
4.5.3	Part load scenario: HeP - 50% NCR . . . . .	68
4.5.4	Part load scenario: HeP - 20% NCR . . . . .	71
4.5.5	Idle/Harbour scenario: HeP - 0% NCR - 100% AUX . . . . .	74
4.6	Heat Pump with BOG feed to Auxiliary engines simulation results (HeP-AUX) . . . . .	77
4.6.1	HeP-AUX: 100% NCR . . . . .	78
4.7	Evaluation of alternative process layouts . . . . .	80
4.7.1	Intercooled heat pump cycle . . . . .	80
4.7.2	BOG recirculation in the Tank Reflux system . . . . .	82
4.8	Discussion of simulation results . . . . .	83
5	Equipment selection . . . . .	91
5.1	LNG pumps . . . . .	91
5.1.1	LNG High Pressure pump . . . . .	91
5.1.2	LNG Low Pressure pump . . . . .	92
5.2	Refrigerant compressor . . . . .	93
5.2.1	Requirements . . . . .	93

5.2.2 Compressor alternatives . . . . .	95
5.3 BOG compressor . . . . .	102
5.4 Heat exchangers . . . . .	103
6 Conclusion	107
Appendix A ME-GI engines	110
Appendices	110
Appendix B Ships Operational Profiles	113
B.1 Main engine . . . . .	113
B.2 Auxiliary engines . . . . .	114
Appendix C Simulation results	116
C.1 Tank energy balance and cooling duty calculations . . . . .	116
C.2 Case studies . . . . .	117
C.2.1 Case HeP - 100 % NCR . . . . .	117
C.3 Sensitivity Analyses . . . . .	120
C.3.1 Case HeP - 100 % NCR . . . . .	120
Appendix D Acronyms	123
Bibliography	125

# List of Figures

2.1	Implementation schedule for Revised MARPOL Annex VI [1, p.2] .	6
2.2	Emission Control Areas under IMO Annex VI [2] . . . . .	6
2.3	Typical thermal efficiency of prime movers [3, p.244] . . . . .	7
2.4	Ship propulsion alternatives for Natural Gas fuelled ships and Carriers sorted by type of fuel [4, 3, 5, 6, 1, 7, 8, 9, 10, 11] . . . . .	8
2.5	Platform supply vessel, Dual fuel Diesel-Electric propulsion [4] . .	9
2.6	Ro-Ro ship, Pure LNG operation, Diesel-Mechanical propulsion, with Diesel backup engine [4] . . . . .	9
2.7	Comparison between LNGC and other LNG fuelled vessels, the blue lines indicate constant ratio between the LNG tank volume and the main engine power, [12, p.9], [13, 14, 15] . . . . .	11
2.8	Propulsion systems for LNG Carriers [5, p.5], the highlighted alternative refers to low speed 2 stroke gas injected diesel engines integrated with a high pressure BOG compressor and a reliquefaction cycle . . . . .	14
2.9	Hamworthy 1st generation BOG Reliquefaction System (Mark I) [16, p.5] . . . . .	16
2.10	Hamworthy 3rd generation BOG Reliquefaction System (Mark III) [16, p.6] . . . . .	17
2.11	Cryostar EcoRel reliquefaction process for LNG Carriers [17, p.5] .	18
2.12	SINTEF Mini LNG Process, PFD [18, p.34] . . . . .	19
2.13	Sketch of a ME-GI engine [19, p.5] . . . . .	21
2.14	Example of ME-GI Gas supply specifications, delivery pressure at varying engine load, for a 250 bar engine feed [20, p.15] . . . . .	21
2.15	Cross section of the Burckhardt Laby-GI fuel gas compressor for ME-GI engine applications [19, p.21] . . . . .	23
2.16	FGSS with Cryostar's HP pump solution and BOG handling alternatives [19, p.31] . . . . .	24

2.17 PFD of HP Fuel Gas Supply System, for a design flowrate of 0.39kg/s [21, p.20] . . . . .	25
2.18 PFD of HP Fuel Gas Supply System for atmospheric tank, equipped with BOG compressor and recondenser, proposed by Samsung Heavy Industries [22, p.10], [13, p.18] . . . . .	26
2.19 Integration of HP FGSS and Hamworthy Mark III reliquefaction cycle, published by MAN in [19, p.19] . . . . .	27
2.20 Integration of HP FGSS and BOG Reliquefaction System LNGRS (or Hamworthy Mark III), published by Wartsila in [23, p.18] . . . . .	28
3.1 Jorn M. Jonas patented heat pump process [24] . . . . .	30
3.2 PFD of the heat pump process (HeP) . . . . .	32
3.3 PFD: Heat pump process, with TR dedicated Pump . . . . .	34
3.4 PFD: Heat pump process with BOG fuelled AUX engines (HeP-AUX) . . . . .	35
3.5 HPK process layout with High Pressure BOG Compressor . . . . .	37
3.6 MIX-AUX process, or "terminal type" . . . . .	37
3.7 BOR as a function of insulation thickness, tank type and size [25], integrated with data from literature [26, 27] . . . . .	42
3.8 Vapor pressure of pure fluids relevant for LNG processes [28] . . . . .	44
4.1 HYSYS® model complete flowsheet . . . . .	47
4.2 Hysys tank model PFD . . . . .	48
4.3 Fuel phase envelopes from HYSYS in the pressure-temperature diagram, LNG (red) and BOG (blue) . . . . .	50
4.4 Hysys model computational sequence . . . . .	51
4.5 HeP-100%NCR: Performance map . . . . .	59
4.6 HeP-100%NCR: Optimum compressor outlet pressure . . . . .	60
4.7 HeP-100%NCR: Refrigerant Temperature-Duty diagram . . . . .	62
4.8 (HeP-100%NCR: Refrigerant cycle in the pressure - enthalpy diagram . . . . .	63
4.9 HeP-100%NCR: Temperature difference profile for process HX . . . . .	63
4.10 HeP-100%NCR: Variation of COP with different parameters . . . . .	64
4.11 HeP-100%NCR: Sensitivity Analysis: Evaporation pressure with constant refrigerant mass flow and high pressure . . . . .	66
4.12 HeP-100%NCR: Sensitivity Analysis: Evaporation pressure, with constant refrigerant high pressure and effective refrigeration duty . . . . .	67
4.13 HeP-50%NCR: Operation map . . . . .	68
4.14 Optimum high pressure for different Main engine load scenarios . . . . .	69

4.15 HeP-50%NCR: Refrigerant Temperature-Duty diagram . . . . .	70
4.16 (HeP-50%NCR: Refrigerant cycle in the pressure - enthalpy diagram	71
4.17 HeP-50%NCR: Temperature difference profile for process HX . . . .	71
4.18 HeP-20%NCR: Operation map . . . . .	72
4.19 HeP-20%NCR: Refrigerant Temperature-Duty diagram . . . . .	73
4.20 (HeP-20%NCR: Refrigerant cycle in the pressure - enthalpy diagram	74
4.21 HeP-20%NCR: Temperature difference profile for process HX . . . .	74
4.22 HeP-0%NCR-100%AUX: Operation map . . . . .	75
4.23 HeP-0%NCR-100%AUX: Optimum refrigerant mass flow . . . . .	75
4.24 HeP-0%NCR-100%AUX: Refrigerant Temperature-Duty diagram . . .	76
4.25 (HeP-0%NCR-100%AUX: Refrigerant cycle in the pressure - enthalpy diagram . . . . .	77
4.26 HeP-0%NCR-100%AUX: Temperature difference profile for process HX . . . . .	77
4.27 Comparison of energy consumption for BOG compression for Aux- iliary engine and recondensation with the heat pump process HeP	78
4.28 HeP-AUX-100%NCR: Optimum heat pump cycle high pressure . . . .	78
4.29 HeP-AUX-100%NCR: Refrigerant Temperature-Duty diagram . . . .	79
4.30 (HePAUX100%NCR: Refrigerant cycle in the pressure - enthalpy di- agram . . . . .	80
4.31 HePAUX100%NCR: Temperature difference profile for process HX	80
4.32 Process layout with refrigerant compressor Intercooling by LP re- frigerant . . . . .	81
4.33 Comparison between isentropic compression paths with and with- out intercooling, in the Nitrogen pressure enthalpy chart gener- ated with RefProp . . . . .	82
4.34 Overall FGSS primary energy consumption, including flared gas in GCU, expressed as percentage of main engine thermal power at 100%NCR. (*Reliquefaction estimated from literature) . . . . .	83
4.35 Comparison of the heat pump performance and capacity with com- mercially available liquefaction processes for LNGC [10, 18, 29], COP and specific work are related to each other through the evap- oration enthalpy of the BOG, so are cooling duty and reliquefac- tion capacity . . . . .	85

4.36 Overall FGSS primary energy consumption of different processes, calculated by the Design model with different values of the Main engine fuel flowrate. . . . .	86
4.37 Boundary conditions for the process and limits for no-flaring operation, in a dimensionless plane . . . . .	88
5.1 Operation range and specifications for the Refrigerant Compressor, in the HeP and HeP-AUX processes . . . . .	94
5.2 Compressor coverage chart [30, p.13-3] integrated with examples of operation ranges for BOG centrifugal compressors in LNG terminals [31] and LNG carriers. The blue rectangle indicates the heat pump specifications. . . . .	96
5.3 Example of isothermal efficiency profile as a function of discharge pressure and number of stages, for a ordinary reciprocating compressor with cooled stages [32] . . . . .	98
5.4 Efficiency of a BOG Oil-free Labyrinth compressor package [33] . . . . .	99
5.5 Heat Exchangers U*A values, calculated by the Design Model to provide a specified MITA of 5°C, for the HeP and HeP-AUX processes.	105
A.1 LNG Carrier estimated BOG evaporation and consumption rate as a function of ship speed [34, p.5] . . . . .	110
A.2 Quantity of pilot fuel at varying load of the ME-GI engine at Minimum Fuel Mode [19] . . . . .	110
A.3 Nomenclature for MAN engines [35, p.18] . . . . .	111
A.4 ME-GI Engine datasheet for the design case selection [35, p.53] . . . . .	112
B.1 (Operation profile of a Panamax-max vessel . . . . .	113
B.2 Operation profile of a North Sea ferry, [36] . . . . .	113
B.3 Main engine operation profile of the vessel, from Table B.1 . . . . .	114
B.4 Anticipated electric power consumption table for a vessel of a similar size than the design case [7] . . . . .	115
C.1 Energy balance control volume . . . . .	116



# List of Tables

2.1	Main technologies for reliquefaction of BOG on LNG carriers [10]	15
2.2	SINTEF Mini LNG Process, main parameters [18, p.35]	19
2.3	SINTEF Mini LNG Process, performance [18, p.39]	20
3.1	Alternative processes	36
3.2	Main engine features	40
3.3	Auxiliary engines lumped features	41
3.4	Calculation of Heat leak for two different scenarios	42
4.1	LNG and BOG composition at 1.04 bara	50
4.2	Adjust settings for Case Studies	52
4.3	Adjust settings for Sensitivity Analysis	52
4.4	Typical LNG Composition form major export terminals, in Volume % [4, p.6]	53
4.5	LNG composition for the Heat Pump (HeP) model, properties calculated with HYSYS at the reference tank conditions -161.5°C, 1.04 bara.	54
4.6	Unit Operations inputs to the Heat Pump (HeP) model	54
4.7	Stream input properties for the Heat Pump (HeP) model	55
4.8	Inputs to simulations for alternative processes	56
4.9	Design cases for the heat pump process (HeP)	57
4.10	HeP-100%NCR: Process Equipment mass and energy balance	61
4.11	HeP-50%NCR: Process Equipment mass and energy balance	70
4.12	HeP-20%NCR: Process Equipment mass and energy balance	73
4.13	HeP-0%NCR-100%AUX: Process Equipment mass and energy balance	76
4.14	HeP-AUX-100%NCR: Process Equipment mass and energy balance	79
5.1	Comparison table of three types of compressors [37]	95

5.2	Specifications for LNG BOG Oil-free Labyrinth compressor package from Burckhardt, at 0.99 bar and -142°C suction, gas composition 11 mole% N <sub>2</sub> , 89 mole% CH <sub>4</sub> at 100% and 50% capacity [33]	99
5.3	Example of material selection guidelines for reciprocating compressor parts depending on suction temperature, from a compressor component manufacturer	101
6.1	Pros and cons of the three best options for BOG handling	108
B.1	Measurement of power consumption of a chemical tanker vessel during the analysed navigation conditions [38]	113
B.2	Operation profile of the vessel with respect to main and auxiliary engines load, calculated from table B.1	114
B.3	Auxiliary engine load in relation to the value at normal operation and as a fraction of the installed capacity, extracted from Table B.4	114

## Abstract

The aim of this thesis is to design and optimize a heat pump process to handle Boil-Off-Gas from Liquefied Natural Gas (LNG) cryogenic fuel tanks onboard LNG fuelled ships. The process is designed for LNG fuelled ship different from LNG carriers, equipped with LNG fuel tanks at atmospheric pressure and 2-strokes low-speed engines with high pressure direct gas injection. It consists in a Nitrogen transcritical cycle integrated with the fuel supply system, operating entirely below ambient temperature. The concept is based on a patent of the norwegian company LNG New Technologies.

Two different versions of the heat pump process are simulated with the commercial software HYSYS® . Based on the simulation results the process is compared to other alternative solutions from the literature.

The results prove that the proposed heat pump process can effectively refrigerate the LNG tank if the ship is operating in the normal mode or at reduced main engine load. However at very low engine loads and especially when the main engine is shut down, the system fails to produce the required refrigeration effect. A similar performance can be obtained with other examined processes, which on the other hand are less complex. The only solutions to handle Boil-Off-Gas when the main engine is off are the commercial reliquefaction processes for the LNG Carriers market. However these are less efficient and more complex than the other solutions.

Finally a preliminary selection of the heat pump process equipment is outlined, with focus on the refrigerant compressor. The results indicate that a reciprocating oil-free machine with cryogenic material specifications should be used. This is considered the most non-conventional and costly unit of the process.

## Keywords

LNG, BOG, cryogenic, transcritical heat pump, LNG fuelled, reliquefaction.

## Acknowledgments

This Master thesis was written in the spring of 2014 at the Energy and Process Engineering faculty of the Norwegian University of Science and Technology NTNU during the second year of a double degree program (TIME) with Politecnico di Milano, where the work was later revised in the winter of 2015.

I would like to thank first my academic supervisors Paolo Chiesa and Petter Nekså for their valuable assistance and experienced mentoring throughout the course of the thesis, and my research advisors Kjell Kolsaker and Dag Stenersen for their great availability and their constructive criticism at every meeting. Special thanks go to the process engineer Jørn Magnus Jonas of the company LNG New Technologies that inspired the concept of the thesis and closely followed its development contributing with his precious industrial knowledge, as well as his colleagues Andreas Norberg and Kjetil Sjølie Strand for their contribution and for hosting me in the company's office in a pleasant and friendly environment.

The NTNU and Sintef researchers Rahul Anantharaman, Lars Nord and Rajesh Kempegowda helped me and other students with process simulations by offering voluntary software training lectures. Filippo Spano' from the Chemical Engineering department of Politecnico brilliantly solved our license connection problems just when every hope was gone.

Finally I am grateful to my family and friends for their moral and material support, in particular to Alfredo, Alberto, Ivana and Riccardo for reading parts of my thesis and to Tina Bautovic for her lovely care.

# Riassunto Esteso

Attualmente il Gas Naturale Liquefatto (GNL) sta diventando un combustibile competitivo nell'ambito della propulsione navale a causa dell'introduzione di norme sempre piú stringenti sulle emissioni marittime. Di conseguenza ci si aspetta che la propulsione a GNL, ad oggi limitata perlopiú alle grandi metaniere e al settore della navigazione costiera di corto raggio, sia destinata a penetrare anche il segmento delle grandi navi non metaniere che navigano in mare aperto. In ragione delle crescenti dimensioni delle navi l'industria ha rilevato la necessitá di soluzioni tecnologiche piú efficienti per lo stoccaggio del GNL, la propulsione e la gestione del Boil-Off-Gas (BOG) generato dall'entrata di calore attraverso l'isolamento del serbatoio criogenico.

Ad oggi la letteratura tecnica e le tendenze dell'industria sembrano confermare che il sistema propulsivo ottimale per grandi navi a GNL (non metaniere) sia costituito dalla combinazione di serbatoi criogenici a pressione atmosferica e motori lenti a due tempi con iniezione diretta di gas ad alta pressione (fino a 300 bar) in ciclo Diesel, prodotti da MAN con il nome commerciale di ME-GI. Entrambi i sistemi sono disponibili sul mercato, tuttavia dalla loro combinazione sorge il problema irrisolto della gestione del Boil-Off. Il serbatoio a pressione atmosferica infatti consente un efficiente utilizzo dei volumi disponibili, tuttavia limita la possibilitá di accumulare BOG al suo interno. I motori ME-GI offrono svariati vantaggi dal punto di vista dell'efficienza globale e delle emissioni, ma l'alta pressione di iniezione complica la possibilitá di alimentarli con il BOG. In questo contesto l'industria ha proposto diverse soluzioni impiantistiche in-

novative per l'alimentazione ad alta pressione. Questa tesi verte sull'analisi di un processo di pompa di calore, ispirato al brevetto dell'azienda norvegese LNG New Technologies.

## Il processo di pompa di calore e le sue alternative

La pompa di calore é costituita da un ciclo chiuso recuperativo ad azoto transcritico, che preleva il calore dal serbatoio criogenico e lo cede al GNL freddo pompato ad alta pressione nella fase densa e diretto al motore ME-GI. L'effetto utile frigorifero della pompa di calore consente di bilanciare l'entrata di calore nel serbatoio e quindi controllare la produzione di BOG.

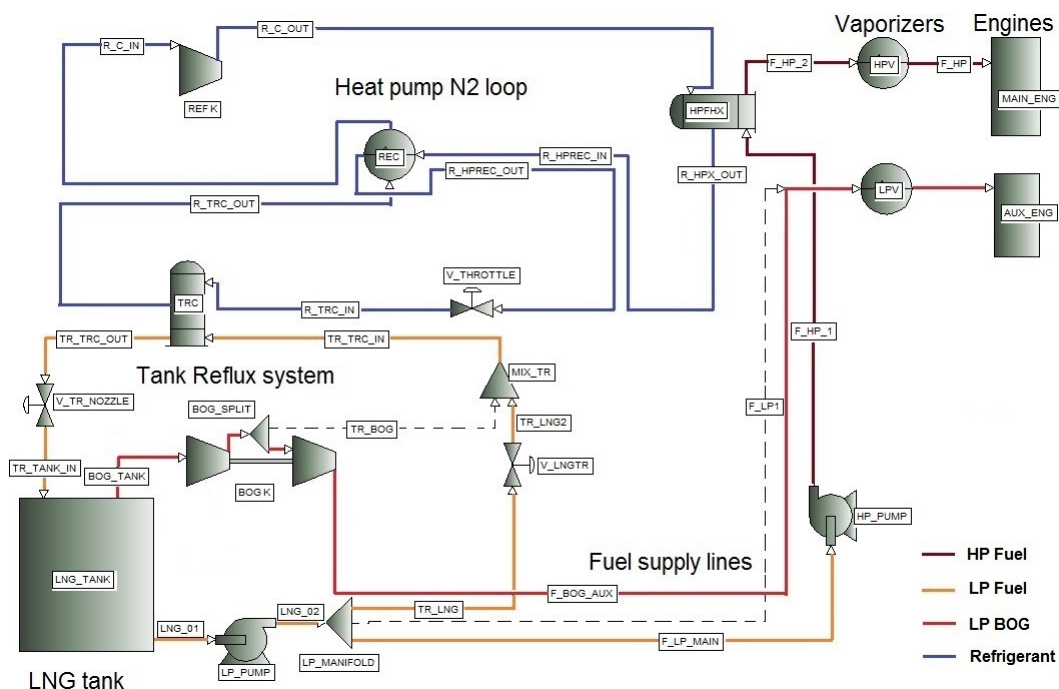


Figure 1: PFD: Processo di pompa di calore, nella versione con BOG alimentato al motore AUX (HeP-AUX)

La Figura illustra l'assetto ottimale del processo (identificato dalla sigla "HeP-AUX"), che prevede di alimentare i motori ausiliari (AUX) per la generazione di potenza elettrica con BOG (a 6 bar) e il motore propulsivo con liquido pompato ad alta pressione. Grazie a tale accorgimento, la pompa di calore é chiamata a

compensare solo la frazione di calore, in ingresso nel serbatoio, che eccede il consumo di BOG da parte degli ausiliari.

Mediante la sigla "HeP" si identifica invece l'assetto che prevede l'alimentazione del liquido a entrambi i tipi di motore. Tale configurazione permette di evitare l'impiego del compressore del BOG, ma si è rivelata svantaggiosa dal punto di vista energetico.

Gli altri processi considerati allo scopo del confronto sono:

- gli scenari in cui tutto il BOG prodotto, o solo l'eccesso al netto degli ausiliari, viene bruciato nelle Gas Combustion Units (GCU), indicati rispettivamente dalle sigle "GCU" e "GCU-AUX";
- la compressione del BOG fino alla pressione di iniezione di 300 bar mediante compressore alternativo multistadio ("HPK");
- il processo di "tipo terminal", standard per i grandi terminal di rigassificazione del GNL, che prevede la ricondensazione del BOG nel liquido pompato ad una pressione intermedia (es. 6.3 bar) e quindi sottoraffreddato (qui indicato con "MIX-AUX");
- la reliquefazione mediante cicli frigoriferi, progettati per le metaniere ("REL" e "REL-AUX")

Lo scenario di riferimento per le simulazioni è una nave con serbatoio di combustibile da 2200 m<sup>3</sup>; potenza di crociera del motore propulsivo di 10.94 MW; carico elettrico coperto dagli ausiliari di 450 kW.

## Simulazioni e risultati

Il processo di pompa di calore è stato simulato e ottimizzato mediante il software Aspen HYSYS®. Le variabili primarie di ottimizzazione sono la pressione

di evaporazione e la pressione massima del ciclo. In base a queste, e dato l'effetto utile richiesto, si determina il flusso di refrigerante necessario. In questo studio la pressione di evaporazione è stata fissata ad un valore di 9 bar, determinato mediante analisi parametriche, che costituisce l'ottimo compromesso fra la riduzione del rapporto di compressione e il mantenimento di una differenza di temperatura adeguata nell'evaporatore. Il valore ottimale della pressione di mandata del compressore è compreso nel range 59-66 bar. L'influenza di altri parametri considerati significativi è stata valutata mediante analisi parametriche. Il software è stato utilizzato anche per modellare i processi alternativi, con l'eccezione del ciclo di reliquefazione, le cui prestazioni sono state stimate dai dati in letteratura.

I risultati delle simulazioni di seguito riportati mostrano che i processi più efficienti, nel caso in esame, sono il processo di compressione (HPK), il processo di pompa di calore (HEP-AUX) e il processo di tipo terminal (MIX-AUX) con un certo vantaggio di quest'ultimo.

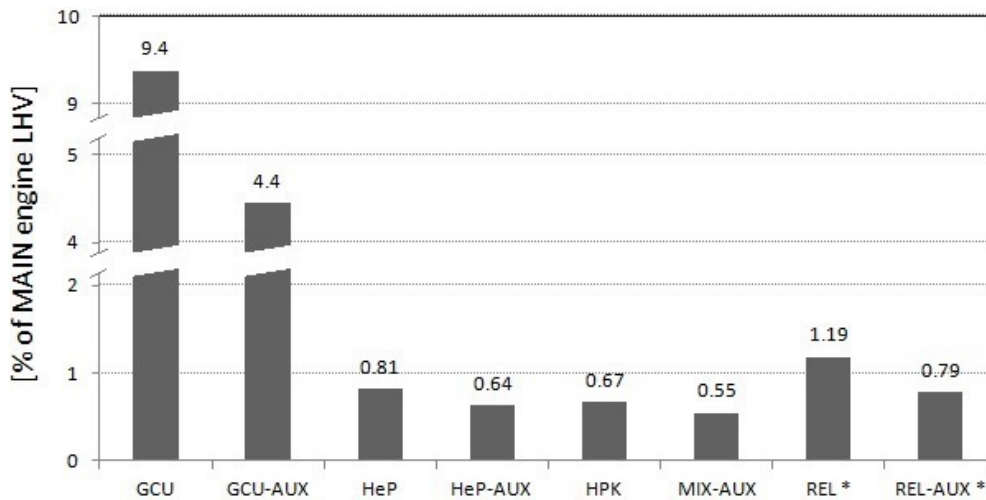


Figure 2: Consumo totale di energia primaria del sistema di alimentazione del combustibile, compreso il gas bruciato nelle GCU, espresso come percentuale della potenza termica del motore primario al 100% del NCR. (\*Reliquefazione stimato dalla letteratura)



## Componenti

Per il ciclo di pompa di calore si é ipotizzato l'utilizzo di scambiatori a piastre, o Shell&Tube laddove la differenza di pressione fra i fluidi lo richiede. Per il compressore del refrigerante si consiglia una macchina alternativa a due stadi non lubrificati, capace di operare ad una temperatura di aspirazione di circa -140°C in uscita dal recuperatore del ciclo. In base al modello di compressione politropica utilizzato la compressione avviene interamente al di sotto della temperatura ambiente; il lavoro di compressione é pertanto contenuto, ma si rende necessario l'utilizzo di leghe speciali che aumentano il costo della macchina.

## Conclusioni

La tabella seguente riassume un confronto di massima fra i tre processi che offrono la migliore efficienza energetica a pieno carico. Si osserva che nessuno dei tre é in grado di controllare la produzione di BOG quando il motore principale é spento. L'unico fra i processi esaminati, che consente in tale situazione di evitare di bruciare il BOG, é il processo di reliquefazione, al prezzo di una minore efficienza e una maggiore complessità.

Table 1: Confronto fra tre processi selezionati

	<b>HeP-AUX</b>	<b>MIX-AUX</b>	<b>HPK</b>
Energy consumption (100%NCR)	good	excellent	good
Main engine turndown tolerance (based on Design model simulations)	good	fair	excellent
BOG handling in Idle/Harbour scenario	GCU	GCU	GCU
Number of additional components (compared to GCU scenario)	5	2	1
Special components	Refrigerant compressor	Recondenser	HPK: 5 stages reciprocating
"Critical" HX	HPFHX, REC	-	-
Overall plant complexity	high	low	medium

In conclusione, per quanto riguarda lo scenario in esame, la maggiore complessità impiantistica della pompa di calore ne scoraggia l'impiego in favore del processo di tipo terminal ("MIX-AUX"), nonostante essa si dimostri competitiva con gli altri per quanto riguarda le prestazioni energetiche.

# Chapter 1

## Introduction

Liquefied Natural Gas (LNG) is becoming a competitive marine fuel due to the introduction of stricter environmental standards for marine emissions, and the market for LNG fuelled ships is expected to grow from local short-sea market to deep-sea shipping on a global scale. The recent orders for large LNG fuelled ships reveal the existence of a growing market and the need for more advanced and efficient technological solutions for LNG fuel systems, propulsion systems and handling of LNG Boil-Off-Gas (BOG) generated from heat transfer through the cryogenic tank insulation (heat leak).

The technical literature and the market players seem to have identified the most efficient design for large LNG fuelled ships in the combination of atmospheric fuel tanks and 2-strokes low speed gas diesel engines with gas injection at high pressure (ME-GI). Both systems are established and commercially available technologies, however their combination poses the practical challenge of BOG handling that is still not fully resolved, due to the high pressure required by the ME-GI engine.

Many manufacturers and technology providers are currently developing high pressure Fuel Gas Supply System arrangements, but it is still not clear how these will provide a reliable and efficient solution to the BOG issue. The Norwegian company LNG New Technologies patented the concept for a heat pump system

that extracts heat from the cryogenic tanks and discharges it to the vaporizing high pressure LNG directed to the ME-GI engine, thereby controlling the BOG generation in the tank.

The purpose of this thesis is to define a process layout of the above mentioned heat pump concept, optimize it by means of computer simulations, evaluate its performance compared to alternative processes and indicate what kind of process equipment would be needed.

The background to the work is described in the 2<sup>nd</sup> chapter of the thesis, which includes an overview of the LNG fuelled ship market, descriptions of the key technologies involved, namely gas engines, cryogenic tanks, BOG handling methods, including reliquefaction cycles, and finally the state of the art of fuel supply solutions for ME-GI engines applications. Chapter 3 is dedicated to the description of the proposed heat pump process in its layout details, and to the definition of a specific scenario as a basis for the calculations. Chapter 4 presents the computer simulations executed with the commercial software HYSYS®, starting from the model structure and inputs, to the simulation results presentation and discussion. This chapter includes a quantitative comparison with alternative BOG handling processes. Finally, chapter 5 outlines a preliminary selection of process equipment on the basis of the simulation results, with particular emphasis on the heat pump refrigerant compressor.

# Chapter 2

## Background

### 2.1 LNG as ship fuel

#### 2.1.1 Motivations for LNG as a ship fuel

LNG has been used as a fuel for propulsion on LNG Carriers (LNGC) since 1964, after the introduction of the first LNG fuelled vessel (non-LNGC) in 2000 the last decade has seen LNG becoming a competitive fuel for marine transport, mainly due to the introduction of restrictions in the international environmental regulations on marine emissions that favour LNG compared to more conventional and polluting marine fuels.

LNG marine projects certainly demand a higher investment cost than conventional projects, related to the tank and fuel gas system, but some savings can be expected on fuel cost depending on the fuel pricing scenarios [39, 40], however as fuel price prediction is critical in a long term project the savings associated with emission regulations are currently the main drive for LNG projects in the shipping industry.

The most influential international regulation is the "MARPOL 73/78", outlined by the International Maritime Organization (IMO) in a diplomatic conference in 1973 and expanded since then with six annexes [40, 38]. The last MARPOL Annex VI sets limits for  $\text{NO}_x$  and  $\text{SO}_x$  emissions from exhaust gas, differentiating

from open sea and selected coastal areas denominated Emission Control Areas (ECA). Figure 2.1 illustrates how the regulations are getting more stringent in the decade 2010-2020, especially in the ECAs. The current global status of the ECAs is illustrated in Figure 2.2.

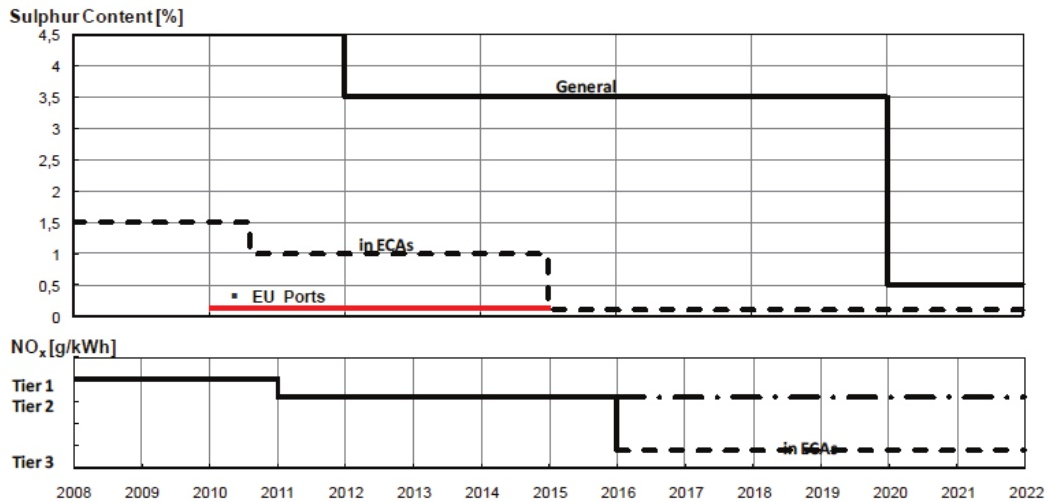


Figure 2.1: Implementation schedule for Revised MARPOL Annex VI [1, p.2]

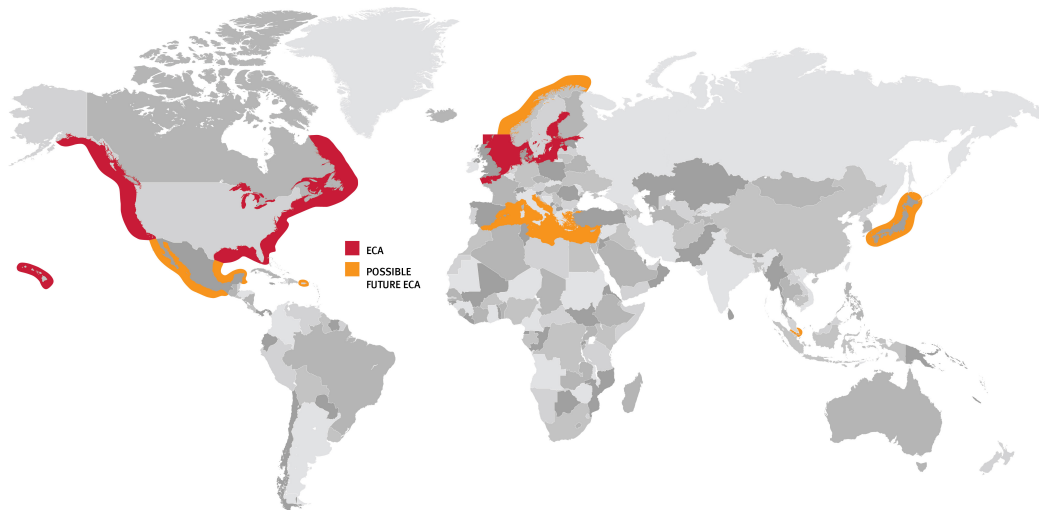


Figure 2.2: Emission Control Areas under IMO Annex VI [2]

In this context LNG is seen as a viable alternative to the conventional more polluting fuels such as Marine Diesel Oil (MDO) and Heavy Fuel Oil (HFO), for an increasing number of shipping segments.

### 2.1.2 Ship propulsion alternatives

To date ship propulsion is largely dominated by diesel engines that replaced steam turbines in the course of the 20<sup>th</sup> century, less frequently ships are driven by gas turbines, almost only LNG Carriers are still driven by steam turbines that guarantee flexibility in the fuel mix.

Diesel engines can be classified by the shaft speed: low, medium or high (the latter being limited to very small vessels), or by the number of strokes: 2-strokes (always low speed) or 4-strokes (usually medium speed) [7]. Figure 2.3 relates the thermal efficiency of commercial ship propulsion technologies with the installed power, it results that diesel low speed engines are the most efficient, followed by medium speed engines, gas turbine cycles and lastly steam turbines.

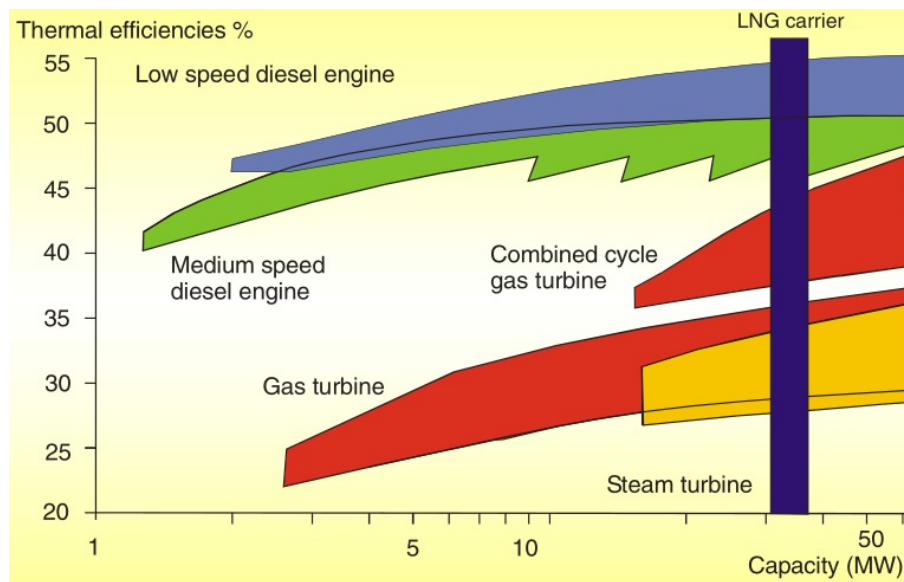


Figure 2.3: Typical thermal efficiency of prime movers [3, p.244]

All of the options listed above are suitable for LNG Carriers propulsion, some of them also for LNG fuelled ships (non-LNGC). Figure 2.4 has been created to offer a more detailed overview of the main propulsion alternatives for LNG fuelled ships and LNG Carriers, mapping the various technology by type of fuel used. The three vertical boxes in the background indicate the possible fuel modes of the machine, for instance steam turbines cover the three fuel modes mean-

ing that the steam boiler can burn either only natural gas, or a mixture of gas and fuel oil, or only fuel oil (MDO/HFO); low speed engines on the other hand cover only the second two modes since they can not run on pure natural gas and require at least a minimum amount of pilot fuel oil for ignition.

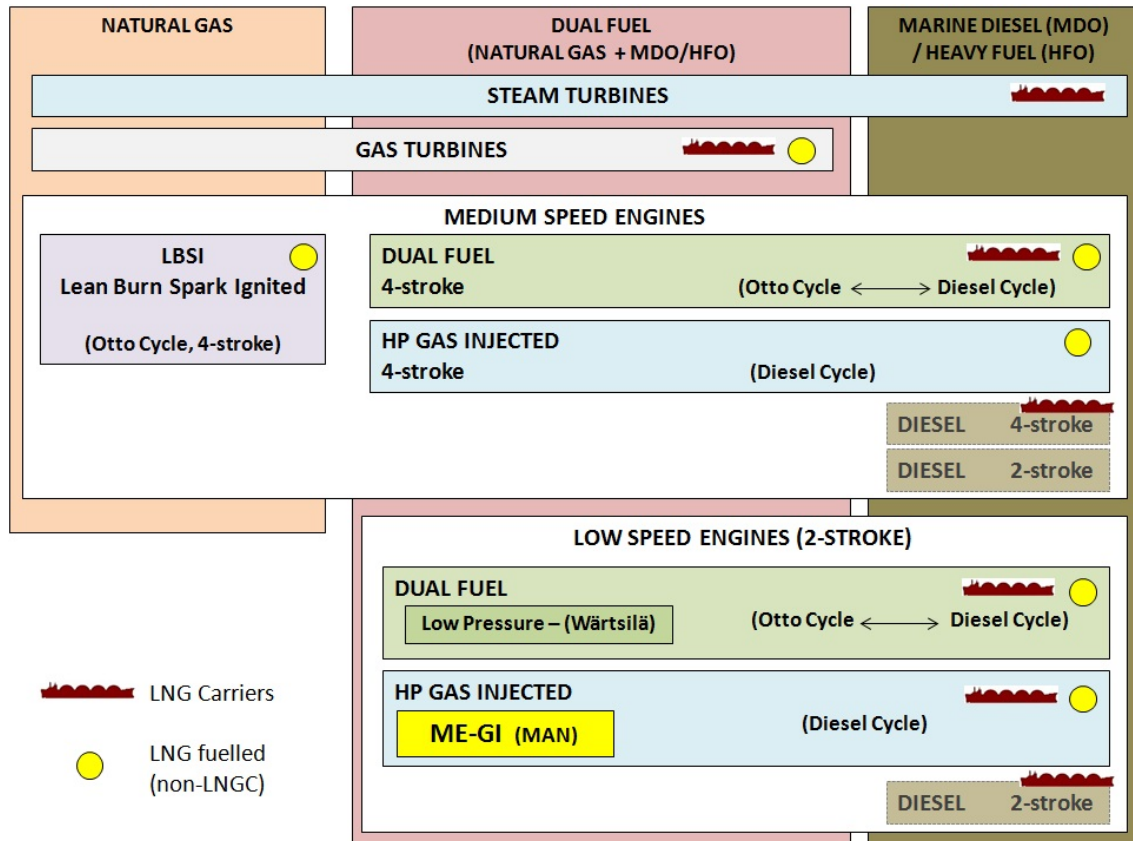


Figure 2.4: Ship propulsion alternatives for Natural Gas fuelled ships and Carriers sorted by type of fuel [4, 3, 5, 6, 1, 7, 8, 9, 10, 11]

The most attractive propulsion alternatives for LNG fuelled ships are reciprocating engines working in dual fuel mode, most of these machine can run on natural gas with a variable amount of fuel oil and easily switch to fuel oil mode if required. In the current state of the art of small LNG fuelled vessels mainly 4-strokes medium speed engines are employed of the types Dual Fuel and LBSI. The shaft speed of these type of engines is too high for the propeller, therefore the power transmission normally goes through a gear or through electric generators (Figures 2.6 and 2.5).



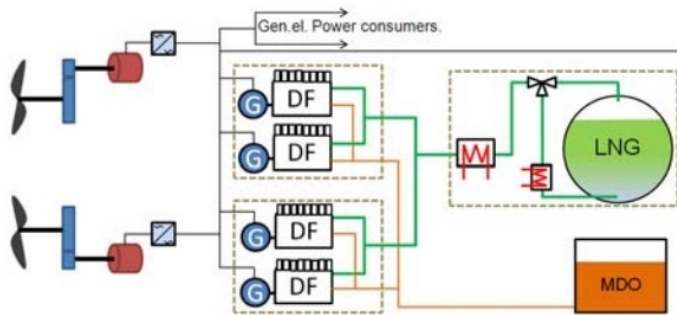


Figure 2.5: Platform supply vessel, Dual fuel Diesel-Electric propulsion [4]

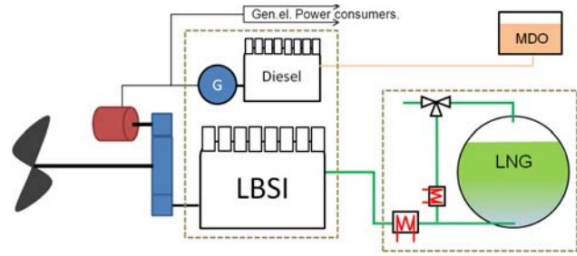


Figure 2.6: Ro-Ro ship, Pure LNG operation, Diesel-Mechanical propulsion, with Diesel backup engine [4]

In addition to the superior thermal efficiency, another advantage of low speed engines is that they can match the optimum propeller speed and be directly coupled to the propeller without a reduction gear and without the need for electric generators [41] [42, p.884]. Among those the High Pressure Gas Injected engines have high efficiency at all loads thanks to the thermal properties of the Diesel cycle [4], MAN Diesel & Turbo is one of the world leading producer of this type of machines that are gaining popularity in the market of medium-large gas fuelled ships under the name of "ME-GI" engines.

The main disadvantage of ME-GI engines is that the high pressure required for gas injection introduces complications and safety concerns in the design of the Fuel Gas Supply System, to overcome this the competitor company Wartsila offers a low pressure dual fuel 2-stroke solution, with direct gas injection during the compression phase and pilot fuel injection for ignition of the premixed charge.

The present thesis aims to develop a system specifically fitted to a ME-GI engine propelled vessel.

### 2.1.3 LNG fuelled ships

As of today a number of different categories of ships are being built or designed for LNG propulsion, the primary distinction for LNG fuelled ships divides them

in two groups:

- LNG Carriers (LNGC);
- LNG fuelled ships (other than LNG Carriers).

The first ships to use LNG as a fuel were LNG Carriers, since 1964. All of the early LNG Carriers were driven by steam turbines, fuelled by marine Heavy Fuel Oil (HFO) and LNG BOG from the cargo tanks [43], in the 1980's started the development of more efficient internal combustion engines systems for LNGC [4, p.2], in 2006 Slow Speed Diesel engines with BOG reliquefaction systems entered the market, together with Dual Fuel engines and electric propulsion [43, p.3].

In 2000 the first LNG fuelled ship (non-LNGC) started sailing in the norwegian coast [44], since then a number of small ferries and vessels for short-sea routes came into service mostly in Norway [38, p.3] [4, p.2]. Most of the early LNG fuelled vessels were car/passenger ferries, Platform Support Vessels (PSV) and similar short-sea vessels, in the recent years also tankers, cargo vessels and tug boats went into operations.

As of today the last confirmed orders include chemical tankers, cargo vessels as well as Ro-Ro vessels, bulk carriers and container ships [45]. The motivation to power these types of ships with LNG could be related to maximize the savings in ECA zones, as a matter of fact ship traffic analyses indicate that small and medium Ro-Ro vessels, tankers, bulk carriers and container vessels spend considerable time sailing in ECA zones [38, p.5], [46, p.26], . In particular it can be observed that fuel cost accounts for the highest share of the running cost for container vessels among the main shipping segments [47, 48] and the industry is showing a particular interest in developing large LNG fuelled container vessels for international shipping routes [39, 49].

For the scope of this thesis, the most relevant difference between LNG Carri-

ers and other LNG fuelled ships is the ratio between the tank size and the power of the propulsion system. This parameter is important when it comes to analyzing and comparing BOG handling alternatives, as the tank size can be considered proportional to the heat leak in the tank and to the BOG flowrate, while the propulsion power is proportional to the fuel consumption of LNG or BOG. It can be observed in Figure 2.7 that the ratio between the LNG tank volume and the installed main engine power is much higher for LNGC, due to the fact that the cargo volume in a LNGC contributes to the total LNG volume and BOG generation.

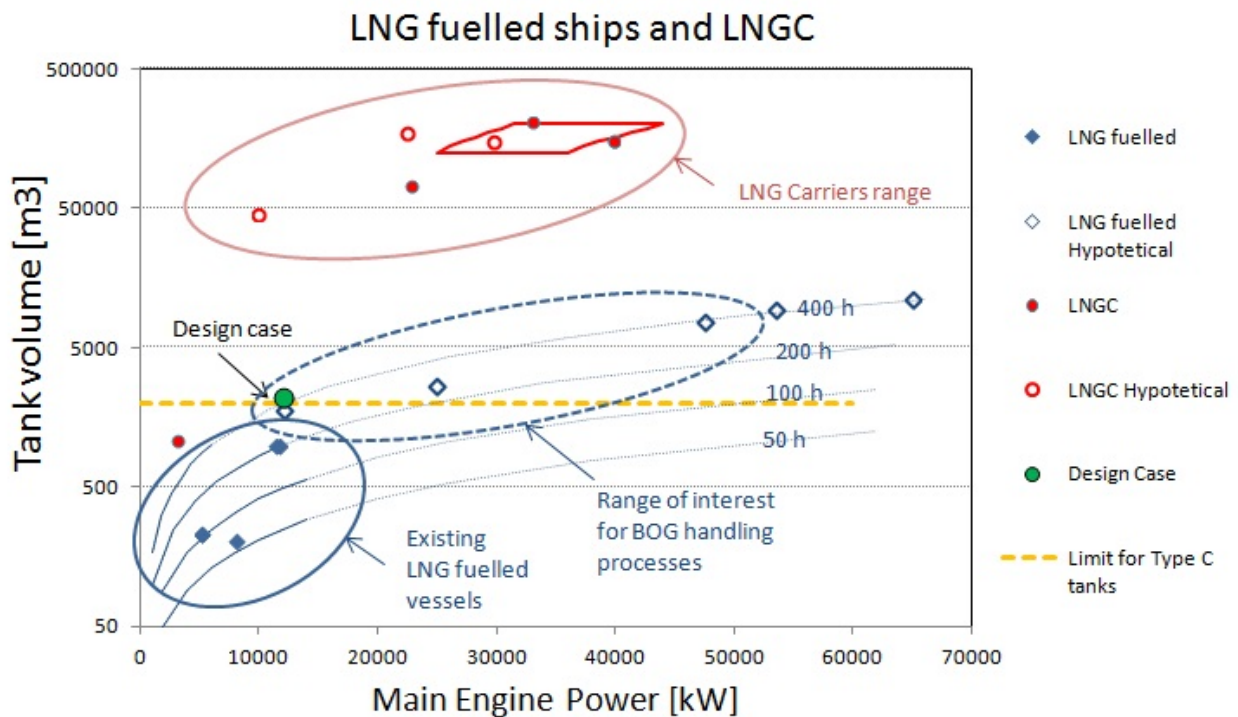


Figure 2.7: Comparison between LNGC and other LNG fuelled vessels, the blue lines indicate constant ratio between the LNG tank volume and the main engine power, [12, p.9], [13, 14, 15]

## 2.2 Tank types

LNG on ships is stored in cryogenic insulated tanks at the temperature of  $-160$  to  $-162^{\circ}\text{C}$ . LNG marine tanks have been classified by the IMO in three categories:

- Type A and Membrane tanks

characterized by complete secondary barrier;

- Type B tanks

characterized by partial secondary barrier, they typically have a self-supporting structure;

- Type C tanks

characterized by absence of secondary barrier, they are in most cases smaller pressurized tanks.

The first LNG tanks for ships were developed for the cargo on LNG Carriers. Since the LNG fuel on LNGCs is taken directly from the cargo tanks a dedicated LNG fuel tank is not needed, however with the introduction of LNG fuelled ships also dedicated LNG fuel tanks had to be developed.

Currently type C pressurized tanks are the only used for the small existing LNG fuelled ships (non-LNGC) [45]. The advantage of this type of tank is that they can operate at a pressure up to 9 bar, this allows the gas to accumulate in the tank atmosphere for some time before this pressure is reached. The main disadvantages of Type C tanks are the large amount of dead space and the tank capacity limits (currently in the order of 500 m<sup>3</sup>) [25, p.13].

It is expected that other types of tanks, different from Type C, will be taken in consideration for larger volumes of LNG fuel [25], for example Germanischer Lloyds estimates that for container ships with LNG volumes larger than 2000-3000 m<sup>3</sup> large type B prismatic tanks would be preferable to small Type C tanks due to lower specific costs [39, p.9]. If Type A and B are utilized as fuel tanks in LNG fuelled ships the maximum pressure of about 1.7 bara will provide very little buffer capacity for containing the BOG generated by the heat leak, as a consequence a different BOG handling approach will be needed.

## 2.3 BOG handling

LNG Boil Off Gas (BOG) is generated in any type of LNG tank due to the heat flow from the environment to the cryogenic tank, this flammable gas rich in Nitrogen and Methane accumulates in the tank atmosphere above the LNG liquid level at a temperature usually higher than the bulk liquid, causing the tank pressure to steadily increase in time. The generation and accumulation of BOG must be controlled to make sure that the tank pressure stays within the limits, in particular a too high pressure could lead to damages to the tank structure.

Depending on the type of tank and the application different BOG handling methods are used alone or in combinations:

- BOG containment in pressurized Type C tanks;
- BOG "flaring" in Gas Combustion Units (GCU);
- BOG as a fuel for ship propulsion;
- BOG as a fuel for Auxiliary engines;
- BOG reliquefaction;
- BOG venting (as a last resource).

As discussed BOG containment is currently the only BOG handling method for LNG fuelled ships non-LNGC, this is an efficient and simple method but its viability is limited to modest tank size for short-sea shipping with frequent bunkering.

Gas Combustion Units are used on LNG Carriers to dispose of the excess BOG when it exceeds the fuel consumption or the reliquefaction capacity, in these reactors the gas is burned and the exhaust vented to the atmosphere, this system is the on board equivalent of flaring.

BOG was used in the first LNGCs as a fuel for propulsion and burned with HFO

in steam turbine boilers, recently more advanced and efficient propulsion systems have been developed for LNGC where the BOG is burned alone or in a mixture with other marine fuels for propelling the ship. Figure 2.8) collects the technologies for LNGC propulsion with respect to utilization of BOG.

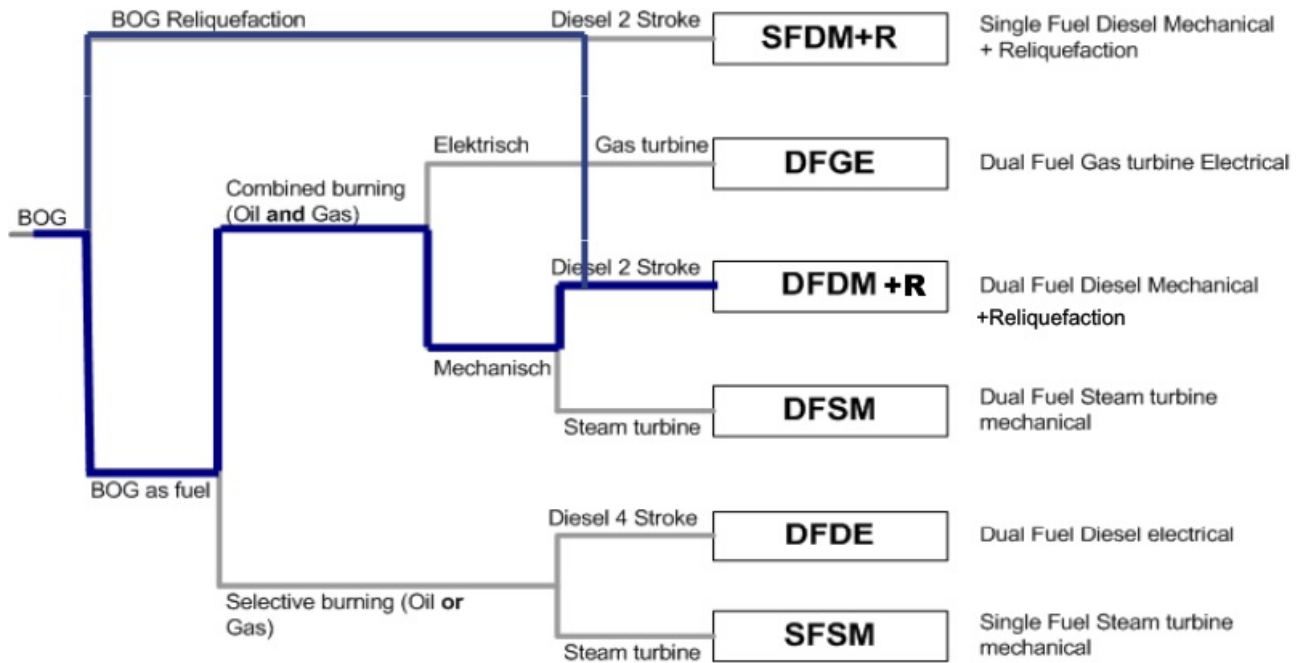


Figure 2.8: Propulsion systems for LNG Carriers [5, p.5], the highlighted alternative refers to low speed 2 stroke gas injected diesel engines integrated with a high pressure BOG compressor and a reliquefaction cycle

BOG can be used for electric power production if the vessel is equipped with a set of Dual Fuel 4-stroke Diesel Auxiliary engines, however due to the variability of the Auxiliary power demand on a ship a parallel system would be needed to handle the BOG under all operating scenarios.

### 2.3.1 BOG reliquefaction on LNG Carriers

On board processes for BOG reliquefaction have been developed for LNG Carriers, the first plant was built in 2000 and since then a number of different technologies became available on the market (Table 2.1).

Table 2.1: Main technologies for reliquefaction of BOG on LNG carriers [10]

Plant model	Manufacturer	Work Cycle	Year	Reliq. Capacity [kg/h]	Power [kW]	Specific work [kWh/kg]
LNG Jamal	Osaka Gas	Brayton	2000	3000	3000	1
TGE	Tractebel	Brayton	2004	6250	5030	0.75
Mark I	HGS	Brayton	2006	6000	5800	0.96
EcoRel	Cryostar	Brayton	2008	7000	6000	0.86
Mark III	HGS	Brayton	2008	7000	5500	0.78
Mark III Laby-GI	HGS	Brayton	2009			
TGE Laby-GI	Tractebel	Cascade	2009			

The most common process for on board reliquefaction is the Nitrogen Brayton refrigeration cycle, produced by several manufacturers with different layouts. Alternatives to the Brayton cycle are the Ethylene/Propylene cascade process produced by Tractebel Gas Engineering (TGE) and Burckhardt Compression [19, p.24] and the mixed refrigerant MiniLNG plant developed by Sintef.

#### Nitrogen Brayton cycle

The main manufacturer of Brayton processes for on board BOG reliquefaction is Hamworthy (recently bought by Wartsila). The first version of the Hamworthy process, also known as Moss process, or Hamworthy Mark I, is shown in Figure 2.9, in this process the BOG from the tank is compressed to about 4.5 bar by a two stage centrifugal compressor and reliquefied in the plate fin heat exchanger in the cold box. The cooling medium is pure Nitrogen which is compressed from 13.5 to 57 bar by a centrifugal 3 stage compressor coupled with a single stage turbo expander [10],[3, p.270].

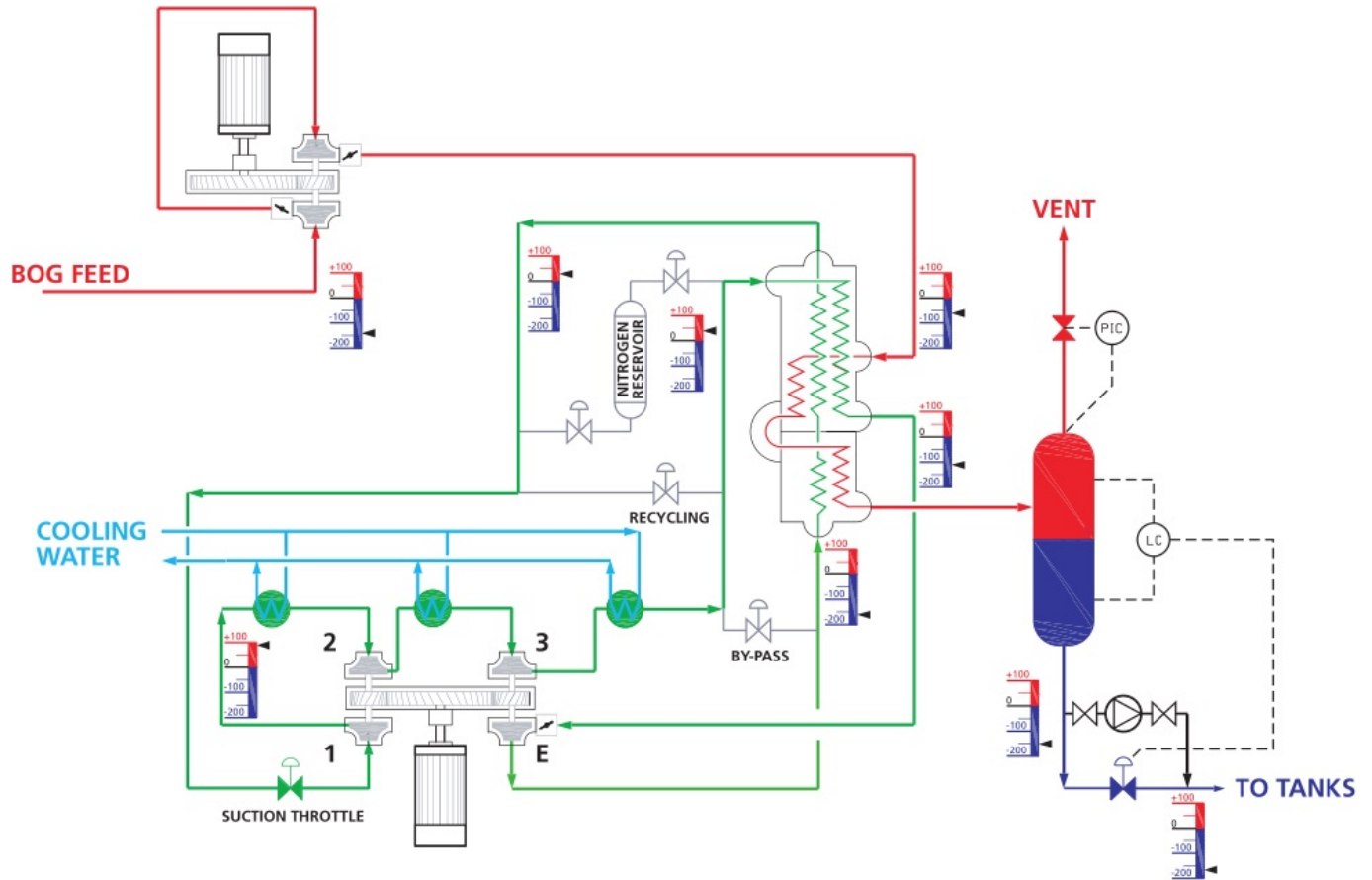


Figure 2.9: Hamworthy 1st generation BOG Reliquefaction System (Mark I) [16, p.5]

A more recent version of this system is the Hamworthy Mark III cycle in Figure 2.10 with the main difference that the tank BOG is preheated by HP warm Nitrogen before entering the compressor, as a consequence 3 stages with inter-cooling are required to compress the BOG to its reliquefaction pressure, with the advantage that part of the compression heat can be discharged to the seawater, thereby increasing the overall efficiency [16, p.6]



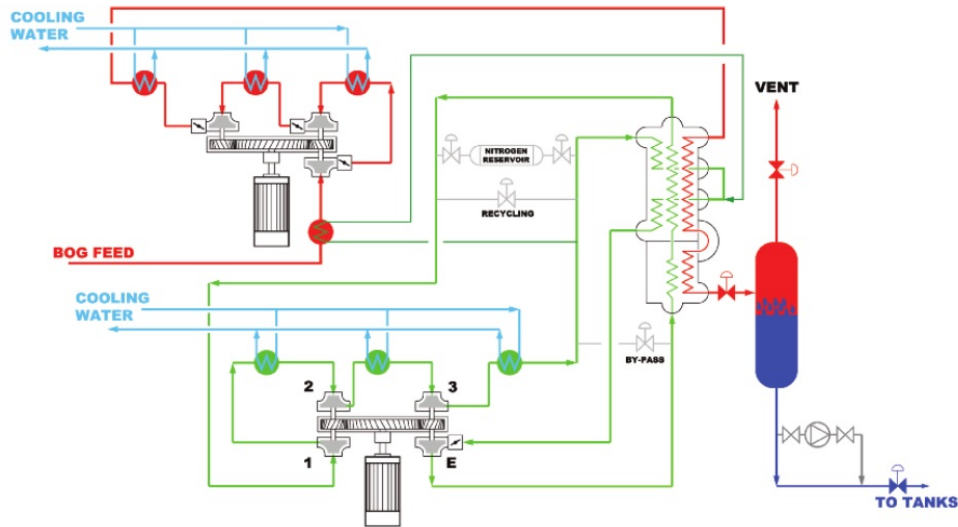


Figure 2.10: Hamworthy 3rd generation BOG Reliquefaction System (Mark III) [16, p.6]

The Cryostar's EcoRel process is a different version of a Brayton cycle with distinct heat exchangers of which one internal recuperative Nitrogen heat exchanger, two separate heat exchanger for BOG desuperheating and liquefaction and one BOG compressor cryogenic intercooler. It can be observed that while Hamworthy moves the BOG compression to the warm temperatures to take advantage of seawater intercooled stages, Cryostar chooses to maintain a cold BOG compression (at about 4.8 bar) using the Nitrogen for the intercooling, in parallel with the BOG desuperheating.

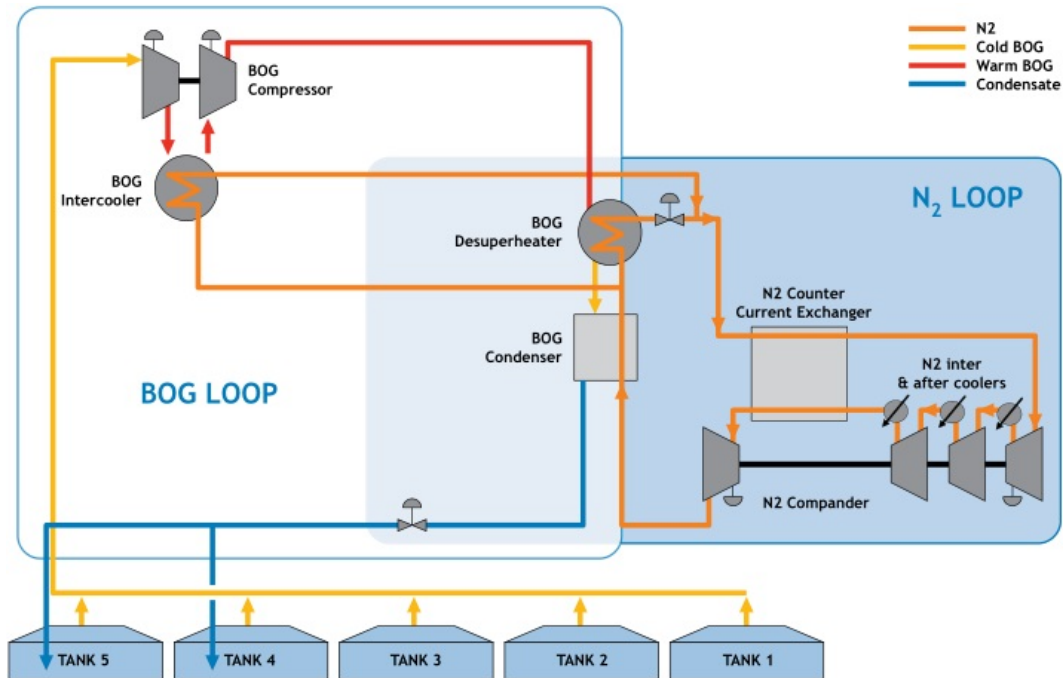


Figure 2.11: Cryostar EcoRel reliquefaction process for LNG Carriers [17, p.5]

### Mini LNG

The Mini LNG system is a mixed refrigerant process that has been developed and tested in the Sintef laboratories in Trondheim, and operated on a small LNGC since 2009 [18]. In this plant configuration the tank BOG is compressed by a oil-free labyrinth compressor to the pressure of 18bara (max 22bara) and above ambient temperature. The warm gas is then cooled by a seawater after-cooler and a Propylene precooling cycle to the temperature of  $-35^{\circ}\text{C}$ , before entering the heat exchanger where it is desuperheated, liquefied and subcooled against the Mixed Refrigerant. At this point the subcooled liquid is throttled to tank pressure [50, p.145]. A full scale Mini LNG plant has been installed on a Multigas Carrier by I.M. Skaugen SE, with a capacity of 20 tonnes LNG/day [51] and a energy consumption of 0.7 kWh/kg of reliquefied LNG [29]. The lower value of energy consumption of 0.47 kWh/kg in Table 2.2, is due to the fact that the Propylene compressor work is not included in the calculations [29].

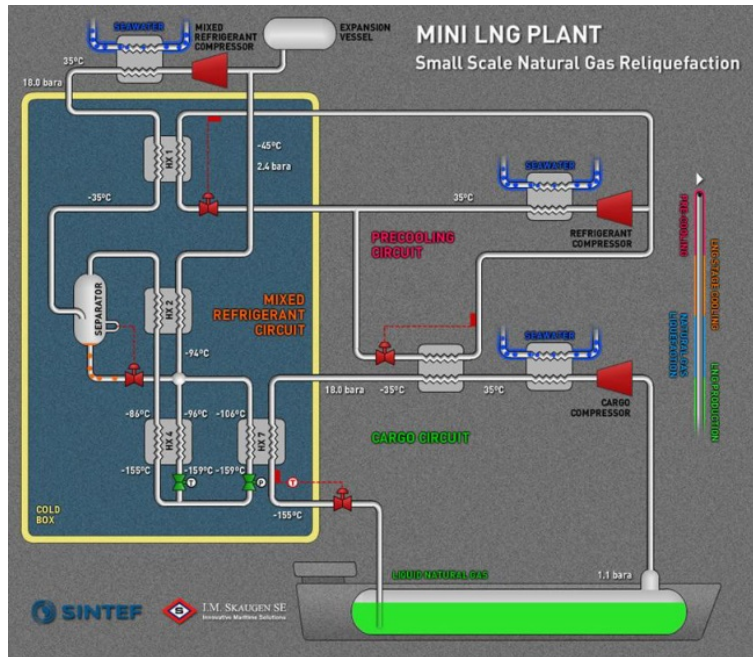


Figure 2.12: SINTEF Mini LNG Process, PFD [18, p.34]

Table 2.2: SINTEF Mini LNG Process, main parameters [18, p.35]  
**BOG NG with 89 mol% CH<sub>4</sub>, 11 mol% N<sub>2</sub> (18 bara)**

Boil-off gas liquefaction capacity	20 tonnes/d
LNG exit temperature (before throttling to tank)	-155 °C
MR (at first vapour-liquid separator inlet) and NG pre-cooling temperature	-35 °C
Mixed refrigerant compressor pressure ratio	9.3 -
Mixed refrigerant compressor power consumption	395 kW
Estimated compressor isentropic efficiency	0.65 -
Mixed refrigerant actual suction volume	1520 m <sup>3</sup> /h
Specific suction volume	1.8 m <sup>3</sup> /kg LNG
Specific power consumption mini-LNG	0.47 kWh/kg LNG

Table 2.3: SINTEF Mini LNG Process, performance [18, p.39]

**Results from full scale tests and simulation model verification**  
Including simulation results for future plant operating conditions (corrects for off-design conditions at full scale tests)

Parameter	Unit	Measured	Simulation	Simulation corrected <sup>1)</sup> (dp and leak)	Simulation corrected <sup>2)</sup> (precooling t)
Liquefaction capacity	tonnes/d	14,4	14,4	17,1	18,8
LNG exit temperature before throttling to tank	°C	-154,1	-154,1	-155	-155
MR precooling temperature at vap-liq separator	°C	-24,9	-24,9	-24,9	-35
NG precooling temperature	°C	-31,7	-31,7	-35	-35
Refrigerating capacity	kW		70,7	84,3	93,2
Volume flow LP MR out of coldbox	m <sup>3</sup> /h		1436	1512	1517

To compare the Mini LNG performance to the one of the process in this study it is useful to estimate its COP. If the refrigeration duty of 70-93 kW is taken from table 2.3, with a mixed refrigerant compressor work of 395 kW [18, p.35] (precooling refrigerant compressor neglected), the resulting COP is 0.18 to 0.24. If refrigeration duty is computed from the BOG mass flow according to the equation

$$\dot{Q}_{\text{ref}} = \dot{m}_{\text{BOG}} \cdot \Delta h_{\text{evap}} = \frac{20000 \text{ kg/day}}{24 \cdot 3600} \cdot 517.1 \text{ kJ/kg} = 119 \text{ kW} \quad (2.1)$$

then the COP becomes 0.3.

## 2.4 Systems for 2-Stroke Low Speed Engine Propulsion

The objective of this thesis is to develop a system for LNG fuelled ships equipped with 2-stroke low speed gas diesel engines. There are two reasons why the topic has been restricted to this specific scenario. The main reason is that this type of engines are expected to have a bright outlook in the market of medium-large LNG fuelled ships due to the remarkable propulsion efficiency given by the thermal features of the gas diesel cycle and by the possibility of direct coupling to large slow propellers. Secondly the BOG handling is particularly critical in this scenario due to the difficulty of feeding it to the engine at high pressure. In

summary it is expected that providing an efficient and reliable solution for the BOG handling in this scenario would open the way to one of the most efficient propulsion solutions for gas fuelled ships.

In the present chapter the state of the art of ship propulsion systems with 2-stroke gas diesel engines is described, including an overview of the engine technology itself and a series of options for fuel supply that are under development.

### 2.4.1 ME-GI engines

MAN Diesel & Turbo is one the world leading manufacturers of large low speed gas diesel engines for ship propulsion, these engines are known by the designation "ME-GI", indicating 2-stroke Dual Fuel Electronically controlled Gas Injected engines. Figure 2.13 shows the cross section of a ME-GI engine.

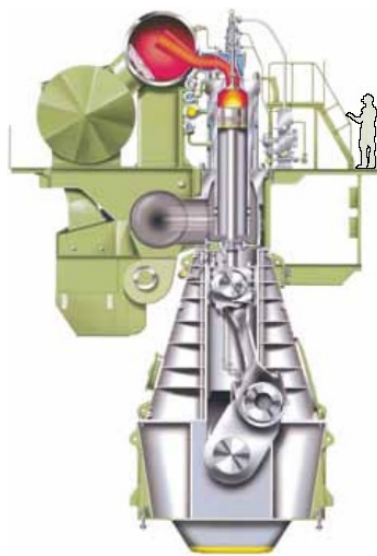


Figure 2.13: Sketch of a ME-GI engine [19, p.5]

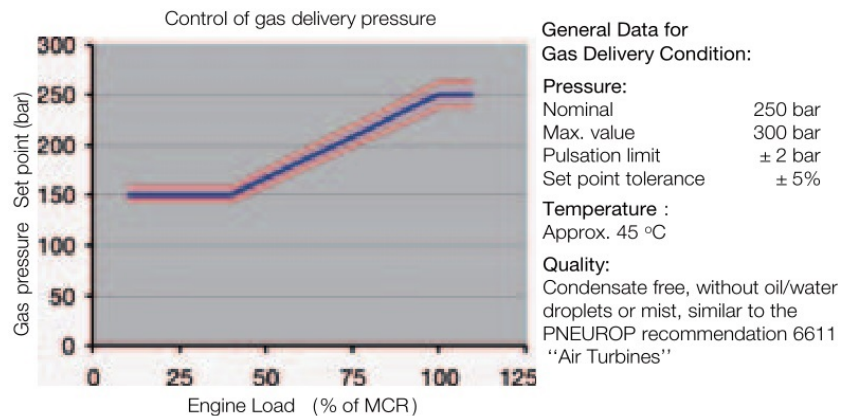


Figure 2.14: Example of ME-GI Gas supply specifications, delivery pressure at varying engine load, for a 250 bar engine feed [20, p.15]

The attribute "Dual Fuel" indicates that the engine can run on fuel-oil alone or on a mixture of fuel-oil and Natural Gas, the amount of injected fuel-oil can be reduced down to a minimum preset of 2-5% of pilot fuel necessary for ig-

nitition, meaning that operation with Natural Gas alone is not possible [19]. The main feature of these machines compared to other Dual Fuel engines is that they always operate in a standard Diesel cycle, the HP gas injection at the end of the compression stroke provides the advantages of the Diesel cycle such as absence of limits for knocking and misfiring, possibility to operate at maximum power and Break Mean Effective Pressure (BMEP) without de-rating and low methane slip [4, 52]. The thermal efficiency of about 50% of the gas injected Diesel cycle is comparable to the conventional fuel-oil cycle, this value is high and fairly stable at different gas/fuel-oil ratios and at reduced engine load [20].

The detailed description and modeling of the engine is out of the scope of this thesis, yet this machine sets the requirements for the Fuel Gas Supply System and therefore the boundary conditions for a related simulation model. In particular ME-GI engines require gas at 250-300 bar and about 45°C during normal operation, at reduced load the pressure can be reduced linearly as shown in Figure 2.14.

The two available options for supplying Natural Gas to such high pressure are LNG cryogenic pumps or multistage reciprocating BOG compressors.

#### 2.4.2 High Pressure BOG compression

High Pressure (HP) compressors are complex and costly machines compared to HP cryogenic pumps but they offer a direct solution to the BOG handling problem. Burckhardt Compression and MAN are developing a BOG HP compressor system for LNG Carriers with ME-GI propulsion, in a configuration where the HP Fuel Gas Supply System is integrated with reliquefaction processes [19],[10, p.8]. The compressor, with the commercial name Laby-GI, is a five stages reciprocating machine, with labyrinth oil-free piston sealing for the first three stages and conventional lubricated piston ring sealing in the last two stages,

[20](Figure 2.15).

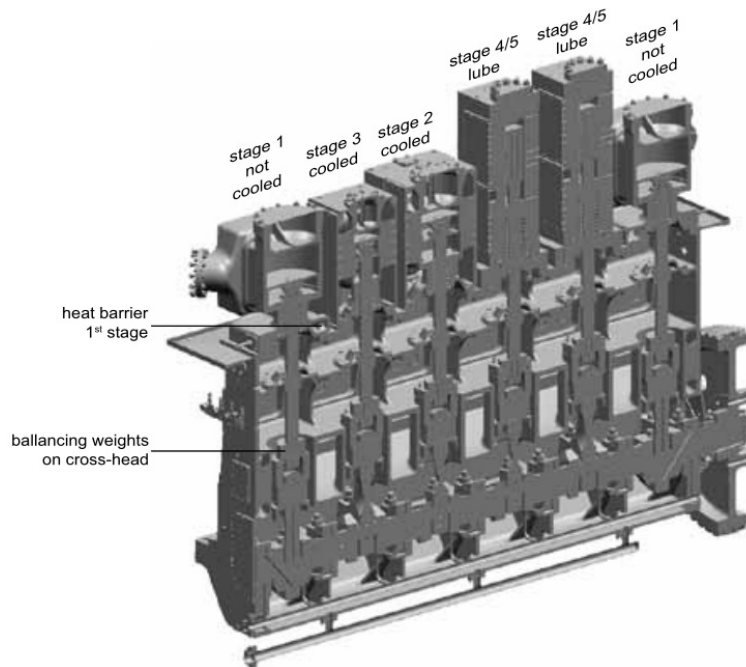


Figure 2.15: Cross section of the Burckhardt Laby-GI fuel gas compressor for ME-GI engine applications [19, p.21]

This machine is designed to compress large quantities of BOG onboard LNG carriers, in the order of 1,5 kg/s for a 210'000 m<sup>3</sup> carrier [20, p.10]), an equivalent system for an LNG fuelled ship would have to be scaled down to a flowrate approximately 30 to 50 times smaller than this value.

### 2.4.3 High Pressure LNG Fuel Gas Supply Systems

When it comes to LNG fuelled vessels, rather than downsizing a solution for the LNGCs segment, many companies have focused in developing new processes that employ standard cryogenic components that are used in the LNG fuelled ships industry or in the LNG terminal industry, adapting them to the HP gas injected engine scenario. Mostly these processes consist in pumping the liquid LNG and evaporating it at high pressure, avoiding the HP BOG compression stages. Some of the industries involved in this type of research are Samsung, HGS, TGE, DSME, Cryostar, HHI and MHI [19, p.29].

Cryostar in [19, p.31] identifies the main components of a HP Fuel Gas Supply System (FGSS) for ME-GI engines:

- Reciprocating LNG HP pump with Variable Frequency Drive (VFD);
- Automatic pump control system (to meet engine delivery pressure);
- Buffer volume for pressure pulsations damping.

Figure 2.16 shows this FGSS layout, including a list of potential BOG handling methods that might be required.

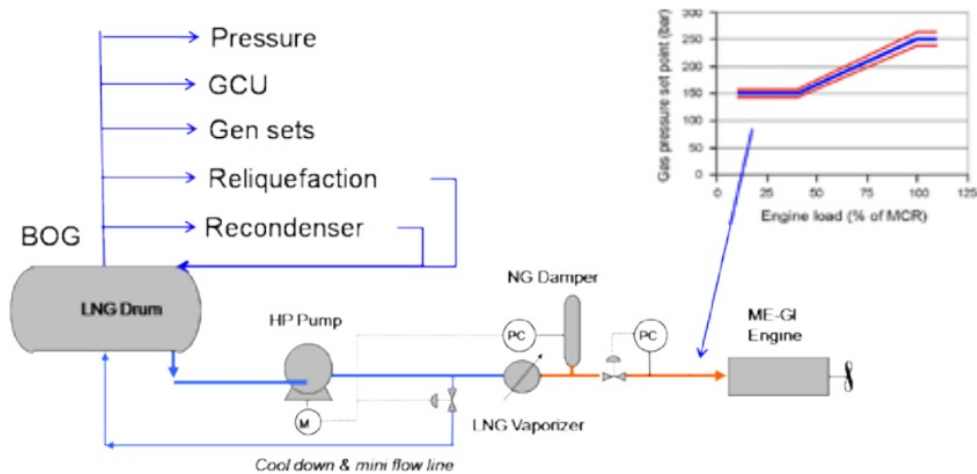


Figure 2.16: FGSS with Cryostar's HP pump solution and BOG handling alternatives [19, p.31]

Hyundai Heavy Industries (HHI) in [21] defines a set of general specifications for HP FGSS for ME-GI engines, the layout suggested in this document is shown in Figure 2.17.



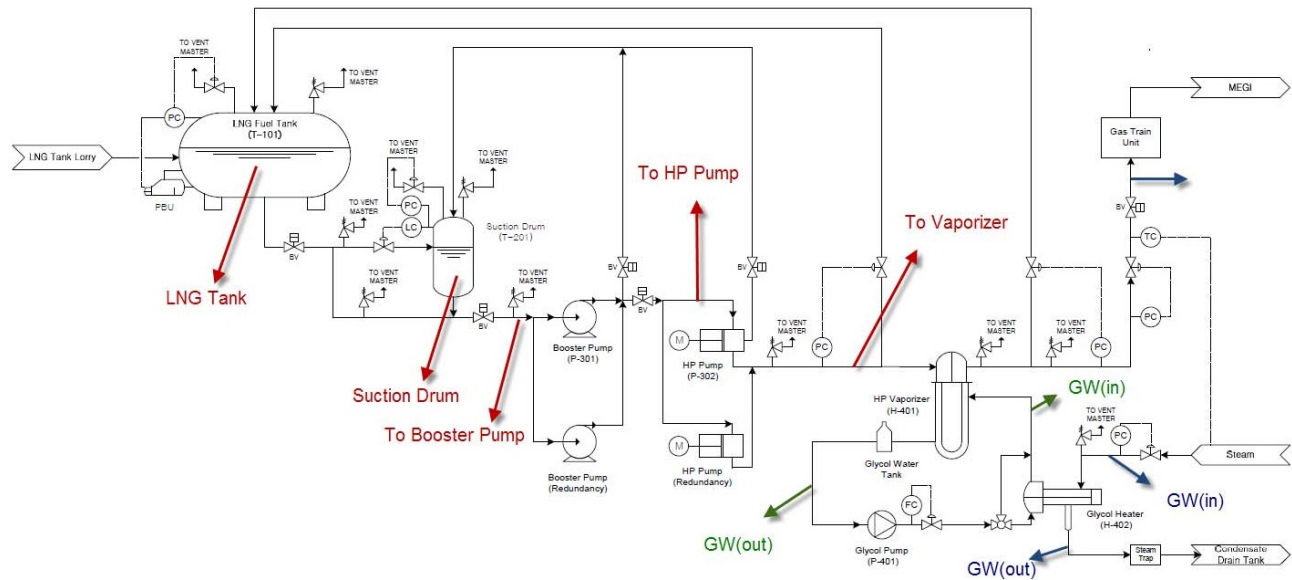


Figure 2.17: PFD of HP Fuel Gas Supply System, for a design flowrate of 0.39kg/s [21, p.20]

This system is designed for LNG fuelled ships (non-LNGC) with a 6.5 bar Type C fuel tank and a fuel consumption of 0.39 kg/s of LNG at 100% engine load, compared to the one in Figure 2.17 this layout does not include a HP buffer tank, but is equipped with a Suction drum and Low Pressure (LP) pumps upstream the HP pumps, these units protect the HP pumps avoiding vapor slip in the pump suction and cavitation. In this configuration the HP vaporizer system is composed by a shell & tube glycol heat exchanger that vaporizes and superheats the LNG to its target temperature, and a glycol closed loop where the fluid is heated by steam generated in boilers [21].

One example of HP FGSS layout for atmospheric tanks is illustrated in Figure 2.18, this layout differs from Type C applications as it includes a BOG handling system with LP BOG feed to the Auxiliary engines, and a BOG recondenser. The recondenser is a contactor that mixes LNG pumped at LP (4-5 bar, in the sub-cooled region) with LP superheated BOG in a suitable ratio, the output is sub-cooled liquid that can be fed to the HP pump. This component is frequently used for BOG handling in LNG receiving terminals [53].

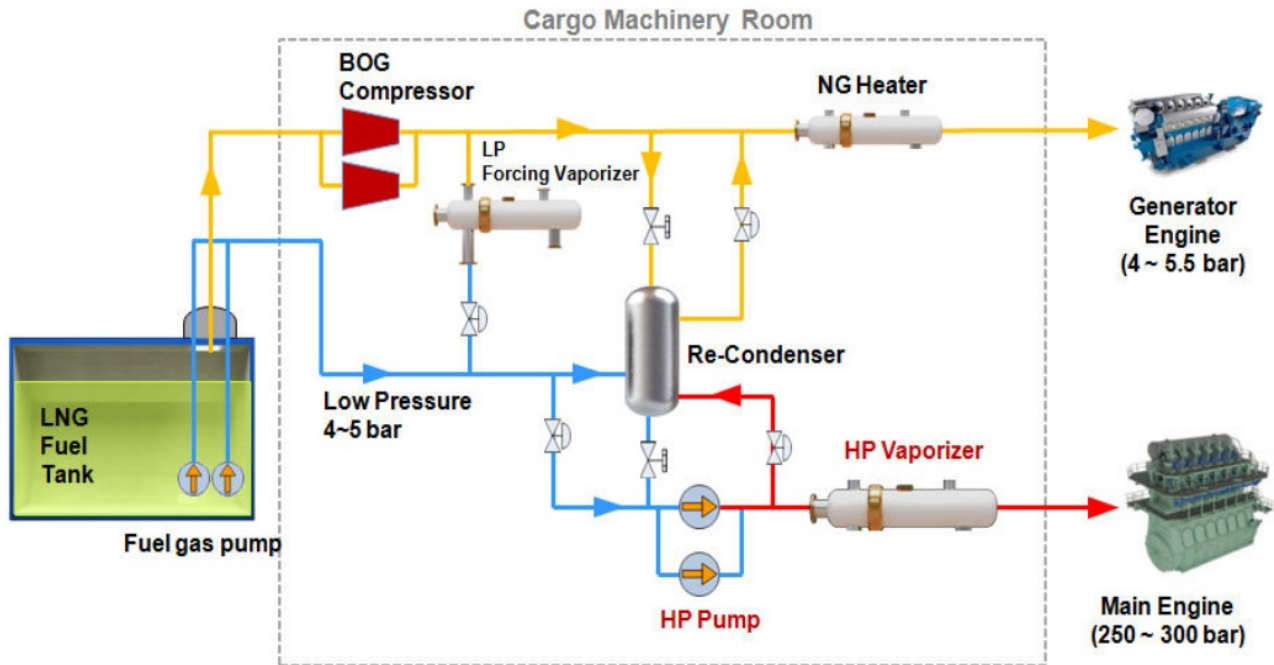


Figure 2.18: PFD of HP Fuel Gas Supply System for atmospheric tank, equipped with BOG compressor and recondenser, proposed by Samsung Heavy Industries [22, p.10], [13, p.18]

#### Integration of HP Fuel Gas Supply Systems and reliquefaction processes

The idea of using pumps rather than compressors to provide HP fuel to the Main engine has been explored also for the design of LNG Carrier's Fuel Gas Supply Systems. In this case, given the high BOG production, the FGSS will necessarily have to be integrated with a BOG reliquefaction process.

Hamworthy studied how to optimize its Mark III reliquefaction cycles for ME-GI applications, in the system shown in Figure 2.19 the FGSS is integrated with the reliquefaction cycle through a heat exchanger named "Optimizer", this component is part of the Brayton cycle in parallel with the "BOG Preheater" and the cold box, and has the function of recovering part of the low temperature exergy of the cold HP LNG stream with a fraction of the HP Nitrogen stream, thereby enhancing the Brayton cycle efficiency.

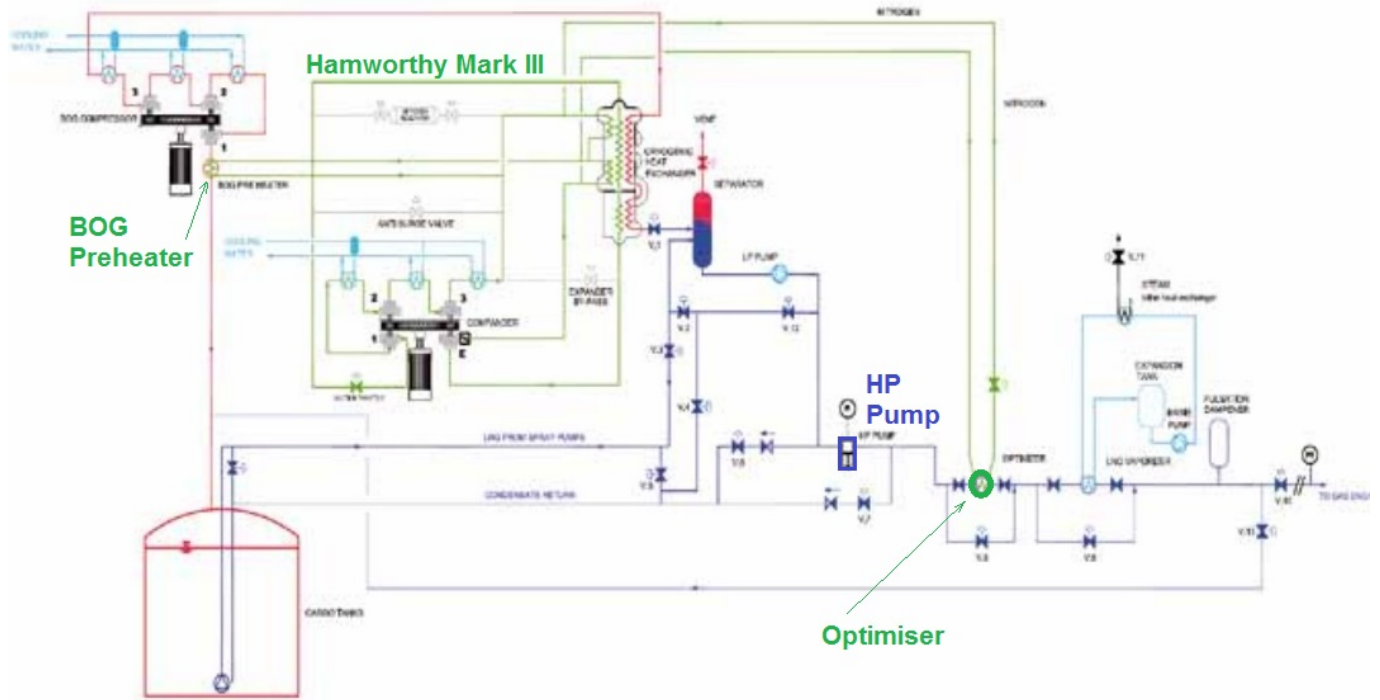


Figure 2.19: Integration of HP FGSS and Hamworthy Mark III reliquefaction cycle, published by MAN in [19, p.19]

Wartsila, that acquired Hamworthy in the beginning of 2012, is also studying this system for applications with HP 2-strokes engines, Figure 2.20 shows a process similar to the one illustrated above, here the BOG compressor is also used to send gas at 5-6 bar to the Auxiliary engines.

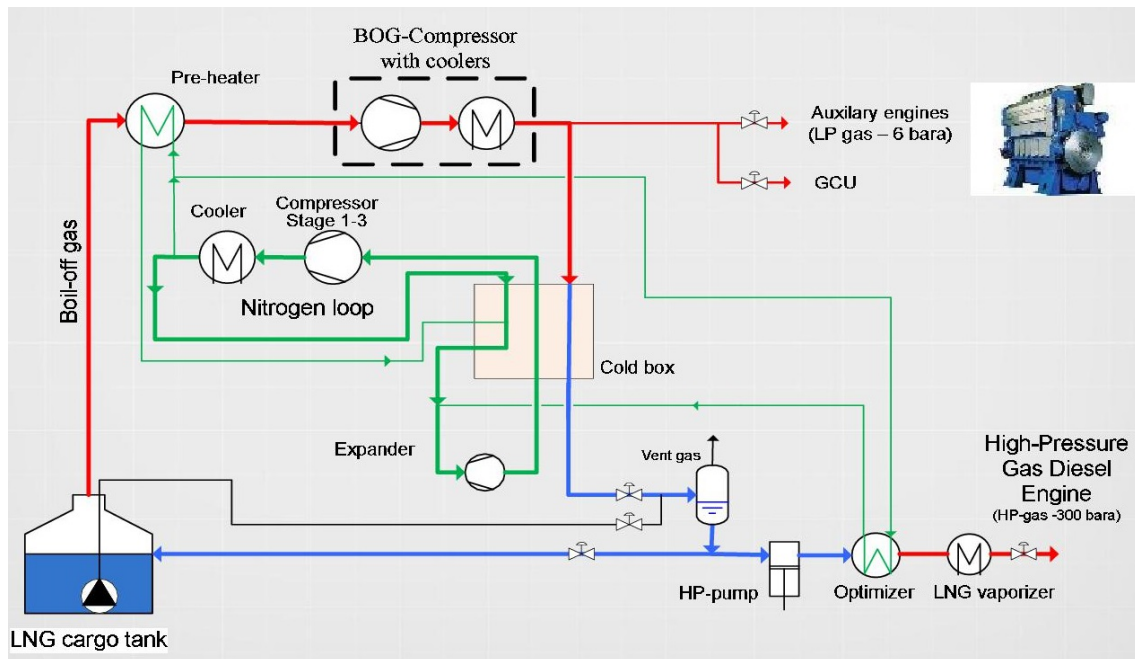


Figure 2.20: Integration of HP FGSS and BOG Reliquefaction System LNGRS (or Hamworthy Mark III), published by Wartsila in [23, p.18]

# Chapter 3

## Heat pump process

The previous chapter outlined a literature review of the most relevant BOG handling strategies. The high pressure compression and the reliquefaction processes have been developed for LNG carriers, in principle they could be downsized to meet the requirement of the LNG fuelled ship segment. On the other hand there are reasons to believe that a different approach could be followed when it comes to LNG fuelled ships instead of LNGCs:

- The amount of BOG generated in LNG fuelled ships is roughly 10-100 times less than for a similar size LNGC (Figure 2.7);
- Downsizing large reliquefaction processes to meet a significantly lower reliquefaction capacity might be uneconomical and inefficient;
- Space and process complexity constraints are tighter on a merchant ship than on a LNGC.

The approach of the present thesis was inspired by the Norwegian company LNG New Technologies that outlined and patented a process to cool the LNG fuel tank and bunkering pipe of a LNG fuelled ship by means of a refrigerant cycle that uses the heat requirement of the HP cold LNG in the FGSS to drive the process. The patented system illustrated in Figure 3.1 is essentially a heat pump process that transfers heat from the cold fuel tank space (5b) and filling pipe (5a) to the LNG Fuel Supply line (8) directed to the engines. The refrigerant fluid

(1) is a inert gas such as Nitrogen subject to compression in (2) and pressure reduction in (4) via throttle valve or expander [24], it can be noted that heat exchangers with external utilities such as seawater, steam or glycol loops are not included in this layout.

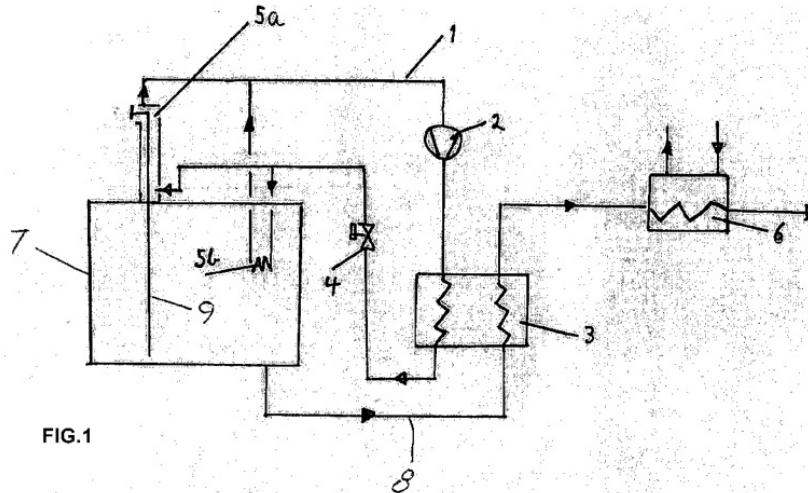


Figure 3.1: Jorn M. Jonas patented heat pump process [24]

The principle of integrating the HP FGSS with the Nitrogen reliquefaction cycle was already investigated by Hamworthy and others as detailed in chapter 2.4.3, the heat pump process as outlined by LNG New Technologies differs from those approaches in the way that it aims to achieve the fullest possible integration between the process streams, until the heat discharge to the environment in the form of external utilities streams is excluded.

In the development of the present thesis, different process layouts than the one suggested by LNG New Technologies were studied but the "philosophy" of full heat integration between the process streams without heat discharge to the environment was maintained as a constant feature, with the intention to assess the limitations of this simple and efficient approach.

### 3.1 Heat pump process layout (HeP)

A number of different process layouts have been explored in the course of this thesis, Figure 3.2 illustrates the main configuration of the heat pump process (HeP). The Process Flow Diagram (PFD) is divided in three parts:

- the Fuel Supply lines, that transfer LNG fuel from the cryogenic tank to the main and Auxiliary engines at the prescribed temperature and pressure;
- the Tank Reflux System, that extracts LNG from the tank and recirculates it back at lower temperature;
- the Heat Pump cycle, that transfers the heat from the Tank Reflux System to the Fuel Supply lines, in a closed refrigerant loop.

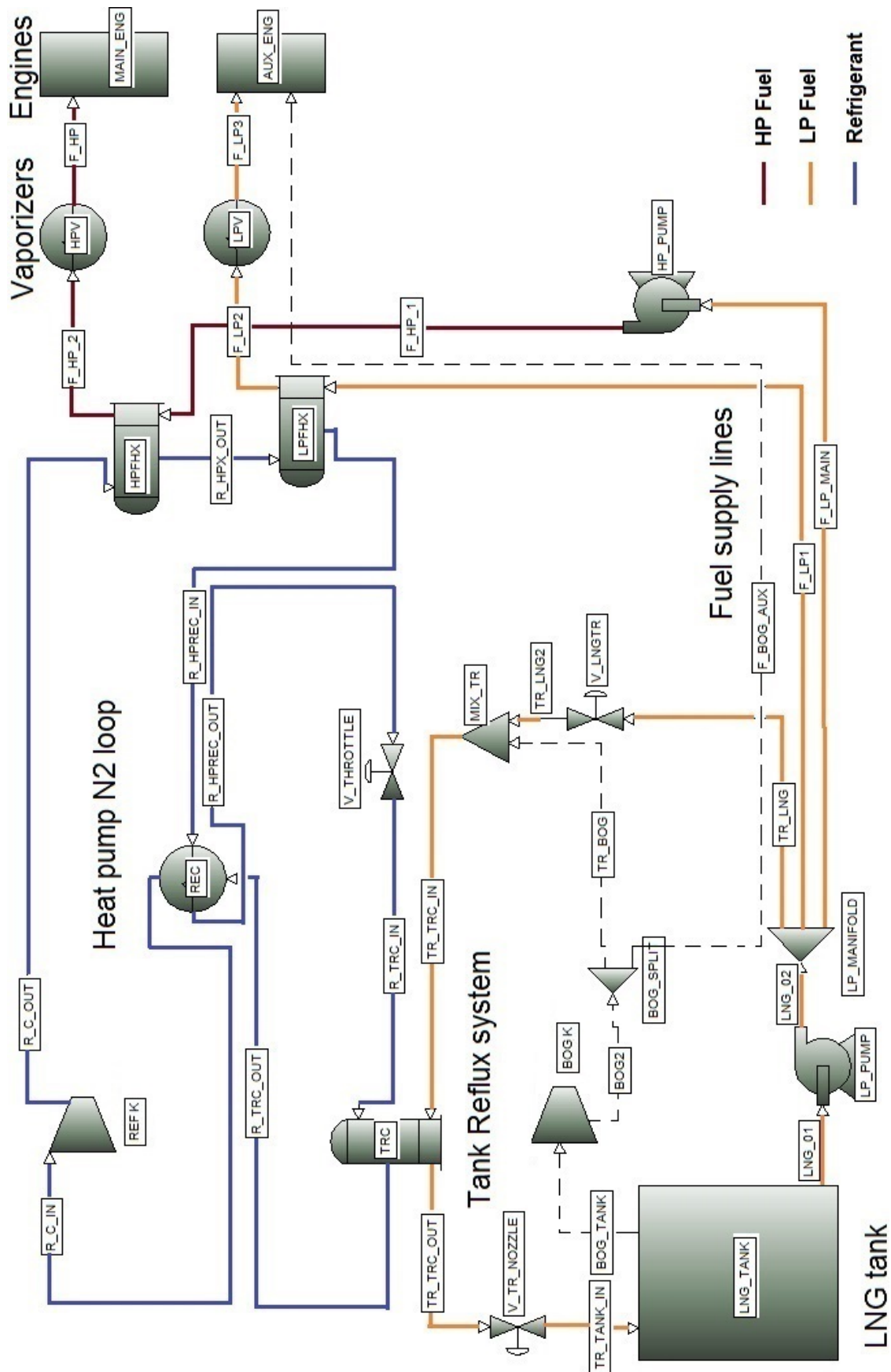


Figure 3.2: PFD of the heat pump process (HeP)



As indicated by the color legend the heat pump loop contains pure Nitrogen refrigerant. The Nitrogen, after being compressed by the Refrigerant Compressor, is cooled by the LNG fuel in the High Pressure Fuel Heat Exchanger (HPFHX) in series with the Low Pressure Fuel Heat Exchanger (LPFHX), following the heat discharge to the Fuel Supply lines it enters the Recuperator (REC) for internal heat exchange. At the Recuperator outlet the refrigerant is throttled to a lower pressure in the two phase region, so it can evaporate in the heat exchanger labeled Tank Reflux Cooler (TRC) providing the necessary cooling duty to the Tank Reflux system. The Fuel Supply lines consist in a HP LNG supply for the main ME-GI engine and a LP LNG supply for the Auxiliary engine. In the present layout of the heat pump process (HeP) the BOG is not used to feed the Auxiliary engines (F-BOG-AUX stream is dotted). The Tank Reflux system is fed by LP LNG that is subcooled in the TRC. Alternatively it is possible to recirculate compressed BOG in the Tank Reflux system (dotted stream TR-BOG), this option is not covered in this study.

### 3.1.1 Heat pump with dedicated Tank Reflux pump layout

One feature of the process in figure 3.2 is that the same LP Pump is used to feed the Auxiliary engine, the HP Pump, and the Tank Reflux system. This design choice has the advantages that it minimizes the number of cryogenic machinery items and it allows the pump to always operate above the minimum flow specification characteristic of cryogenic pumps (this is related to the fact that the heat leak in the piping and in the pump body might lead to cavitation in the pump if the flow is too low [54]). On the other hand this configuration has one important disadvantage with respect to the efficiency of the process. The LP Pump needs to work with a outlet pressure of 6 bar for the Auxiliary engine feed, but the required inlet pressure to the Tank Reflux system only needs to compensate the pressure drop in the piping, in the TRC heat exchanger and in the tank spray system. A Tank Reflux system pressure higher than required would

increase the specific work of the LP Pump and therefore the enthalpy of the "TR-LNG" stream, yielding to an increased energy input to the tank.

One way to limit this effect is to use a dedicated cryogenic Pump to recirculate the LNG to the tank ("TR-PUMP" in Figure 3.3, with valve "V-LNG-TR" closed) with a lower outlet pressure determined by the pressure drop in the Tank Reflux system, this option needs to be evaluated comparing the expected gain in efficiency and the added complexity and investment cost of the process, as well as possible operational problems related to the minimum flow specifications of the LP Pump.

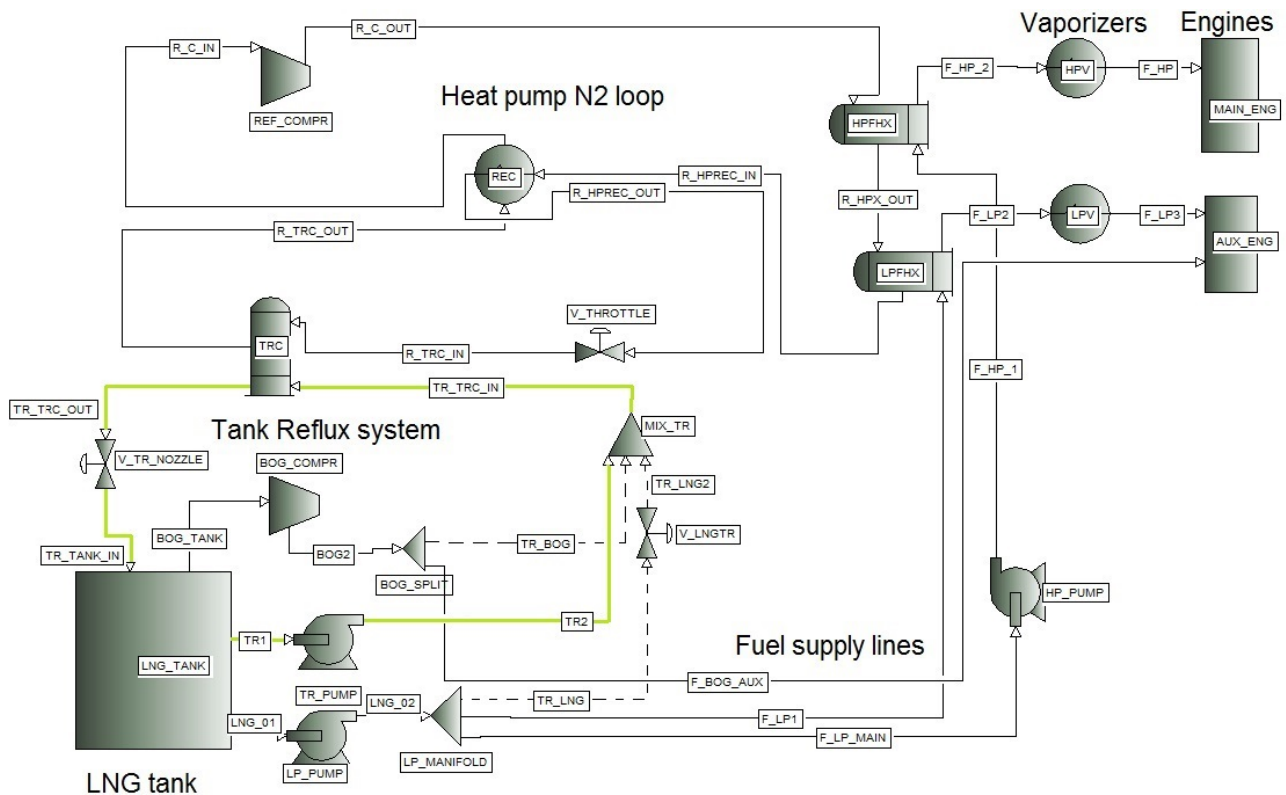


Figure 3.3: PFD: Heat pump process, with TR dedicated Pump

### 3.1.2 Heat pump with BOG fed Auxiliary engine layout (HeP-AUX)

A more relevant change to the layout shown in Figure 3.2 is to remove the LPFHX and use a BOG Compressor to feed the tank BOG to the Auxiliary engines. This alternative will be interesting if the specific energy consumption for compress-

ing the BOG is low compared to the specific energy consumption of the heat pump process. The advantages of this configuration compared to the one previously described are the following:

- the heat exchanger (LPFHX) can be removed, saving one unit;
- the LP Pump now can work with a much lower outlet pressure, within the limitation of the NPSH required by the HP Pump.

Compared to the layout in Figure 3.3 this layout requires less units and the Tank Reflux system allows the LP Pump to fulfill the minimum flow requirements.

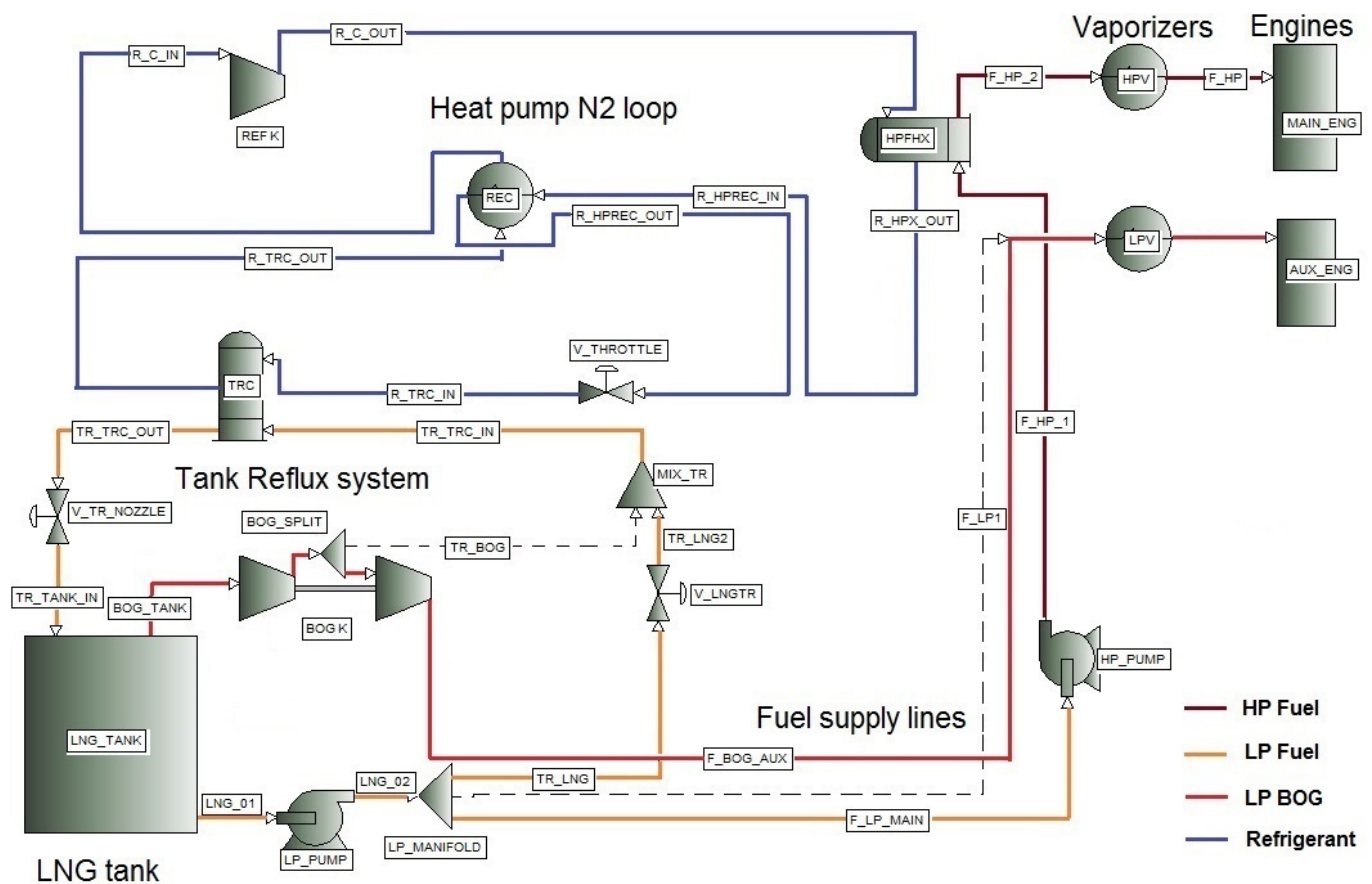


Figure 3.4: PFD: Heat pump process with BOG fuelled AUX engines (HeP-AUX)

In the course of this thesis the heat pump process (indicated as "HeP", in Figure 3.2) and its version with BOG fuelled AUX engines (indicated as "HeP-AUX", in figure 3.4) have been simulated.

## 3.2 Alternatives to the Heat Pump process

For a quantitative comparison a number of other processes mentioned in the literature review have been simulated and compared to the heat pump process. Table 3.1 collects the names of these processes, a simple abbreviation to identify them, and indicates whether each engine is fuelled by liquid or vapor.

Table 3.1: Alternative processes

Name	Tag	Main feed	AUX feed	description
Base	GCU	LNG	LNG	all BOG to GCU
Base +	GCU-AUX	LNG	BOG	only excess BOG to GCU
Heat pump	HeP	LNG	LNG	
Heat pump +	HeP-AUX	LNG	BOG	
HP compressor	HPK	LNG+BOG	BOG	similar to Laby-GI
Terminal type	MIX-AUX	LNG+BOG	BOG	recondenser at 6.3 bar
Reliquefaction	REL	LNG	LNG	estimated from literature
Reliquefaction +	REL-AUX	LNG	BOG	estimated from literature

In any of these cases the Auxiliary engine fuel can either be supplied by the LP LNG pump or by a BOG compressor, in the latter case the "-AUX" acronym is attached to the abbreviation.

As a base case the BOG is burnt in Gas Combustion Units (GCU), the simplest improvement that can be made to this configuration is to compress a part of the BOG to the AUX engine feed pressure wasting only the excess BOG (GCU-AUX). The High Pressure compression process (HPK), inspired by the Laby-GI five stage compressor process for LNG carriers, is illustrated in figure 3.5.

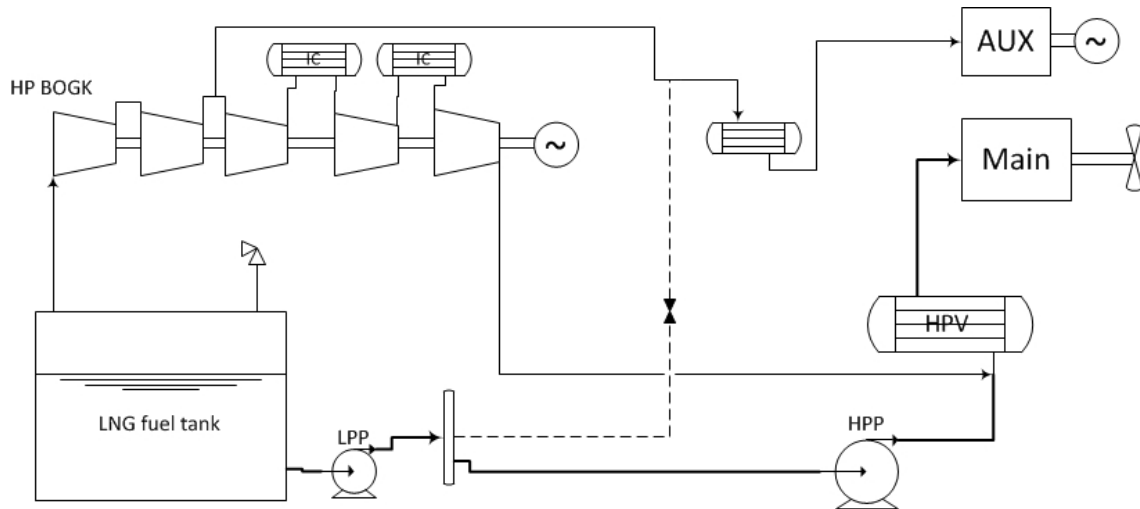


Figure 3.5: HPK process layout with High Pressure BOG Compressor

The process indicated as "MIX-AUX" resembles LNG regasification terminal processes, where LP subcooled LNG is saturated with compressed BOG in a contactor named "Recondenser". The terminal type process illustrated in Figure is similar to the one proposed by Samsung for LNG fuelled vessels (Figure 2.18 from [22]).

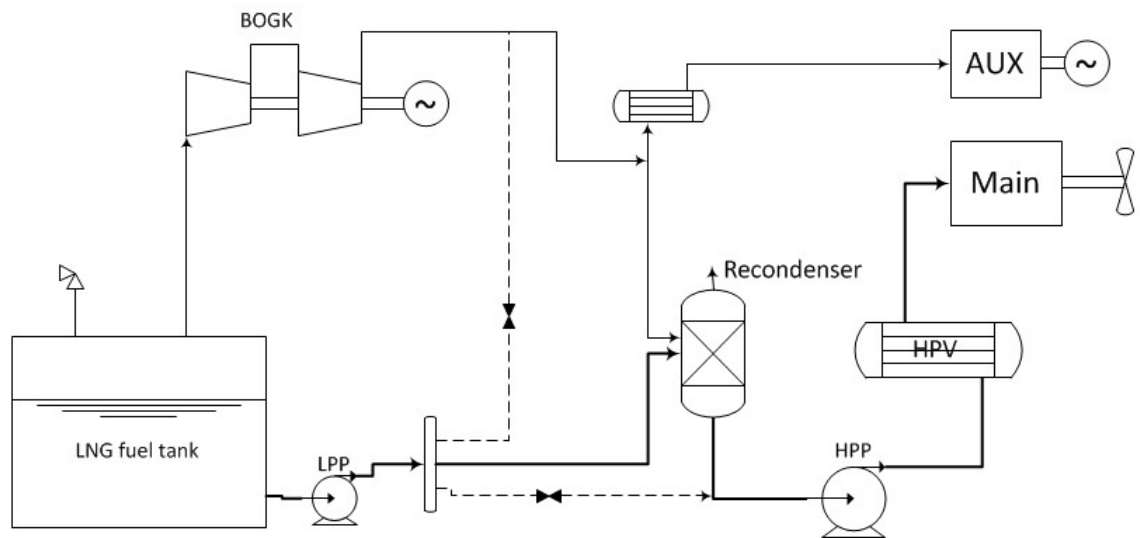


Figure 3.6: MIX-AUX process, or "terminal type"

Liquefaction processes have not been simulated in this thesis, the results have been extrapolated from the literature cited in the previous chapter.

### 3.3 Selection of a reference case

Since the described heat pump process is based on a full integration with different systems of a LNG fuelled vessel, its performance is expected to be dependent on the proportions between those systems. Therefore a particular effort has been dedicated to adopt a realistic and conservative reference case in order to define the boundary conditions for the process.

From the market trends discussed in chapter 2.1.3 it appears that there is a need for new BOG handling systems on medium-large LNG fuelled ships for deep-sea routes that require a fuel tank size larger than 2000-3000 m<sup>3</sup> and spend long time in the Emission Control Areas (ECA). According to these description a generic merchant ships is taken as a reference case, this could correspond to a bulk or chemical carrier, a Ro-Ro vessel or a container vessel.

In order to quantitatively define the reference case, three parameters have been identified as essential to characterize the FGSS and thus set the boundary conditions for the heat pump process, namely:

- the tank volume, used to estimate the average heat leak and set a target for the refrigeration duty;
- the Main engine Power, related to the flowrate of HP fuel in the Fuel Supply system and heat pump heat exchanger (HPFHX);
- the Auxiliary engine Power, related to the flowrate of LP fuel in the Fuel Supply system, and to the possibility of directly consuming the BOG at low pressure.

Taking into account the market trends the company LNT [54] suggests as a base case for the process design and optimization a medium size ship with the following characteristics:

- Tank volume: 2200 m<sup>3</sup>;

- Main engine power during normal voyage: 10.94 MW;
- Aux engine power: 450 kW.

The power of the engines refers to the operation under normal conditions, it is therefore lower than the installed power.

### 3.3.1 Main engine

It is assumed that the ship is propelled by a single ME-GI main engine with power of 10.94 MW. This value refers to the engine power for driving the propeller under normal ship operation, i.e. the condition at which the ship operates most of the time during voyage, engine manufacturers refer to this parameter as "Service Power", or "Normal Continuous Rating" (NCR), or "continuous Service rating for Propulsion" (SP) [55, p.28]. The NCR is lower than the maximum power that the engine can deliver, for example the NCR is usually 85-90% of the Specified Maximum Continuous Rating (SMCR) that represents the owner's requirement for the continuous operation of the engine. The SMCR has to be lower or equal to the Nominal Maximum Continuous Rating (NMCR) that is a characteristic of the engine corresponding to the mean effective pressure and engine speed limits in the layout diagram [55, p.29].

In order to perform a correct selection of the Main engine and thereby accurately calculate the fuel consumption, the present section refers to studies conducted by technology suppliers, and catalogues by the engine manufacturer MAN Diesel&Turbo.

The company Samsung Heavy Industries conducted a comparative study of different types of shipping gas engines [13] for A-max (Aframax [56]) oil tankers propulsion, using the ME-GI engine model 6S60ME-GI8.2 [13, p.30], with a NCR of 10,860 kW. This engine corresponds to 6S60ME-C8-GI in the most recent catalogue [35, p.53] in figure A.4. According to the MAN designation in figure A.3 this is a 6 cylinders Super long stroke, 60 cm diameter cylinder, Electronically controlled, Compact, Gas Injected engine.

A second study on different fuel gas supply system for LNG carriers has been carried out by MAN Diesel&Turbo for smaller size 5 cylinders engine 5S60ME-C82-GI [14], with a SMCR of 10,000 kW at 105rpm, operating at a NCR equal to 81% of the SMCR. This engine is more similar to the new model 5S60ME-C8-GI in figure A.4 in the appendix. In this thesis, with reference to the similar examples reported above, the 6 cylinders 6S60ME-C8-GI engine was selected to supply the NCR of 10,940 kW. As described in table 3.2 the SMCR is a fraction of the NMCR, here 85% [57, p.66], also the NCR is 91% of the SMCR and 77% of the NMCR, which gives a Specific Fuel Consumption (SFC) of about 133.1 g/kWh of gas fuel extracted from the datasheet in figure A.4. This fuel consumption for the design fuel LHV in table 4.5, taking into account the pilot fuel, gives a thermal efficiency of the engine of 53%.

Table 3.2: Main engine features

Engine	6S60ME-C8-GI	
NMCR ("L1")	14280	kW
SMCR ("M")	12070	kW
NCR ("S")	10940	kW
SFC (NG)	0,133	kg/kWh
SFC (pilot)	0,006	kg/kWh
mass flow (NG)	0,404	kg/s
thermal efficiency	53	%

### 3.3.2 Auxiliary engines

Usually 2 or 3 Auxiliary engines are installed on merchant or container vessels for the so called "hotel" consumption, port operations, and other utilities power requirement [7]. The Auxiliary engines' load during normal operation is expected to be modest, and their fuel consumption is also negligible if compared to the main engine's. For this study a Auxiliary engines' power of about 450 kW is chosen as a design value for the normal operation of the ship [54] [14] (Table B.3). It is assumed that the Auxiliary engines are Dual Fuel 4-strokes engines,



fuelled by natural gas at about 6 bara, with injection of Diesel pilot fuel for ignition. The Specific Fuel Consumption for the set of Auxiliary engines is expected to be higher than for the main engine, as they are based on the ignition of a premixed charge. Here a SFC of 0.16 kg/kWh is used to calculate the Auxiliary engine fuel flowrate in table 3.3, [7].

Table 3.3: Auxiliary engines lumped features

Number of Engines	2 - 4	-
Power Installed	2500-3500	kW
Normal Power	450	kW
SFC (NG)	0,160	kg/kWh
SFC (pilot)	0,005	kg/kWh
mass flow (NG)	0,020	kg/s
thermal efficiency	44	%

### 3.3.3 Heat leak calculations

The amount of BOG produced in a on board LNG tank during voyage depends on a number of factors, the most relevant are the tank type, size and geometry, the insulation material and thickness Secondly also liquid level, ambient temperature and sea state have an influence [27, 34]. An averaged parameter to quantify the production of BOG is the Boil Off Rate (BOR), defined as the percentage of the total LNG volume evaporating daily. From the data found in the literature it is estimated that the BOR for this size of atmospheric tanks varies between 0.18%/day [54, 19] and 0.4%/day [13, 26].

Figure 3.7 shows BOR values for vacuum insulated Type C tanks, and atmospheric Polyurethane insulated tanks of the same size, as a function of insulation thickness.

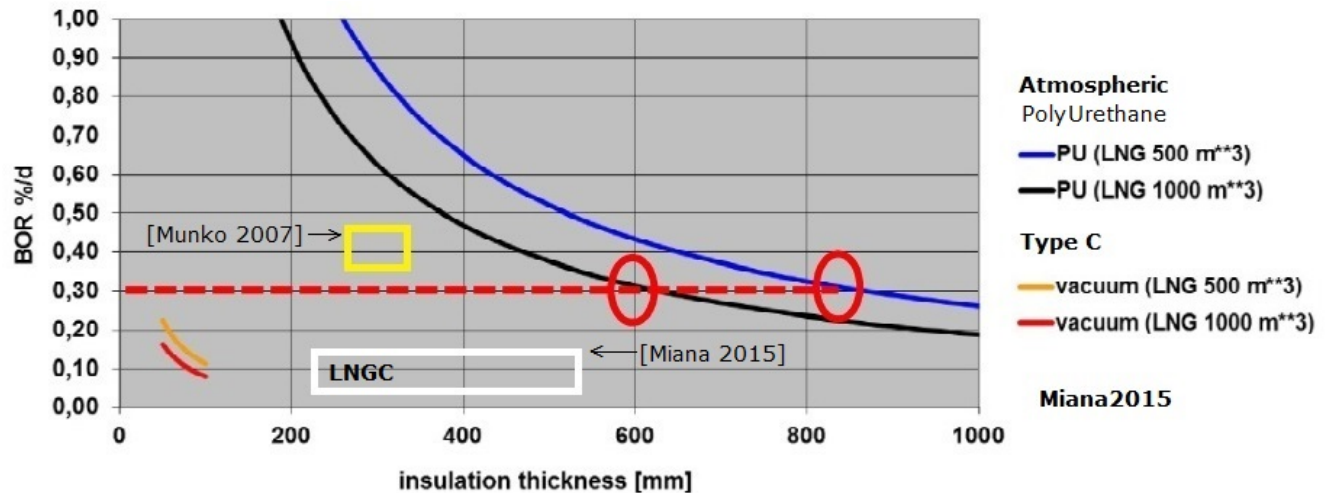


Figure 3.7: BOR as a function of insulation thickness, tank type and size [25], integrated with data from literature [26, 27]

At constant insulation thickness the BOR decreases with the tank volume, due to the increasing ratio between volume of fluid and heat transfer area. Taking into account the typical BOR values from the literature and that a 2200 m<sup>3</sup> tank is much smaller than a typical LNG Carrier cargo tank, a BOR value of 0.325 %/day is assumed in the course of this thesis. Based on this value, the mass flow of BOG and the corresponding refrigeration effect required are estimated as detailed in Table 3.4.

Table 3.4: Calculation of Heat leak for two different scenarios

	HeP	HeP-AUX	UOM
Fuel tank size	2200	2200	m <sup>3</sup>
BOR	0.325	0.325	%/day
mass flow (BOG)	0.0359	0.0359	kg/s
BOG to AUX	0	0.0200	kg/s
Excess BOG	0.0359	0.0159	kg/s
Q ref required	18.6	8.2	kW

A conservative estimate of the BOG evaporation rate can be obtained by multiplying the BOR with the volume of LNG corresponding to the 95% filled tank, using a density of 457 kg/m<sup>3</sup> calculated with HYSYS for the given composition, as in equation 3.1.

$$\dot{m}_{\text{BOG}} = \frac{\rho_{\text{LNG}} \cdot (V_{\text{tank}} \cdot 95\%) \cdot \text{BOR}}{24 \cdot 3600 \cdot 100} \quad (3.1)$$

Assuming that all the heat that leaks into the tank is only absorbed by the phase change of the LNG, the heat leak can be estimated by equation 3.2 [58, p.126]. The evaporation enthalpy of 527.1 kJ/kg is an output of the HYSYS reports for the BOG stream at tank pressure.

$$Q_{\text{leak}} = \dot{m}_{\text{BOG}} \cdot \Delta h_{\text{LNG, ev}} \quad (3.2)$$

The goal of the Heat Pump process (HeP) is to supply a refrigeration effect that compensates the estimated heat leak

$$Q_{\text{ref}}^{\text{HeP}} = Q_{\text{leak}} = 18.6 \text{ kW} \quad (3.3)$$

In case that part of the BOG is compressed for the Auxiliary engine consumption the Heat Pump process (HeP-AUX) needs to cover only a part of the heat leak that corresponds to the excess BOG

$$Q_{\text{ref}}^{\text{HeP-AUX}} = (\dot{m}_{\text{BOG}} - \dot{m}_{\text{AUX}}) \cdot \Delta h_{\text{LNG, ev}} = 8.2 \text{ kW} \quad (3.4)$$

### 3.4 Refrigerant

The only refrigerant fluid used in the present thesis is pure Nitrogen, the reasons for this choice are:

- Nitrogen changes phase at temperatures that are near to the LNG tank temperature (Figure 3.8);
- Nitrogen is safe, non-flammable, non-polluting, cheap and available, and already used as inerting fluid in on-board LNG processes.

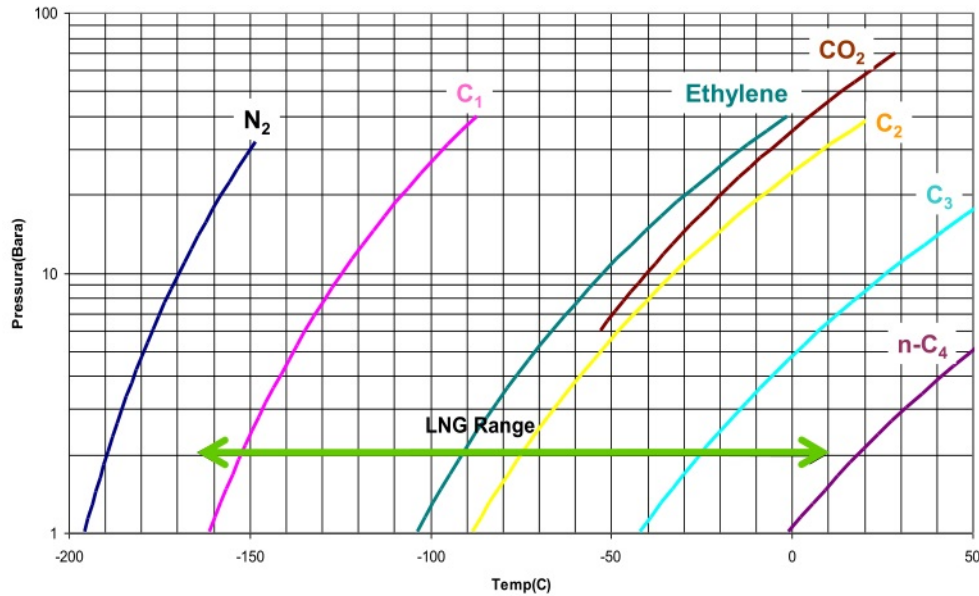


Figure 3.8: Vapor pressure of pure fluids relevant for LNG processes [28]

Other refrigerants could have been considered, in particular Methane and mixtures of Nitrogen and Methane, that in principle could be produced onboard mixing Nitrogen with light tank BOG. However introducing flammable components in the refrigerant mixture would require many additional safety measures (e.g. double wall ventilated piping, gas dangerous designation for valves, flanges, etc...) and increase the plant complexity and cost. This can be acceptable on a LNG Carrier where gas handling systems already exist and the personnel is trained to operate them, but it is not desirable when it comes to merchant ships [54]. For this reasons these options were not investigated in this thesis.

# Chapter 4

## Computer simulations

This chapter presents the structure and the results of a HYSYS® Steady State model that was built to simulate the performance of the process described in the main Process Flow Diagram in Figure 3.2. The commercial software HYSYS® version 8.3 provided by Aspen has been used, linked to the Aspen Simulation Workbook v8.2® . Results have been extracted in form of text reports and case studies and postprocessed with Excel® and Matlab® to generate plots and tables.

The same HYSYS model was used to simulate the system operation in different scenarios, this model is referred to as "Design" model because it is used to quantitatively define the main equipment characteristics for the design of the process. General equipment performance parameters were specified as inputs of the Design model, examples of these are Minimum Internal Temperature Approach (MITA) specifications or constraints for the heat exchangers and constant efficiencies of the rotating machinery.

Other parameters related to the size of the equipment (e.g. heat exchanger UA value and flowrates, compressor and pump pressures and flowrates) are outputs of the Design model.

## 4.1 Heat Pump Model flowsheet

Figure 4.1 shows the HYSYS® model complete flowsheet, that includes the heat pump loop, the FGSS and the Tank Reflux system, arranged in a similar layout as in the main PFD in Figure 3.2. The engines are not included in the model, but rather define the boundary conditions to the FGSS. The Streams and Unit Operations correspond mostly to actual process piping and equipment, in addition to those the flowsheet contains Adjust and Set operators (green) to manipulate the process variables and Spreadsheet operators to perform calculations. This model can simulate different configurations of pure Nitrogen refrigerant processes activating or deactivating the optional streams or pieces of equipment (Intercooler IC, REC, Expander, BOG Tank Reflux) by changing specifications or stream connections. A number of virtual Tees and Mixers (white) are used to split the connection between two consecutive unit operations in order to provide flexibility for editing the model and also to attribute simple and logical names to the streams in relation to the equipment they flow in or out of.



### 4.1.1 LNG fuel tank model

The model includes a simple steady state model of the LNG fuel tank, shown in the orange box in Figure 4.2. The function of this part of the flowsheet is not to simulate the real thermodynamics of the cryogenic tank, which is out of the scope of the thesis, but merely to provide accurate boundary conditions for the FGSS and for the Tank Reflux system. In other words the tank model is a calculation tool to define the thermodynamic properties of the streams "LNG1" and "BOG1" that are respectively the suction of the LNG LP pump and the suction of the BOG compressor.

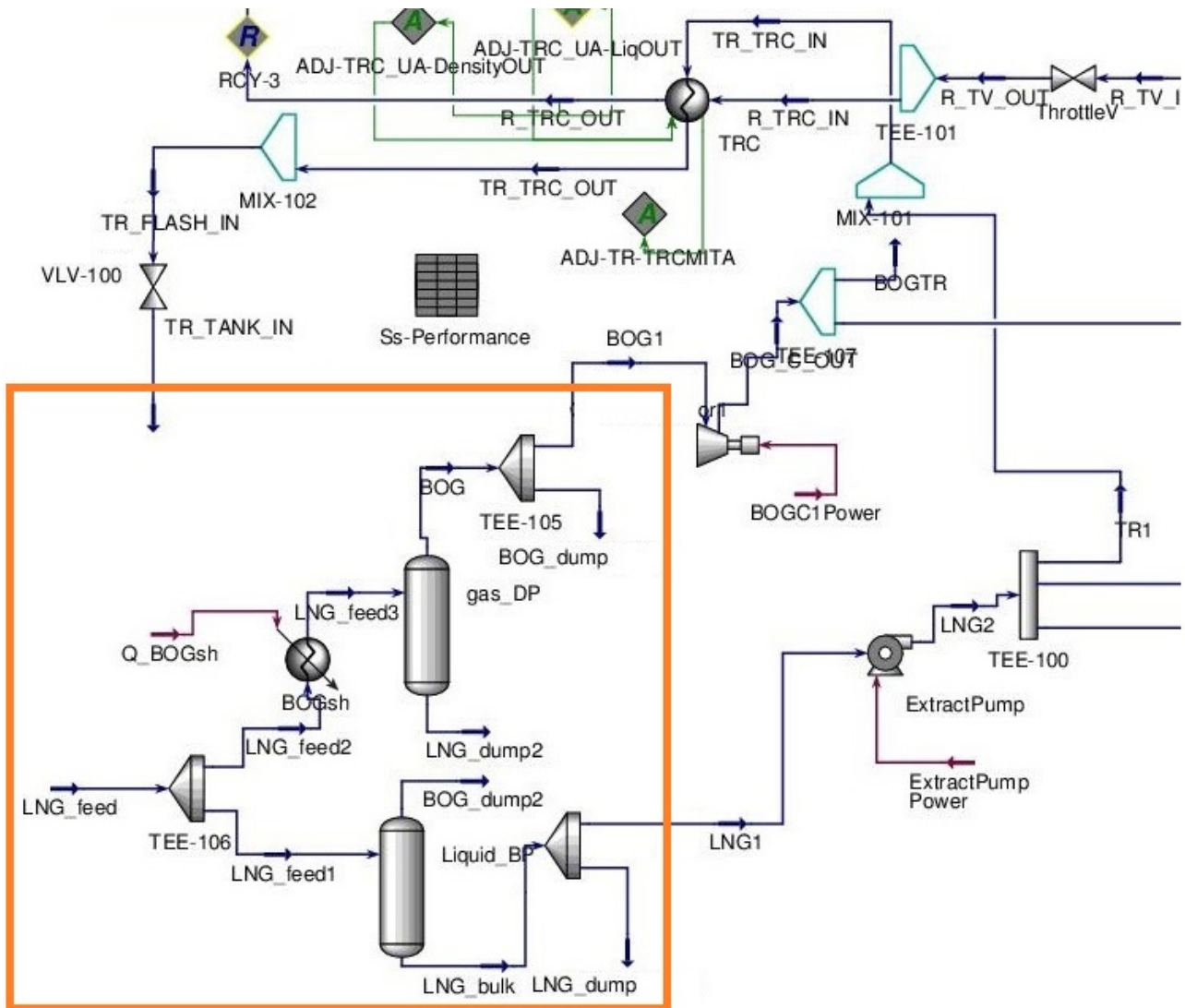


Figure 4.2: Hysys tank model PFD



In this model the LNG composition is defined in the stream "LNG-feed" which feeds the whole fuel system, here also the pressure and temperature of the bulk liquid in the tank are specified. Part of this stream is directed to the separator "Liquid-BP" where saturated LNG liquid is separated and extracted with a specified flowrate defined by the inputs to the simulation. A second fraction of the "LNG-feed" stream is superheated to a slightly higher temperature corresponding to the tank atmosphere (BOG) temperature in equilibrium with a thin liquid layer on the gas liquid interface [29]. It is possible to set the superheat of the BOG to zero in the "BOGsh" specifications, if the BOG is assumed to be in thermal equilibrium with the bulk liquid. The two phases of the superheated stream are also separated and a specified amount of BOG is extracted from the gas phase.

This model gives different compositions for the LNG and BOG that are extracted from the tank, as can be seen in table 4.1 and in the phase envelopes in figure 4.3, it is possible to tune the "LNG-feed" composition and temperature and the degree of BOG superheat to get realistic values of the bulk LNG and BOG composition and temperature. In this case the compositions and phase envelopes of the "LNG-feed" and "LNG1" streams are identical because the "LNG-feed" stream is saturated at the specified conditions.

Table 4.1: LNG and BOG composition at 1.04 bara

Mole %	LNG -feed	LNG -161.5°C	BOG -160°C
N2	0,22	0,22	0,81
C1	91,21	91,21	99,17
C2	5,95	5,95	0,02
C3	1,95	1,95	0,00
n-C4	0,33	0,33	0,00
i-C4	0,33	0,33	0,00
C5	0,01	0,01	0,00

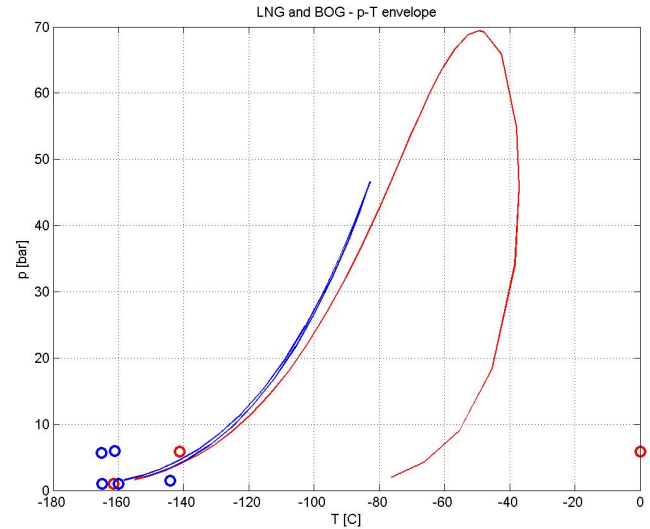


Figure 4.3: Fuel phase envelopes from HYSYS in the pressure-temperature diagram, LNG (red) and BOG (blue)

## 4.2 Heat pump model structure

It has been observed that, even though the model flowsheet does not count a very large number of components, the tight integration between the various parts of the process can increase the calculation effort and undermine the model convergence, in particular in the circumstances where logical operators (like "Adjust" and "Recycle" [59]) compete with each other or with equipment specifications. In this section the term "Adjust" indicates a logical operator that varies one process variable to fulfill a specification that is to equalize a second variable to a target value, the "Recycle" instead is a non-sequential iterative operator that matches two consecutive streams and is used to resolve closed loops [59].

In order to solve convergence problems a considerable effort has been dedicated to achieving an effective placement of logical operators and a correct definition of constraints and specification. It was found that forcing a sequential solution of the flowsheet (ie. solving the flowsheet in the direction of the flow, from upstream to downstream) gives more stable and convergent model, to achieve

this the heat pump loop was solved following the logical sequence described in Figure 4.4.

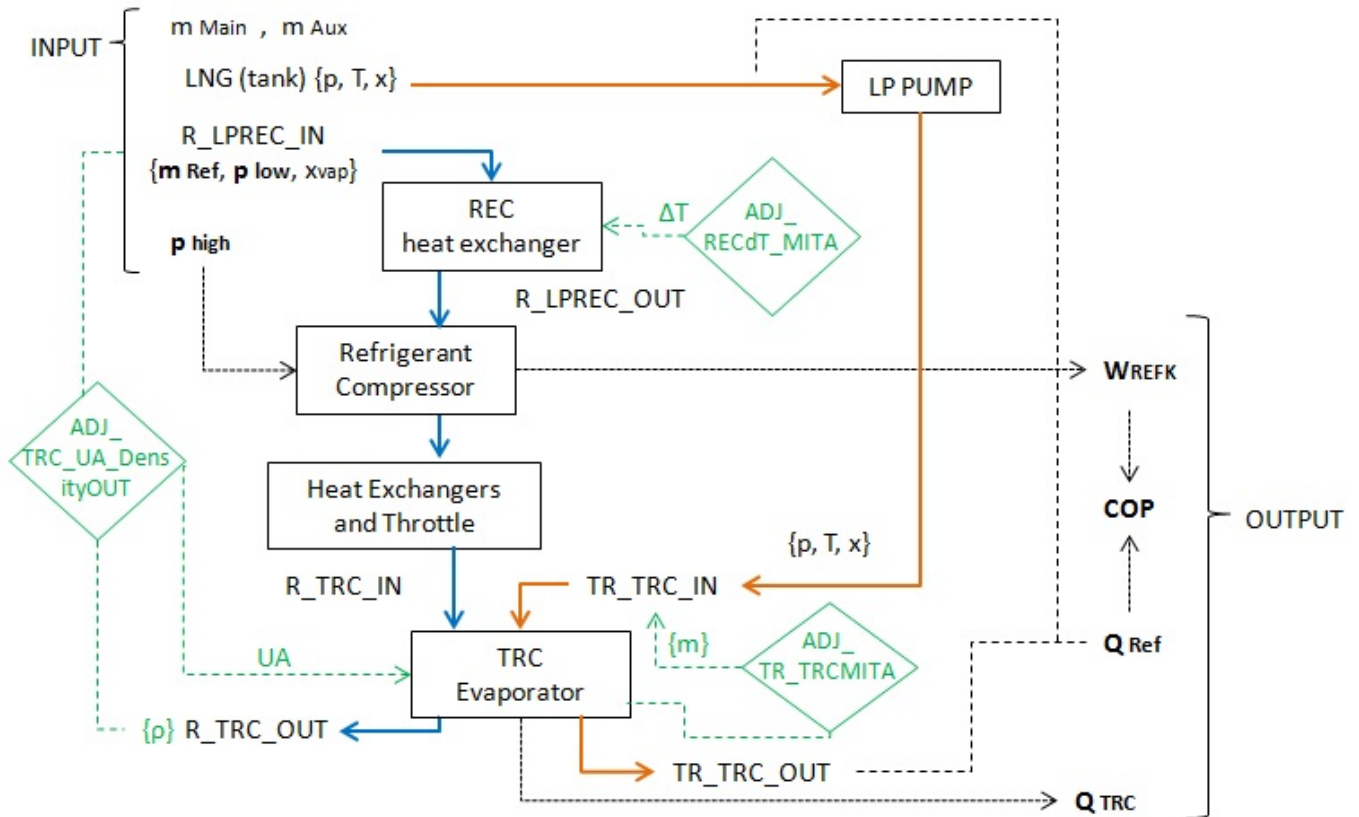


Figure 4.4: Hysys model computational sequence

The computational sequence takes as inputs the fuel consumption of the engines, and the three main variables that define the heat pump cycle, namely low pressure, high pressure and mass flowrate of the refrigerant. The cooling duty of the evaporator, and the net refrigeration duty are outputs of the model. The heat pump pressures and flowrate are tuned such that the net refrigeration duty equals the estimated heat leak. The computational sequence can be described in the following steps:

- Fully define the heat pump loop feed stream "R-LPREC-IN": composition, pressure, vapor fraction (or superheat), flowrate;
- Adjust the REC Low Pressure side temperature increase to match the REC MITA ("AJD-RECdT-MITA");

- Input the heat pump high pressure value (Refrigerant Compressor outlet pressure);
- Calculate the throttle valve pressure drop to compensate compressors and heat exchangers pressure differences;
- Adjust the LNG reflux ("TR-LNG") flowrate to match TRC MITA ("ADJ-TR-TRCMITA");
- Adjust the TRC heat exchanger UA value so that its outlet matches the loop feed stream ("ADJ-TRC-UA-DensityOUT");
- Thanks to the previous operation the loop is consistent and the Recycle operator ("RCY-3") is not necessary.

The input parameters of the Adjust operators are shown in tables 4.2 and 4.3 for the Case Study and for the Sensitivity Analysis respectively, more relaxed tolerances on the MITA were adopted in the Case Studies to enhance the convergence of the model, the tolerance on the density of the TRC outlet heat pump stream was not relaxed because this operator determines the convergence of the energy balance of the system.

Table 4.2: Adjust settings for Case Studies

Name	Control Variable	Min	Max	Step	Specification	Value	Tolerance
ADJ-TR-TRCMITA	TR mass flow [kg/s]	1	9	0.3	TRC MITA [C]	9	4
ADJ-RECdT-MITA	REC LP side $\Delta T$ [C]	5	60	4	REC MITA [C]	6	1
ADJ-TRC-UA-DensityOUT	TRC UA [MJ/C-h]	1.5	70	1	density [kg/m <sup>3</sup> ]	feed	0.1

Table 4.3: Adjust settings for Sensitivity Analysis

Name	Control Variable	Min	Max	Step	Specification	Value	Tolerance
ADJ-TR-TRCMITA	TR mass flow [kg/s]	1	9	0.3	TRC MITA [C]	5.5	0.5
ADJ-RECdT-MITA	REC LP side $\Delta T$ [C]	5	60	4	REC MITA [C]	5.2	0.2
ADJ-TRC-UA-DensityOUT	TRC UA [MJ/C-h]	1.5	70	1	density [kg/m <sup>3</sup> ]	feed	0.1

### 4.3 Inputs to the Heat Pump Model

This chapter lists the assumptions and the numerical inputs to the HYSYS Heat Pump (HeP) model. The Equation Of State used in all the simulations is the cubic Peng Robinson, which is a reasonable choice for non-polar hydrocarbon mixtures [60], [61, p.51]. The LNG composition was calculated from a database of compositions from different production plants in the world (Table 4.4), the average adjusted composition that was used in this study is reported in Table 4.5, where Butane is split between Normal and Iso Butane. As previously shown in Table 4.1 this composition was specified in the virtual feed stream "LNG-feed" in the fuel tank model.

Table 4.4: Typical LNG Composition form major export terminals, in Volume % [4, p.6]

Plant	Country	C <sub>1</sub>	C <sub>2</sub>	C <sub>3</sub>	C <sub>4</sub>	C <sub>5+</sub>	N <sub>2</sub>	LHV (MJ/kg)	Methane N (-)
Arzew	(ALG)	87.4	8.6	2.4	0.05	0.02	0.35	49.11	72.7
Bintulu	(MAS)	91.23	4.3	2.95	1.4	0	0.12	49.35	70.4
Bonny	(NGR)	90.4	5.2	2.8	1.5	0.02	0.07	49.35	69.5
Das	(UAE)	84.83	13.39	1.34	0.28	0	0.17	49.26	71.2
Badak	(INA)	91.09	5.51	2.48	0.88	0	0.03	49.48	72.9
Kenai	(USA)	99.8	0.1	0	0.1	0	0.1	50.02	98.2
Lumut	(BRU)	89.4	6.3	2.8	1.3	0.05	0.05	49.36	69.5
Point	(TRI)	96.2	3.26	0.42	0.07	0.01	0.01	49.91	87.4
Ras	(QAT)	90.1	6.47	2.27	0.6	0.03	0.25	49.32	73.8
Skikda	(ALG)	91.5	5.64	1.5	0.5	0.01	0.85	48.97	77.3
Withnell	(AUS)	89.02	7.33	2.56	1.03	0	0.06	49.36	70.6
Snohvit	(NOR)	91.9	5.3	1.9	0.2	0	0.6	49.20	78.3
Average	-	91.07	5.95	1.95	0.66	0.01	0.22	49.39	75.98

Table 4.5: LNG composition for the Heat Pump (HeP) model, properties calculated with HYSYS at the reference tank conditions -161.5°C, 1.04 bara.

Property	Value	UOM
N <sub>2</sub>	0,22	mole%
C <sub>1</sub>	91,21	
C <sub>2</sub>	5,95	
C <sub>3</sub>	1,95	
n-C <sub>4</sub>	0,33	
i-C <sub>4</sub>	0,33	
C <sub>5</sub>	0,01	
LHV	49,33	MJ/kg
density	456,3	kg/m <sup>3</sup>

The specifications for the process equipment, modeled by HYSYS Unit Operations, are listed in Table 4.6.

Table 4.6: Unit Operations inputs to the Heat Pump (HeP) model

Unit Operation	Tag	Property	Value	UOM
LP Pump	LPP	efficiency	75	%
HP Pump	HPP	efficiency	65	%
Refrigerant Compressor	REFK	polytropic efficiency	75	%
BOG Compressor	BOGK	polytropic efficiency	75	%
All HXs		MITA	5	°C
All HXs		pressure drop	0.3	bar
HX: LPFHX	LPFHX	pressure drop	0.1	bar
HX: evaporator	TRC	outlet liquid fraction	10	%

The first part of the table reports the efficiencies of the rotating machinery, the second part describes the specifications of the process Heat Exchangers (HXs). The Minimum Internal Temperature Approach (MITA) of all the process heat exchangers is set to be 5°C, this is a conservative value for a cryogenic process where pinch temperature differences can be as low as 1-3°C [62, p.215], [63]. A constant pressure drop of 30 kPa (0.3 bar) was attributed to all heat exchangers, except for the LPFHX that was assumed to be smaller. All process components have been considered adiabatic and the heat leak neglected. Finally the liquid fraction of the low pressure evaporating Nitrogen stream ("R-TRC-OUT")

at the outlet of the TRC heat exchanger was specified with an arbitrary value of 10%, this value together with the pressure and flowrate fully defines the stream properties, therefore this can be considered the anchor point of the thermodynamic cycle.

Table 4.7 reports the input properties of some process streams that represent the boundary conditions to the model, since the heat pump cycle is only integrated with the FGSS and with the Tank Reflux System, the only boundary conditions are the LNG fuel tank conditions and the ship engines' feed requirements.

Table 4.7: Stream input properties for the Heat Pump (HeP) model

Stream	Property	Value	UOM
LNG (fuel tank)	Temperature	-161,5	°C
LNG (fuel tank)	pressure	1,04	bar
BOG (fuel tank)	Temperature	-160	°C
LP Fuel (AUX)	pressure	6	bar
HP Fuel (MAIN)	pressure	300	bar
Fuel (MAIN+AUX)	Temperature	45	°C

The tank is assumed to be slightly above atmospheric pressure, and the BOG almost in thermal equilibrium with the bulk LNG, a similar situation can be expected if the recirculated subcooled LNG is sprayed in the tank top. If instead the liquid was injected below the free surface the temperature difference between the two phases would be larger. Typical values for the BOG atmosphere temperature are  $-160^{\circ}\text{C}$  to  $-140^{\circ}\text{C}$  for large LNG carriers cargo tanks [3, p.128] and up to  $-100^{\circ}\text{C}$  for LNG terminals [64, 65, 10]. With respect to the heat pump process the BOG temperature is not a variable of influence, since only liquid is recirculated to the tank. In case the BOG is fed to the AUX engine this variable can affect the operation and the energy consumption of the compressor.

Regarding the engine feed, the pressure and temperature correspond to the specifications of ME-GI engines and 4-stroke dual fuel generators discussed in the previous chapters.

## 4.4 Inputs to other models

The inputs for the other models described in chapter 3.2 are the same as for the Heat Pump model with a few exceptions listed in the following Table.

Table 4.8: Inputs to simulations for alternative processes

Unit Operation	Property	HeP	HeP-AUX	MIX-AUX	HPK	UOM
BOG Compressor	suction Temperature	-160	-160	-140	-140	°C
BOG Compressor	outlet pressure	-	6.3	6.3	300.3	bar
HP Pump	Min subcooling at inlet	high	sufficient	5	high	°C
LP Pump	outlet pressure	6	2	6.3	6.3	°C

The BOG compressor suction temperature is assumed to be higher for the MIX-AUX and HPK process because, contrary to the Heat Pump, in these configurations no fluid is recirculated in the tank, therefore a certain degree of superheat in the tank atmosphere can be expected.

As already discussed, in the HeP-AUX scenario the LP Pump does not need to match the AUX engine injection pressure, therefore a lower value, such as 2 bar, can be enough to win the pressure drop in the evaporator (TRC) and spray system and provide a sufficient NPSH for the HP Pump.

Thanks to the LP Pump the HP Pump does not risk cavitation, except in the MIX-AUX case where the liquid can approach saturation in the "Recondenser". In this case a minimum specified subcooling at HP Pump suction of 5°C has been specified.

## 4.5 Heat Pump Model Simulation Results (HeP)

As already mentioned the results presented in this chapter have been obtained with a Design model. Modeling the Off-Design operation of the process is outside the scope of this thesis.

However it can be expected that the Off-Design conditions of the process, such



as part load of the main engine, could be relevant not only to assess the performance, but also to define the size and specifications of some process components. In particular the maximum pressure of the cycle and therefore the compressor type and specifications, as well as the heat transfer area of the heat exchangers crossed by the fuel flow are expected to increase at part load of the main engine. This means that if these components were dimensioned based on the Design conditions only, they might be insufficient to comply with part load operation. For this reason the Design model was used not only to simulate the process at design conditions but also to estimate the process variables at part load of the main engine, in order to better assess the components characteristics. It should be clear to the reader that the results of the scenarios different from the normal operation scenario do not represent the operation of the same physical system at reduced load, but rather generate a new design, fit to the new operating conditions.

In this chapter the Design model results are reported for four different scenarios: normal operation of the Main engine (HeP-100%NCR), part load operation (HeP-50%NCR and HeP-20%NCR) and idle or harbour operation with zero gas flowrate to the Main engine (HeP-0%NCR-100%AUX), as shown in Table 4.9.

Table 4.9: Design cases for the heat pump process (HeP)

Case tag	MAIN % NCR	MAIN Power [kW]	MAIN m Fuel [kg/s]	AUX m Fuel [kg/s]
A-100%NCR	100%	10940	0.404	0.02
A-50%NCR	50%	~5470	0.202	0.02
A-20%NCR	20%	~2188	0.081	0.02
A-0%NCR-100%aux	0%	0	0.000	0.02

In the four scenarios the power of the AUX engine is held constant to 450kW, while the power of the main engine is scaled down to zero. The part load cases refer to a main engine gas fuel flowrate that is respectively 50% and 20% of the value at normal operation (100% Normal Continuous Rating). Assuming a con-

stant SFC the power of the engine can be estimated proportionally with an error of about 5% for ME-GI engines [35].

#### 4.5.1 Normal operation scenario: HeP - 100% NCR

After setting the fuel flowrates to the engines as boundary conditions, the heat pump is tuned to hit a refrigeration duty of 18.6kW in order to compensate the total heat leak. The transcritical cycle is defined by three variables:

- the evaporation pressure;
- the high pressure (or compressor outlet pressure);
- the refrigerant flowrate.

In this study the evaporation pressure is kept constant to 9 bara (8.7 bara compressor suction) and the effect of its variation is assessed in the Sensitivity Analyses.

If the refrigeration duty is given, then the two other variables are related and only one variable is left for the optimization.

Figure 4.5 shows the main outputs of the simulations for the normal operation scenario (100%NCR) with varying high pressure and mass flow of the refrigerant. The figure is generated from Hysys Case Study tables postprocessed with Matlab. Since the evaporation pressure is kept constant the compressor outlet pressure on the vertical axis is directly related to its pressure ratio.

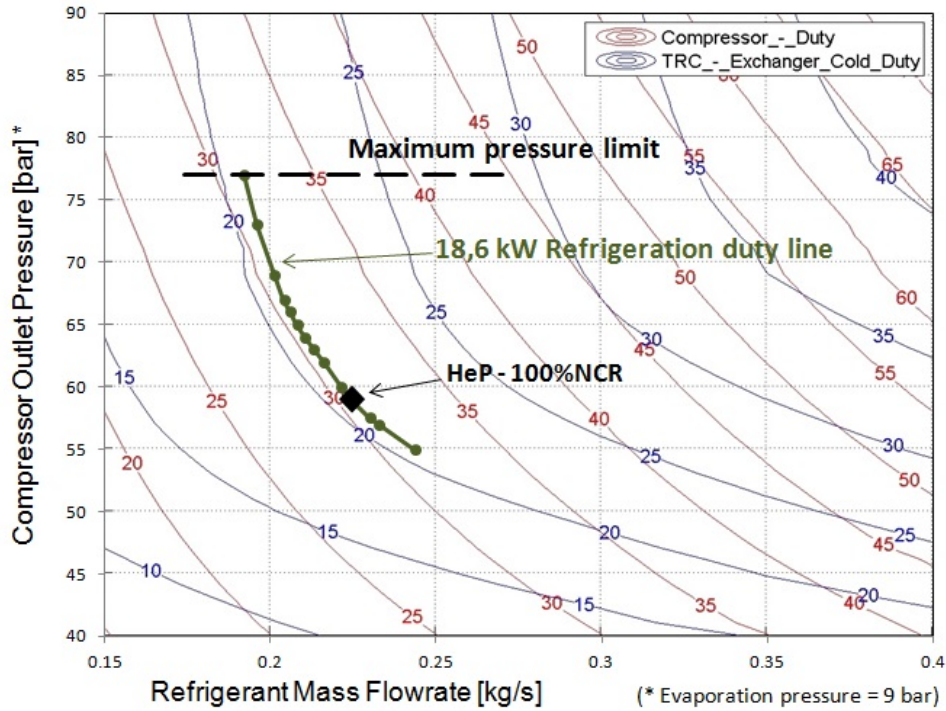


Figure 4.5: HeP-100%NCR: Performance map

The contour lines on the map indicate the refrigerant compressor's work, the duty of the evaporator (TRC heat exchanger) and the effective refrigeration duty. The refrigeration duty  $\dot{Q}_{\text{Ref}}$  is the net cooling effect seen by the tank as a result of the recirculation of the subcooled stream (TR). It is calculated with the equation

$$\dot{Q}_{\text{Ref}} = \dot{m}_{\text{TR}} \cdot (h_{\text{LNG}} - h_{\text{TR\_TANK\_IN}}) = \dot{m}_{\text{TR}} \cdot (\Delta h_{\text{TRC}} - \Delta h_{\text{LPP}}) \quad (4.1)$$

this value is slightly lower than the TRC evaporator duty due to the LP Pump (LPP) work input to the recirculation stream (TR-LNG). The green line in the Figure is the locus of simulated points where the refrigeration duty is equal to the specified value of the heat leak of 18.6 kW.

The compressor work contour lines evidence a minimum power requirement in the range 55-75 bar, for the specified refrigeration duty. Since the pure Nitrogen refrigerant's critical pressure equals 33.96 bar a cycle designed with such high pressure constitutes a transcritical heat pump.

The dotted line represents an arbitrary limit on the high pressure of the cycle

set to 77 bar, that could correspond to an hypothetical structural requirement for the compressor, the heat exchangers and the piping.

The performance of the system on the green contour line is detailed in Figure 4.6 as a function of the compressor outlet pressure only.

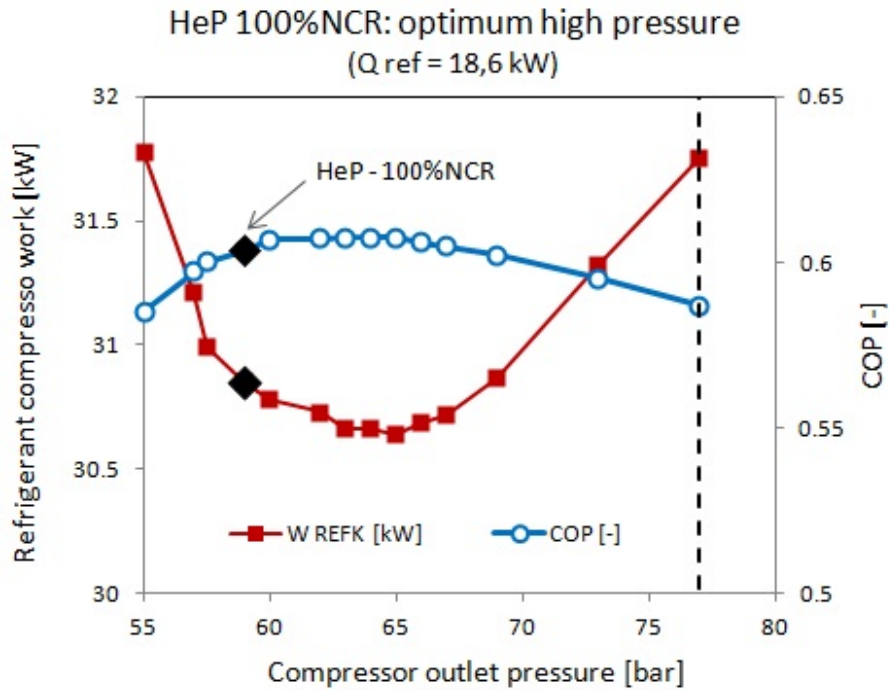


Figure 4.6: HeP-100%NCR: Optimum compressor outlet pressure

The COP is obtained dividing the refrigeration duty by the refrigerant compressor (REFK) work

$$\text{COP} = \frac{\dot{Q}_{\text{Ref}}}{\dot{W}_{\text{REFK}}} \quad (4.2)$$

The Figure shows that there exists an optimum for the compressor outlet pressure to supply the specified refrigeration duty. The same behaviour has been extensively studied for CO<sub>2</sub> transcritical heat pumps in a number of studies [66, 67, 68, 69] which proved that the shape of the isotherms and of the compression path determine the existence of a optimum pressure for heat rejection in the supercritical region.

The near optimum operation point HeP-100%NCR has been selected as Design

case for the normal operation scenario. This point is identified with a square in the previous Figures, and its main system parameters are reported in the following Table 4.10 and in Figures 4.7 to 4.3.

Table 4.10: HeP-100%NCR: Process Equipment mass and energy balance

Equipment	Duty [kW]	m Ref [kg/s]	m Fuel [kg/s]	LP [bara]	HP [bara]
LP Pump	2.93		2.02	1.04	6.00
HP Pump	40.17		0.40	6.00	300.90
Ref Compr	30.85	0.22		8.70	59.00
Total Work	73.95				
HPFHX	50.46	0.22	0.40	59.00	300.60
LPFHX	1.29	0.22	0.02	6.00	58.70
REC	11.32	0.22		9.00	58.60
TRC	20.94	0.22	1.60	6.00	9.30
Cooling Duty	18.62				
COP	0.60				

Figure 4.7 shows the heat pump cycles in the Temperature-Duty diagram, where duty is calculated multiplying the refrigerant's enthalpy and mass flowrate. In this diagram the nitrogen cycle shape is the same as in a Temperature-Enthalpy diagram, stretched on the horizontal axis. The red curves refer to the LNG tank, fuel streams and recirculation stream for the heat pump heat exchangers, each LNG curve is shifted along the horizontal axis to be aligned with the correspondent refrigerant curve so that the plot can be read also as a heat release curve plot for each heat exchanger. The advantage of this choice of thermodynamic variables is that a single diagram can be used to visualize the heat transfer profiles and the absolute value of the heat transferred by all heat exchangers, together with the shape of the cycle in relation to the refrigerant saturation curve [28, p.20].

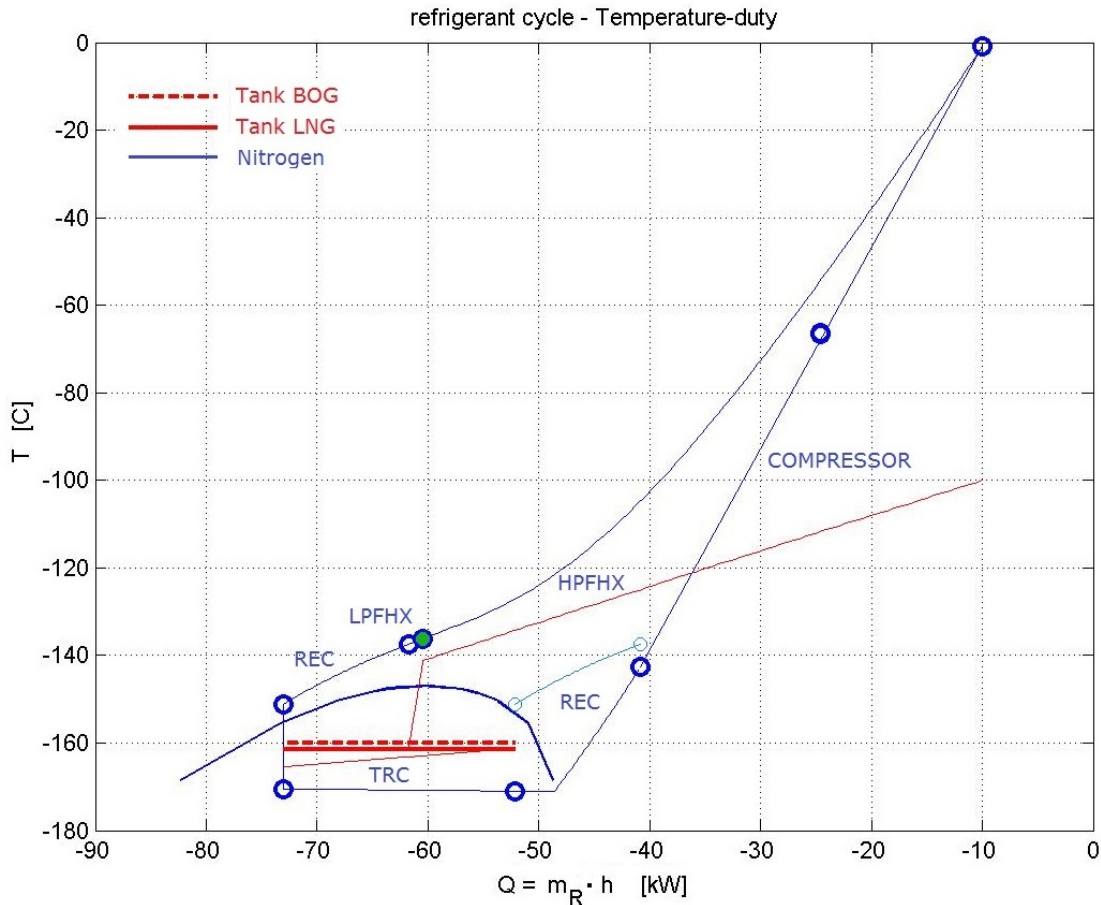


Figure 4.7: HeP-100%NCR: Refrigerant Temperature-Duty diagram

The diagram shows that the cold Nitrogen gas is compressed (in two consecutive stages without intercooling) and enters the HPFHX still below ambient temperature where it is cooled by the HP LNG, the green dots at the cold end of the HPFHX show the specified 5°C pinch point. The Nitrogen in the dense phase is further cooled in the LPFHX and in the recuperator (REC) before being throttled to the lower pressure inside the two-phase region. Here the fluid at 9 bar and -170°C evaporates with the heat from the subcooling LNG in the Tank Reflux system, after that it enters the REC that evaporates the 10% residual liquid and superheats the gas to the compressor suction temperature.

Figures 4.8 and 4.9 show respectively the cycle in the pressure enthalpy diagram and the heat exchangers' temperature difference curves.

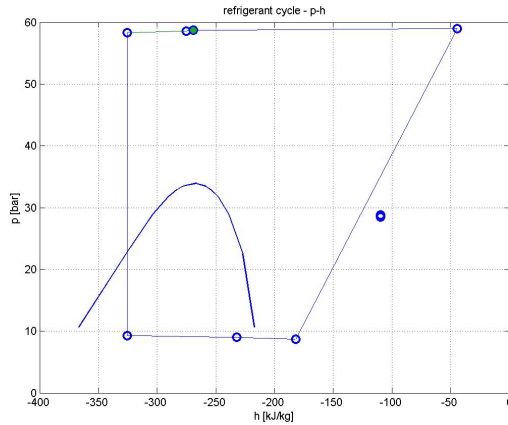


Figure 4.8: (HeP-100%NCR: Refrigerant cycle in the pressure - enthalpy diagram

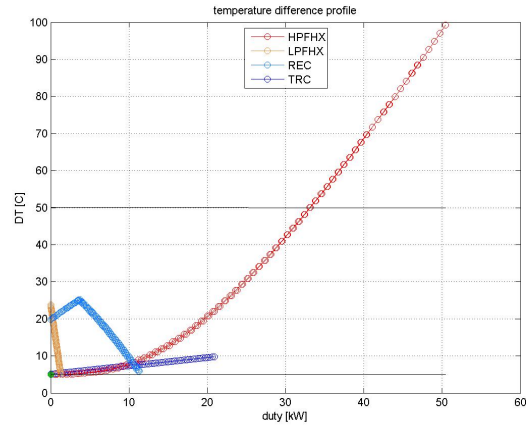


Figure 4.9: HeP-100%NCR: Temperature difference profile for process HX

The HPFHX is pinched at the cold end meaning that it is possible to decrease the HP LNG fuel flowrate by some extent without changing the shape of the cycle, as confirmed by the sensitivity analysis in Figure C.22. The REC heat exchanger has a pinch at the hot end which sets a superior limit to the compressor's inlet temperature. If a warmer compressor's inlet is desired heat must be provided by another stream or in a different configuration.

The refrigeration duty of 18.6 kW corresponds to a reliquefaction capacity of about 130 kg/h of BOG (Table 3.4), giving a energy consumption of 857-938 kJ/kg of reliquefied BOG inside the tank (0.24-0.26 kWh/kg) (the higher value includes the LP Pump energy consumption).

#### 4.5.2 Sensitivity Analysis on the normal operation scenario: HeP - 100% NCR

Sensitivity Analyses (also called Parametric Studies) have been carried out on the design model for the normal operation scenario (HeP-100%NCR) to understand which parameters influence the performance of the cycle and where a more accurate estimate of the equipment properties is needed. Several parameters were varied in a range containing the normal value and the response of selected dependent variables relevant for the system performance was moni-

tored.

In Figures C.18 to C.27 in the appendix Sensitivity Analyses are shown for each different parameter, Figure 4.10 below shows a summary of all the Analyses, the horizontal axis reports the percent variation of the parameters from the normal value, the COP value is on the vertical axis.

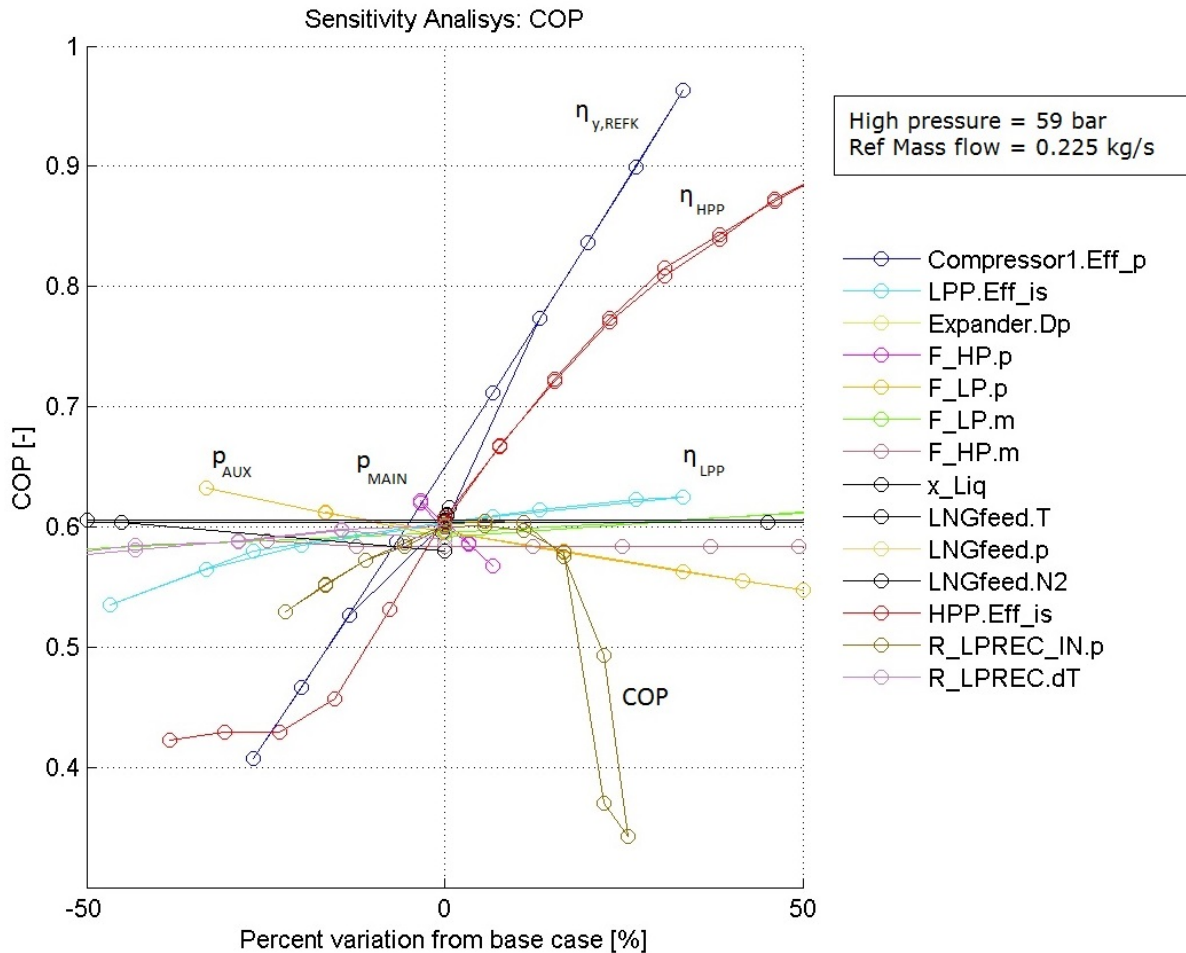


Figure 4.10: HeP-100%NCR: Variation of COP with different parameters

It can be observed from Figure 4.10 that the most sensitive parameters for the COP are the following:

- HP Pump efficiency (Figure C.18);

The HP LNG at the outlet of the HP pump is causing a process pinch in the HPFHX, this means that the temperature of the LNG at the inlet of the



heat exchanger limits the amount of heat that can be extracted from the HP Nitrogen, and consequently the cooling capacity of the process. If the efficiency of the HP pump is reduced the temperature of the HP LNG increases and the performance of the system drops drastically. It is therefore important to assume a reasonable and conservative value of the efficiency of the HP Pump.

- Refrigerant Compressor efficiency (Figure C.16);

As obvious the power requirement is affected by the compressor efficiency, however if the refrigerant flowrate is held constant this parameter does not affect the refrigeration duty, because a higher Nitrogen inlet temperature to the HPFHX can be handled by a further temperature increase of the HP fuel.

- TRC evaporation pressure (Figure 4.11).

A higher evaporation pressure gives a lower compressor pressure ratio and work, at the same time if the evaporation temperature is too high the TRC evaporator will have to extract heat from the LNG under a small temperature difference and will require a higher LNG flowrate (TR-LNG) and a correspondently higher LP pump work. As the LNG recirculation stream (TR-LNG) is flashed back to the tank part of the LP pump work constitutes a energy input to the tank, which has to be subtracted to the TRC duty to get the effective refrigeration effect. For this reason an excessive LNG recirculation flowrate reduces the refrigeration duty and the COP. If the refrigerant flowrate and high pressure are held constant the Sensitivity Analysis on the evaporation pressure in Figure 4.11 evidence an optimum in the COP at 9-10 bar, if the flowrate is constant an increase in the evaporation pressure implies a reduction in the refrigeration duty.

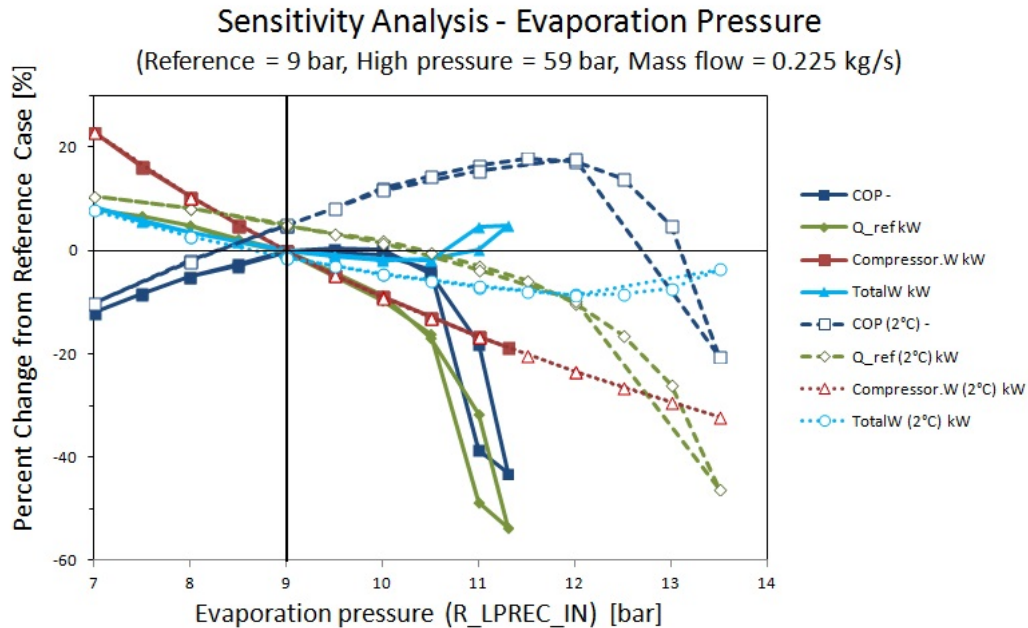


Figure 4.11: HeP-100%NCR: Sensitivity Analysis: Evaporation pressure with constant refrigerant mass flow and high pressure

This analysis refers to a 5°C MITA specification for the evaporator (TRC), if the evaporator MITA was lower the evaporation pressure could be slightly higher, for example if the evaporator MITA was set to 2°C (dotted line in Figure 4.11) the optimum evaporating pressure could be as high as 11-12 bar, for a COP about 18% higher than the reference case.

Figure 4.12 below shows the same analysis, this time with the refrigeration duty set to the design value, and the refrigerant mass flow tuned accordingly. The COP curve is the same as in the previous figure, the orange curve shows the steep increase of LNG reflux (TR), the compressor work has a minimum given by the opposing effects of the increasing evaporation pressure, and increasing refrigerant flow.

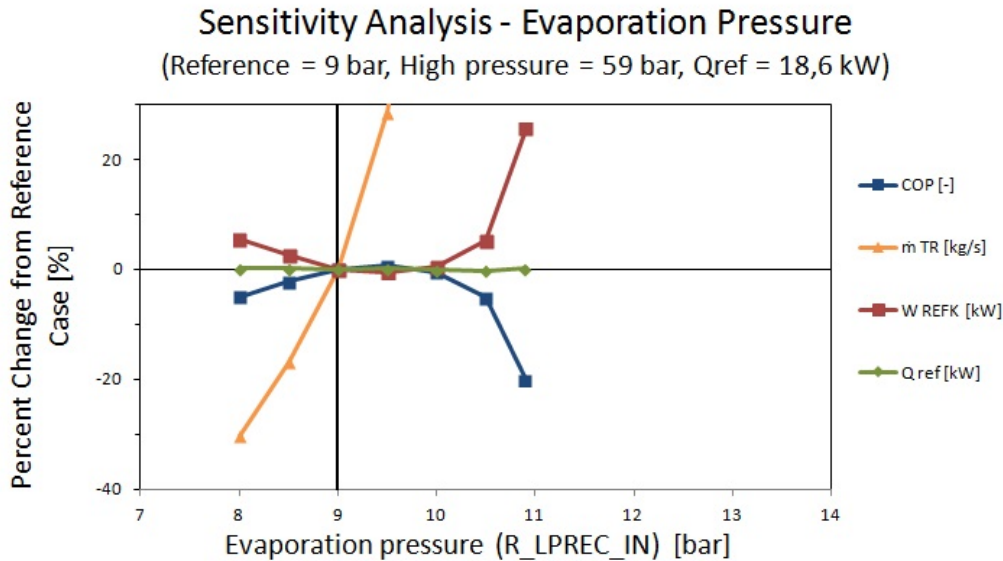


Figure 4.12: HeP-100%NCR: Sensitivity Analysis: Evaporation pressure, with constant refrigerant high pressure and effective refrigeration duty

In addition to the above mentioned other important parameters are:

- REC low pressure side Temperature increase (Figure C.26);

Even though it is not immediately visible from Figure 4.10 the role of the Recuperator (REC) heat exchanger is determinant to achieve a large refrigeration duty in the TRC heat exchanger and to improve the COP. Because of this observation in all the simulations carried out in this study the duty of the REC heat exchanger, or equivalently the temperature increase of its low pressure side stream, has been maximized until allowed by the MITA constraint.

- Use of expander instead of throttle valve;

The benefit of using an expander upstream the throttle valve has been evaluated and the results are reported in Figures C.24 and C.25 in the appendix. In the sensitivity analysis the expansion was stopped near the Nitrogen critical pressure giving a increase in efficiency of 2-4%, depending on expander efficiency. Extrapolating the linear pattern it can be estimated that if the pressure was lowered until the evaporation pressure the efficiency

would increase of about 4-8%. Since this gain in efficiency was considered modest the expander was switched off and it is not included in the results.

#### 4.5.3 Part load scenario: HeP - 50% NCR

The present chapter contains the results of the Design model run with 50% of the main engine fuel flowrate. Figure 4.13 shows the operation map generated by the two variable case study, similarly to Figure 4.5.

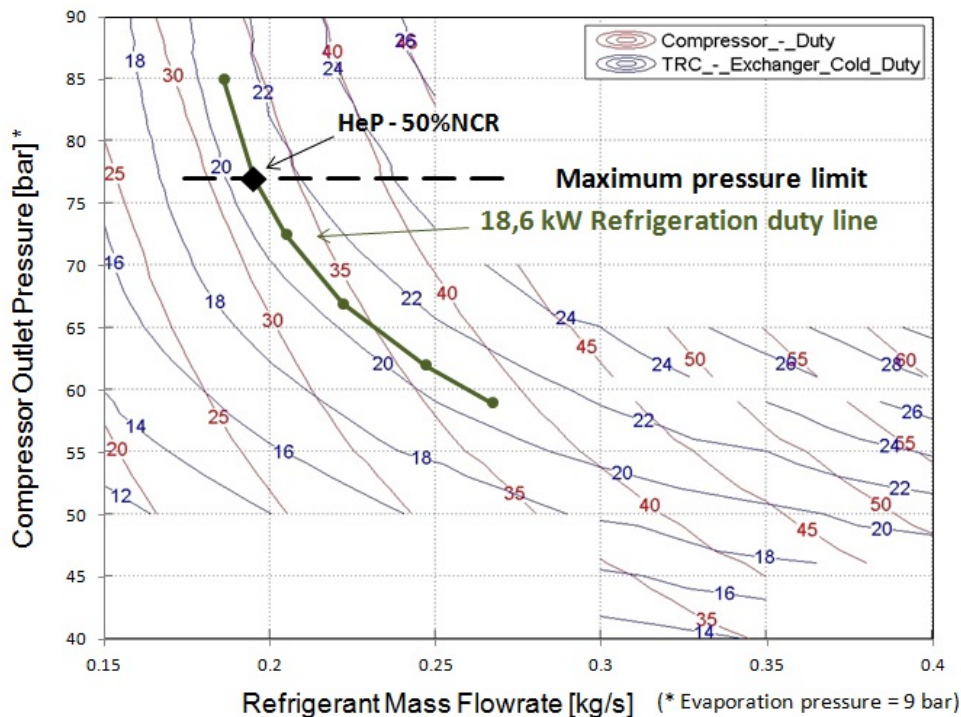


Figure 4.13: HeP-50%NCR: Operation map

The compressor work contour lines still show that for a given cooling duty (e.g. 18.6 kW) there exist an optimum pressure for heat discharge, however in this case the optimum pressure is higher than in the normal operation scenario. Figure 4.14 shows the COP as a function of high pressure for the normal operation and for the 50%NCR and 20%NCR cases.

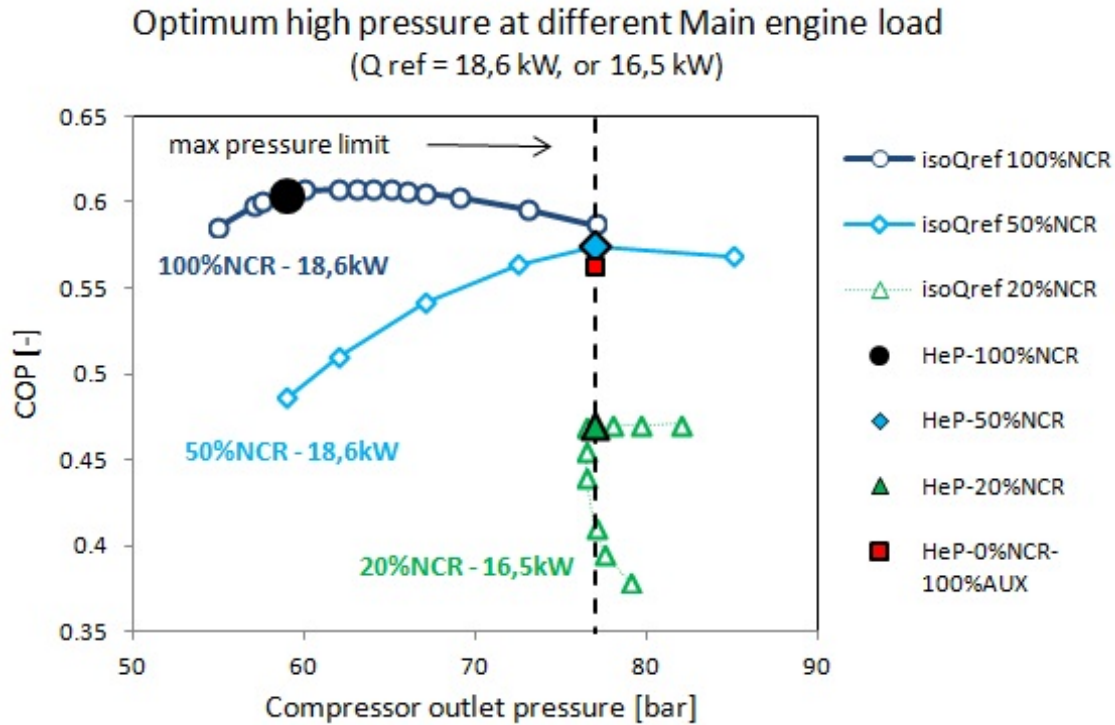


Figure 4.14: Optimum high pressure for different Main engine load scenarios

While in the 100%NCR case the optimum pressure is in the range 59-66 bar, for the 50%NCR case the COP has a maximum in the 75-85 bar region, due to the different heating curves profiles in the HPFHX. As the diagram anticipates, the pressure in the 20%NCR case would need to increase even more to supply the required duty.

Even if an accurate Off-Design model is out of the scope of the thesis, it was considered useful to report these results obtained with the Design model to evidence that the design of the process and the equipment selection should take into account the part load of the main engine. In fact if the process was sized for a design pressure of 59 bar (as for HeP-100%NCR) it would be inefficient at 50% fuel flow, and almost totally unable to perform at 20% fuel flow. The 77 bar limit on the high pressure was chosen based on this considerations.

The design point for the case HeP-50%NCR, with a outlet pressure of 77 bar, is analyzed in detail in Table 4.11 and in Figures 4.15 to 4.17.

Table 4.11: HeP-50%NCR: Process Equipment mass and energy balance

Equipment	Duty [kW]	m Ref [kg/s]	m Fuel [kg/s]	LP [bara]	HP [bara]
LP Pump	2.64		1.82	1.04	6.00
HP Pump	20.08		0.20	6.00	300.90
Ref Compr	32.47	0.20		8.70	77.00
<b>Total Work</b>	<b>55.19</b>				
HPFHX	52.06	0.20	0.20	77.00	300.60
LPFHX	1.35	0.20	0.02	6.00	76.70
REC	9.82	0.20		9.00	76.60
TRC	20.94	0.20	1.60	6.00	9.30
<b>Cooling Duty</b>	<b>18.62</b>				
<b>COP</b>	<b>0.57</b>				

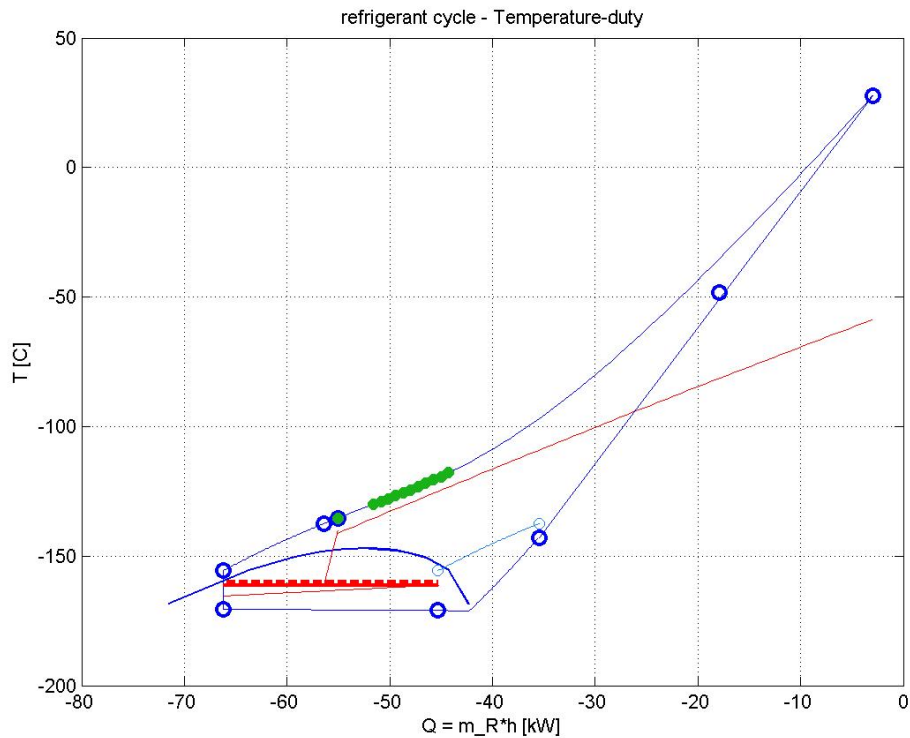


Figure 4.15: HeP-50%NCR: Refrigerant Temperature-Duty diagram

Compared to the normal operation case "HeP-100%NCR" the optimum pressure is now higher, the reason of this is that the HP fuel flowrate has decreased, correspondently its heat capacity in the HPFHX has decreased leading to a steeper heating path and pushing the cooling curve of the refrigerant to higher temper-

atures and pressure as shown in Figure 4.15. The pinch point of the HPFHX shown by the green dots is now internal to the heat exchanger.

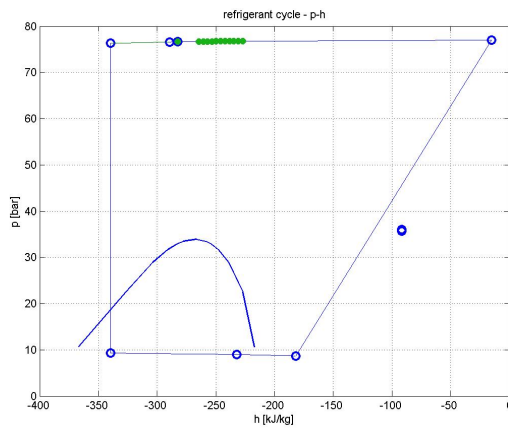


Figure 4.16: (HeP-50%NCR: Refrigerant cycle in the pressure - enthalpy diagram

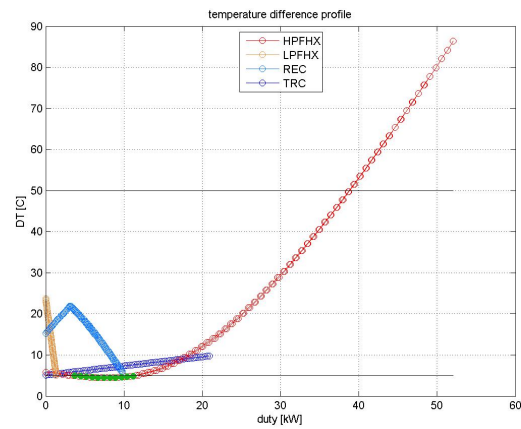


Figure 4.17: HeP-50%NCR: Temperature difference profile for process HX

#### 4.5.4 Part load scenario: HeP - 20% NCR

Figure 4.18 represents the operation map for the part load scenario at 20% of the main engine fuel flowrate. The difference with previous scenarios is that for a given high pressure (e.g. 77 bar) there is a value of the flowrate that gives maximum cooling duty. This means that given a target cooling duty there exists a minimum high pressure below which the target can not be reached by such process.

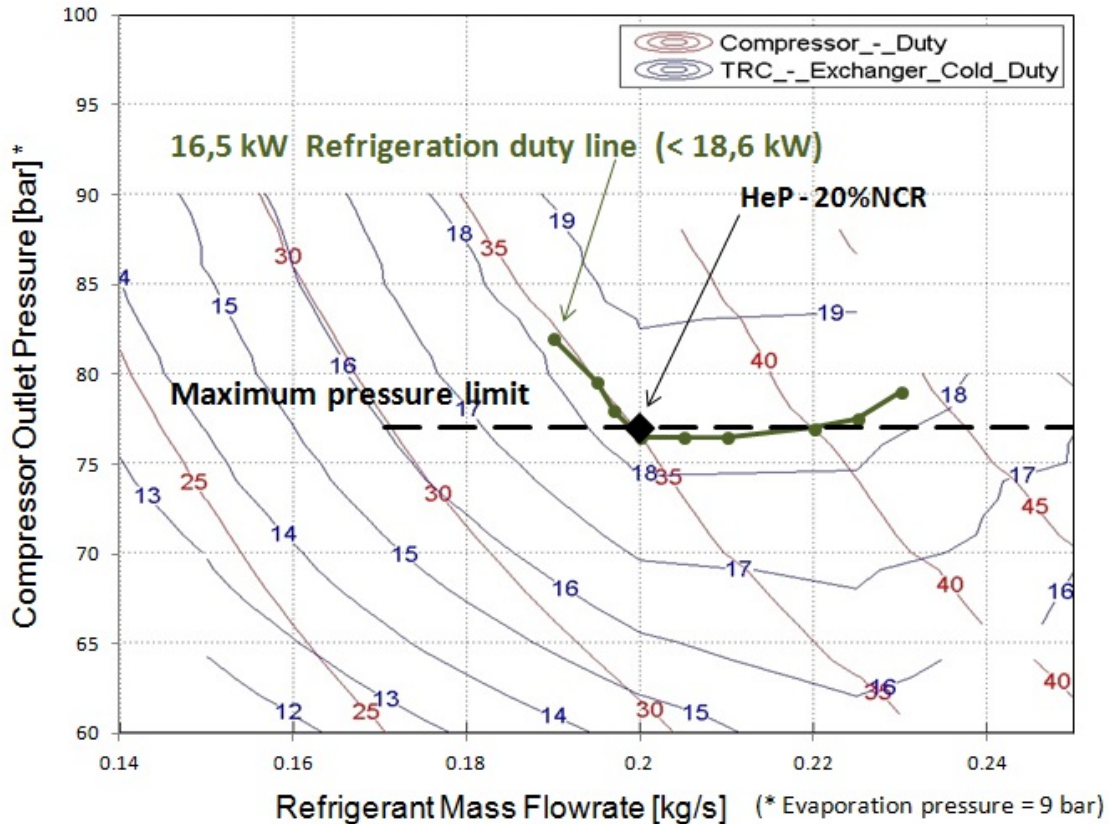


Figure 4.18: HeP-20%NCR: Operation map

Since the limit for the heat pump high pressure has been set arbitrarily to 77 bar in all scenarios, the Figure shows that the maximum refrigeration duty achievable by the system with this high pressure is about 16,5 kW, that is lower than the target of 18,6 kW. As a consequence in the 20%NCR scenario one can expect that some BOG, corresponding to the difference between the refrigeration duty and the heat leak, will need to be flared in GCUs. If the process was designed based on the "HeP-100%NCR" scenario only, with a 59 bar high pressure, its maximum achievable cooling duty at 20%NCR would be further reduced by about 2-3 kW, increasing the amount of flared BOG.

The design point HeP-20%NCR is detailed in Table 4.12 and in Figures 4.19 to 4.21.



Table 4.12: HeP-20%NCR: Process Equipment mass and energy balance

Equipment	Duty [kW]	m Ref [kg/s]	m Fuel [kg/s]	LP [bara]	HP [bara]
LP Pump	2.20		1.52	1.04	6.00
HP Pump	8.03		0.08	6.00	300.90
Ref Compr	35.38	0.20		8.70	77.00
<b>Total Work</b>	<b>45.61</b>				
HPFHX	44.52	0.20	0.08	77.00	300.60
LPFHX	9.35	0.20	0.02	6.00	76.70
REC	11.54	0.20		9.00	76.60
TRC	18.67	0.20	1.42	6.00	9.30
<b>Cooling Duty</b>	<b>16.62</b>				
<b>COP</b>	<b>0.47</b>				

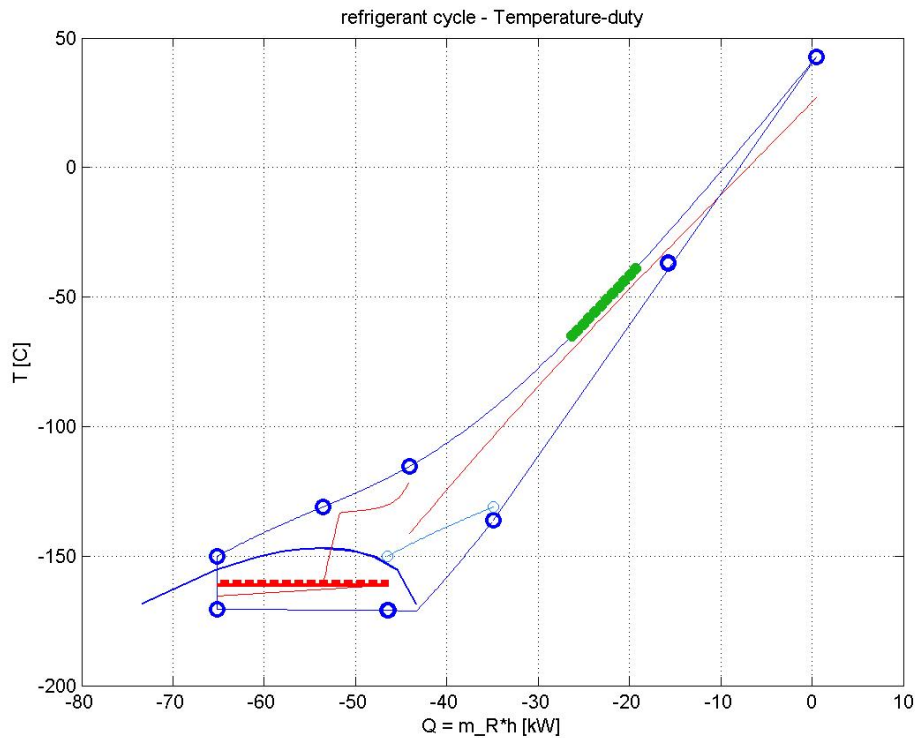


Figure 4.19: HeP-20%NCR: Refrigerant Temperature-Duty diagram

The plots show that the pinch point of the HPFHX has moved towards the center of the heat exchanger where the cooling curves are very sensitive on a variations in heat capacity of the two streams.

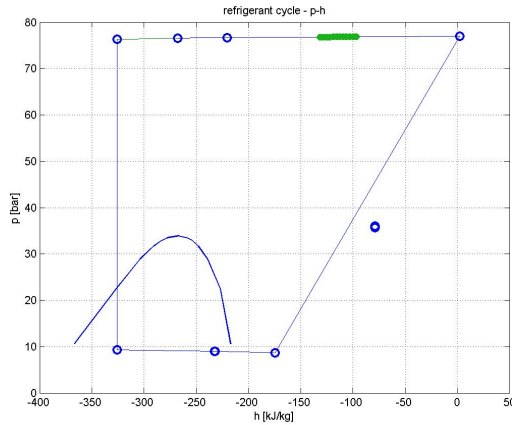


Figure 4.20: (HeP-20%NCR: Refrigerant cycle in the pressure - enthalpy diagram

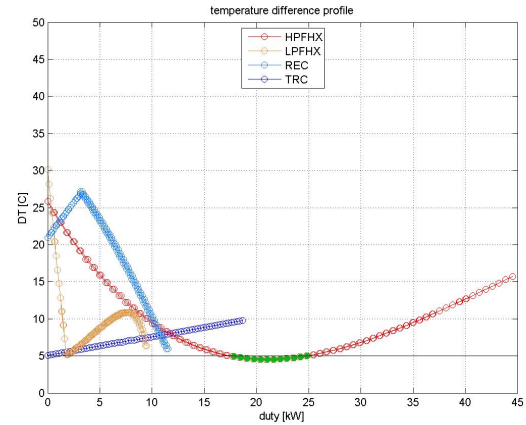


Figure 4.21: HeP-20%NCR: Temperature difference profile for process HX

Unlike the previous scenarios, the LP LNG is evaporated in the LPFHX and not just heated in the liquid phase, and most importantly this heat exchanger's contribution to the cycle's energy balance is more substantial. The LPFHX in this scenario is handling 9.35 kW against the 1.29 kW of the HeP-100%NCR case, consequently the required UA value calculated by the design model increases from 0.1 for the normal operation scenario to 1.1 in this scenario. This another reason why the part load operation should be taken into account in the definition of the equipment size.

#### 4.5.5 Idle/Harbour scenario: HeP - 0% NCR - 100% AUX

This section describes the operation of the heat pump in the scenario where the main engine does not receive any HP gas fuel, this can occur at very low loads when the engine needs to switch to fuel oil mode, or when it is turned off. In this case the HPFHX is not anymore contributing to the heat pump cycle which now uses only the LPFHX to discharge the heat. Figure 4.22 shows that the performance of the system is very poor in this scenario and it is not possible to achieve the target cooling duty of 18,6 kW. However keeping the refrigerant flowrate to very low values (roughly 1/3 of the normal and part load scenarios) it is still possible to produce a cooling effect of 5-6 kW, this is expected to be very

much dependent on the load of the Auxiliary engines.

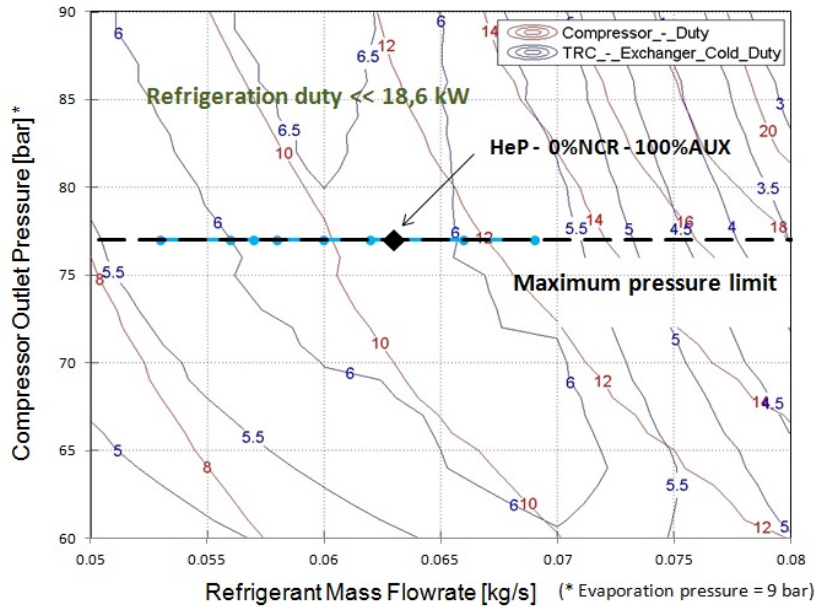


Figure 4.22: HeP-0%NCR-100%AUX: Operation map

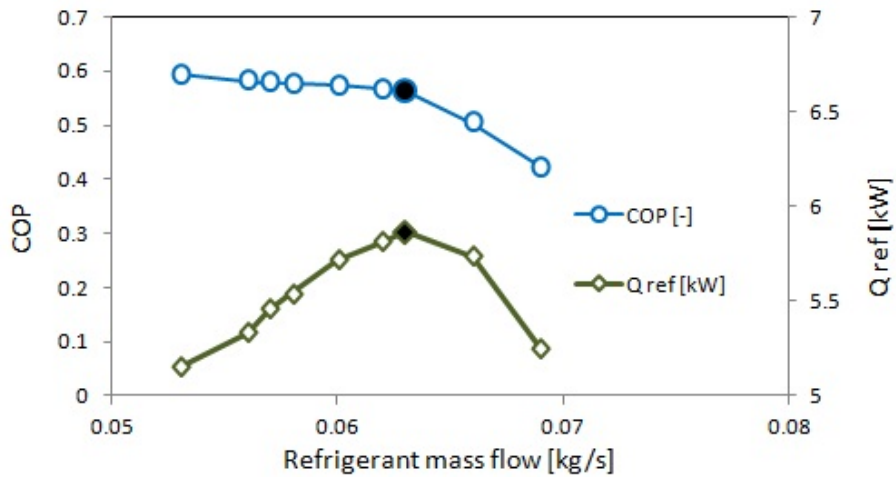


Figure 4.23: HeP-0%NCR-100%AUX: Optimum refrigerant mass flow

An example of operation of this system is analyzed in the following Table 4.13 and in Figures 4.24 to 4.26. The red curve in Figure 4.24 shows that the LPFHX is now able to vaporize and superheat the LP LNG fuel up to ambient temperature.

Table 4.13: HeP-0%NCR-100%AUX: Process Equipment mass and energy balance

Equipment	Duty [kW]	m Ref [kg/s]	m Fuel [kg/s]	LP [bara]	HP [bara]
LP Pump	0.77		0.53	1.04	6.00
HP Pump	0.00		0.00	6.00	300.90
Ref Compr	10.42	0.06		8.70	77.00
<b>Total Work</b>	<b>11.20</b>				
HPFHX	0.00	0.06	0.00	77.00	300.60
LPFHX	16.53	0.06	0.02	6.00	76.70
REC	3.13	0.06		9.00	76.60
TRC	6.61	0.06	0.51	6.00	9.30
<b>Cooling Duty</b>	<b>5.86</b>				
<b>COP</b>	<b>0.56</b>				

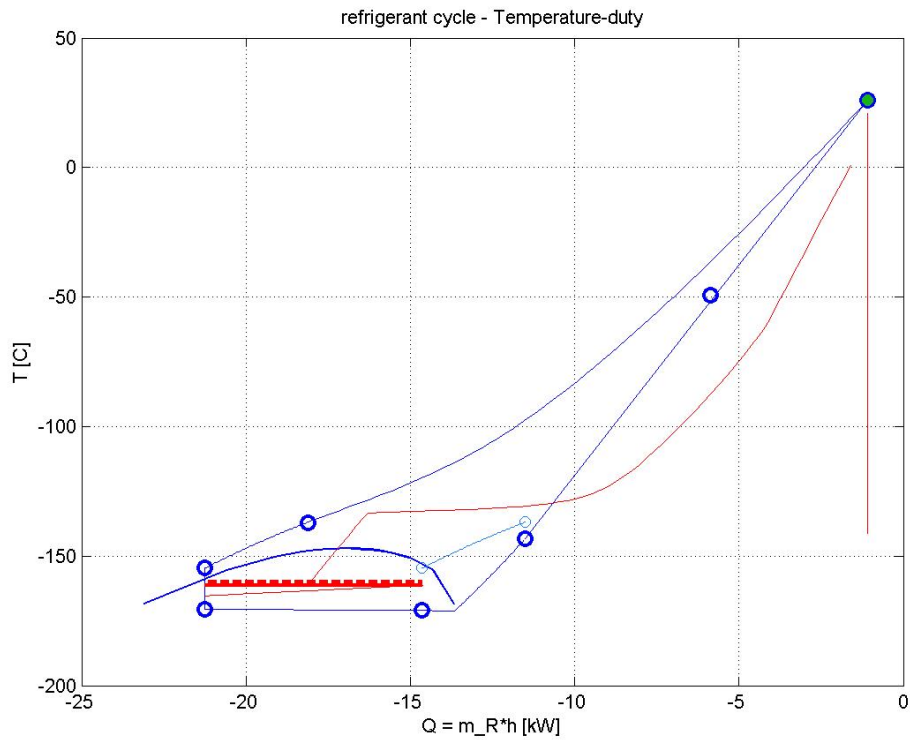


Figure 4.24: HeP-0%NCR-100%AUX: Refrigerant Temperature-Duty diagram

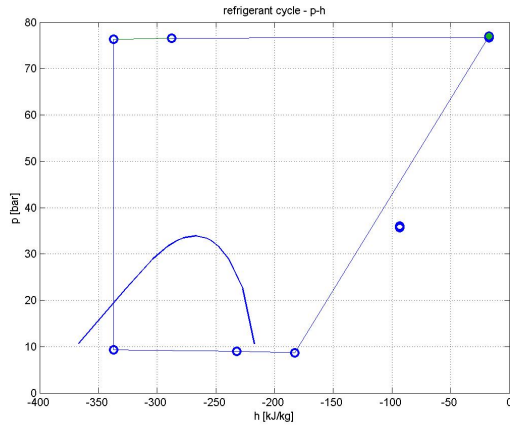


Figure 4.25: (HeP-0%NCR-100%AUX: Refrigerant cycle in the pressure - enthalpy diagram

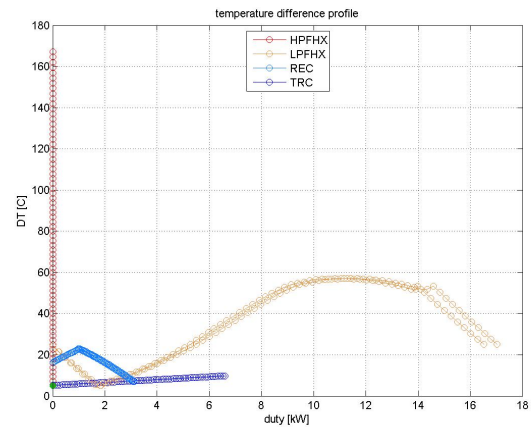


Figure 4.26: HeP-0%NCR-100%AUX: Temperature difference profile for process HX

## 4.6 Heat Pump with BOG feed to Auxiliary engines simulation results (HeP-AUX)

This section illustrates the results of the model of the heat pump with BOG feed to auxiliary engine (HeP-AUX), in this process some BOG is allowed to evaporate in the tank and be compressed by a dedicated compressor (BOGK) for the Auxiliary engine. The heat pump provides the refrigeration duty to compensate the excess heat leak. According to the heat leak calculations in chapter 3.3.3 the refrigeration duty required amounts to 8.2 kW which is significantly lower than the previous 18.6 kW.

Figure 4.27 compares the specific work per unit of mass of compressed BOG with that of the heat pump process (HeP), since the BOG compressor work is 4 to 5 times lower there is reason to believe that compression should be the preferred option to feed the Auxiliary engines in most situations where BOG is available in sufficient amount.

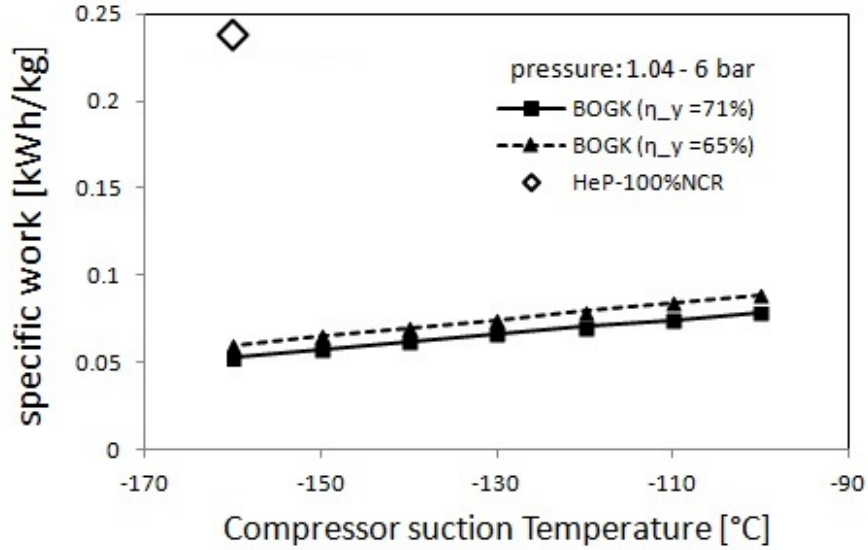


Figure 4.27: Comparison of energy consumption for BOG compression for Auxiliary engine and recondensation with the heat pump process HeP

#### 4.6.1 HeP-AUX: 100% NCR

In this section the results of the "HeP-AUX" process are shown for the normal operation scenario at full main engine load. The optimum high pressure of the heat pump in this scenario is similar to the "HeP" process, as in Figure 4.28

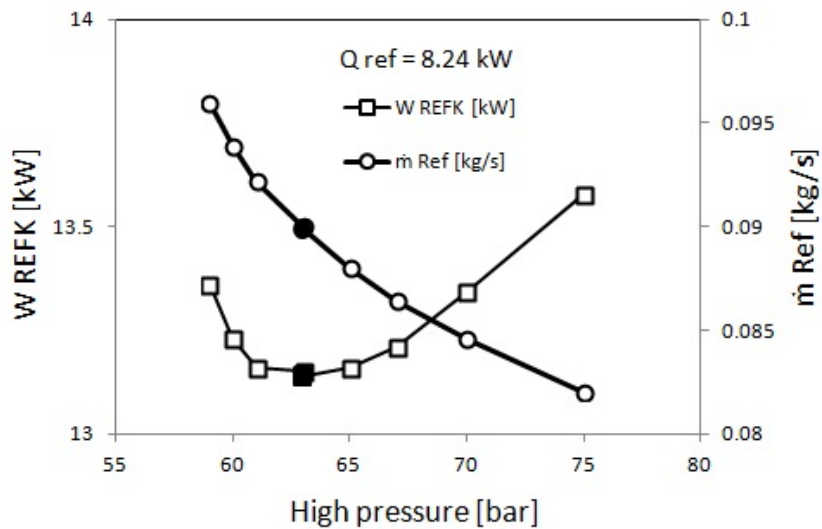


Figure 4.28: HeP-AUX-100%NCR: Optimum heat pump cycle high pressure

The details of the design point "HeP-AUX-100%NCR", highlighted with a black

marker in the previous figure, are listed below.

Table 4.14: HeP-AUX-100%NCR: Process Equipment mass and energy balance

Equipment	Duty [kW]	m Ref [kg/s]	m Fuel [kg/s]	LP [bara]	HP [bara]
LP Pump	0.30		1.07	1.04	2.00
HP Pump	40.71		0.40	2.00	300.90
Ref Compr	13.14	0.09		8.70	63.00
BOG Compr	3.70		0.02	1.04	6.30
<b>Total Work</b>	<b>57.85</b>				
HPFHX	21.56	0.09	0.40	63.00	300.60
REC	4.67	0.09		9.00	62.70
TRC	8.43	0.09	0.67	2.00	9.30
<b>Cooling Duty</b>	<b>8.24</b>				
<b>COP</b>	<b>0.63</b>				

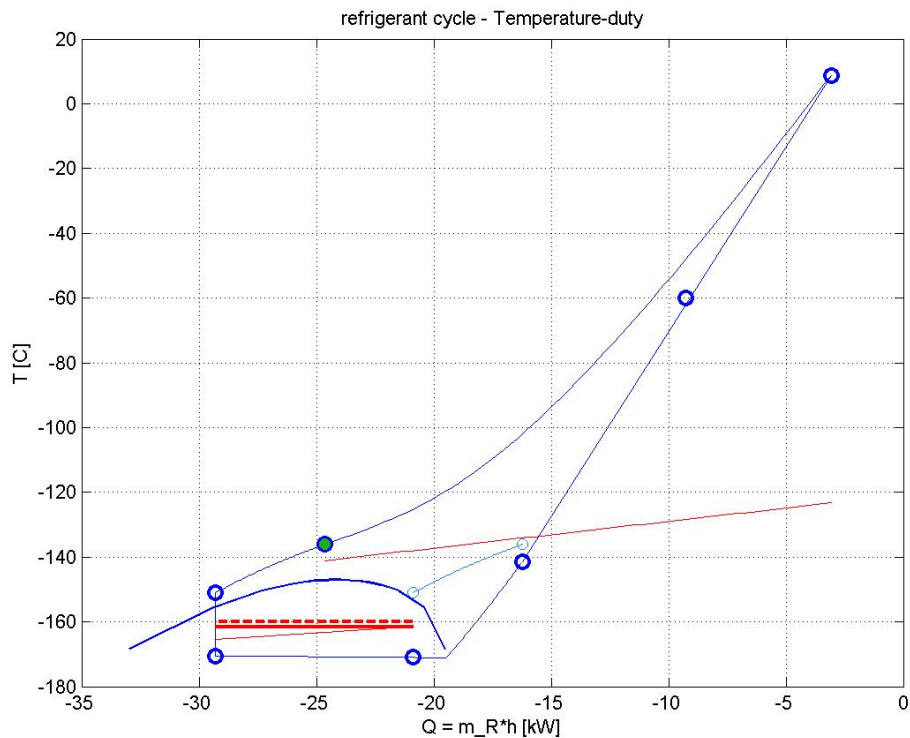


Figure 4.29: HeP-AUX-100%NCR: Refrigerant Temperature-Duty diagram

The "HeP-AUX" cycle at full main engine load is similar to the "HeP". The LPFHX has been removed with a negligible detrimental effect on the cycle effi-

ciency. However, thanks to the dedicated BOG compressor, the LP pump does not need to work at 6 bar discharge pressure, then the pressure can be reduced by some extent, in this case to 2 bar. As a consequence the specific work of the LP pump is reduced and its impact on the refrigeration duty decreases with a positive effect on the COP. Comparing the TRC evaporator duty with the net refrigeration duty one can see that the LP pump work input "dissipates" 2.3% of the TRC duty, instead of 11% in the HeP scenario.

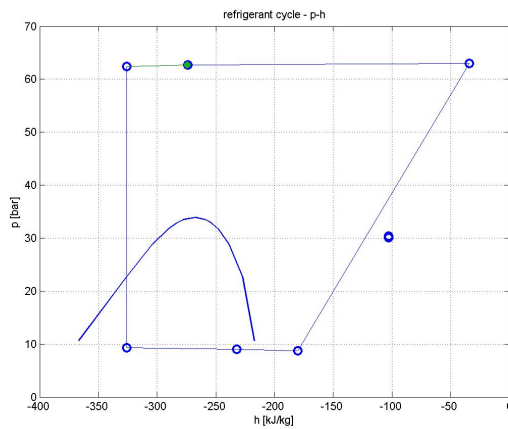


Figure 4.30: (HePAUX100%NCR: Refrigerant cycle in the pressure - enthalpy diagram

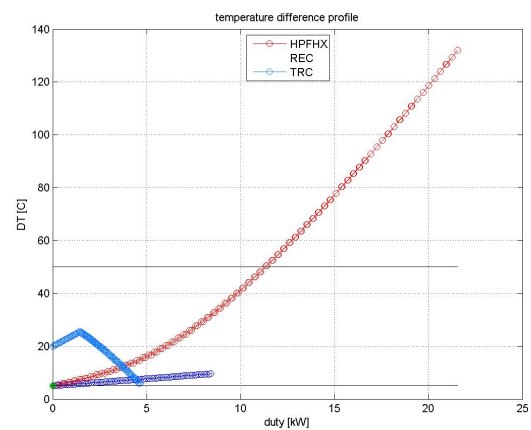


Figure 4.31: HePAUX100%NCR: Temperature difference profile for process HX

## 4.7 Evaluation of alternative process layouts

### 4.7.1 Intercooled heat pump cycle

As will be motivated later on in the course of the thesis, the low temperature at compressor suction is expected to increase the cost of the machine due to the more demanding material requirements. A solution to this would be to force an increase in the suction temperature of the compressor, accepting an correspondingly higher energy consumption. A more efficient solution could be to exchange the heat between the inlet and the outlet of the first stage of the compressor, as described by the layout in Figure 4.32.



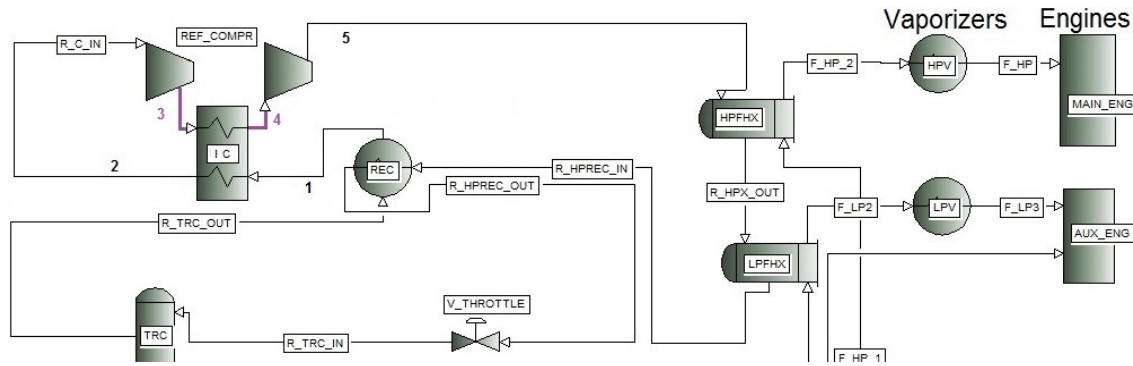


Figure 4.32: Process layout with refrigerant compressor Intercooling by LP refrigerant

In this layout, that was not simulated in the course of the thesis, the heat exchanger IC acts as an intercooler for the refrigerant compressor and as a heater for the LP refrigerant at suction. The inlet temperature of the first compressor stage is increased by some extent, thereby relaxing the materials specifications for the cryogenic compressor, and the intercooling effect on the second stage mitigates the increase in energy consumption. In particular regarding the energy consumption of the compressor the following two effects are expected:

- the higher temperature at the first stage inlet would necessarily increase the stage compression work;
- despite the mitigating effect of the intercooler, the compressor work of the second stage would increase due to the diverging shape of the isentropic lines, as shown by the position of point 4 in Figure 4.33.

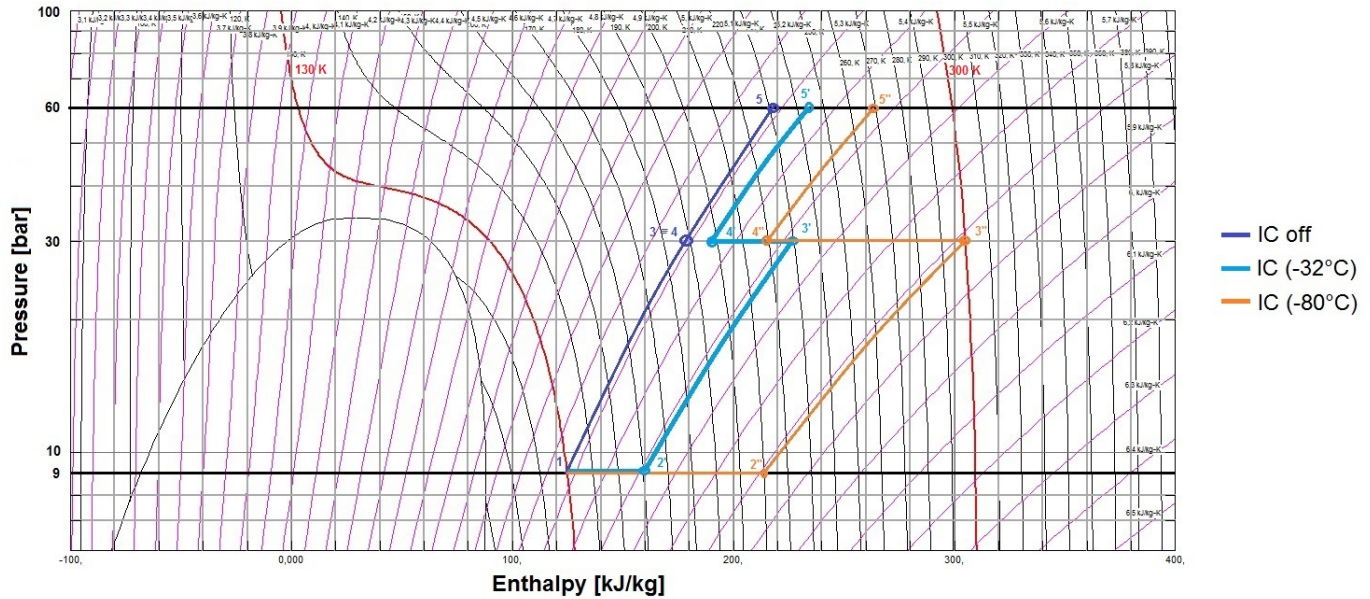


Figure 4.33: Comparison between isentropic compression paths with and without intercooling, in the Nitrogen pressure enthalpy chart generated with RefProp

In conclusion this layout of the intercooled cycle would increase the compressor work and penalize the COP but it could lead to a reduction in refrigerant compressor cost, therefore the existence of a trade off could be expected in which case the use of the intercooler would need to be evaluated based on a more detailed cost analysis.

#### 4.7.2 BOG recirculation in the Tank Reflux system

All the simulation results presented so far refer to a process configuration where LNG liquid is subcooled in the Tank Reflux system and recirculated in the tank, it is however possible to recirculate BOG in the Tank Reflux system by means of a BOG compressor (dotted stream in the main process PFD in Figure 3.2). The expected advantage of reliquefying the BOG instead of subcooling the LNG is that the higher temperature on the hot side of the TRC heat exchanger allows to rise the evaporation pressure and improve the heat pump performance.

This option has been assessed with explorative simulations in a early stage of the model development. It was found that if the BOG compressor operates at 6 bar outlet pressure (i.e. the Auxiliary engine specification) the specific work of

compression will constitute a too large energy input to the Tank Reflux system heavily reducing the effective refrigeration duty. However, if the BOG is compressed just high enough to compensate the pressure drop in the system, this operation mode might be competitive with the basic subcooling mode.

For simplicity the successive analyses have been limited to the configuration with recirculation of liquid, and this option has not been investigated further in the course of the thesis.

## 4.8 Discussion of simulation results

In this chapter the simulation results of the heat pump process model in its two versions "HeP" and "HeP-AUX" are compared with other alternative solutions for BOG handling introduced in chapter 3.2. The results of the simulations at 100% main engine load are summarized in Figure 4.34, the bars represent the primary energy consumption of the FGSS that includes pumps, compressors, and flare gas.

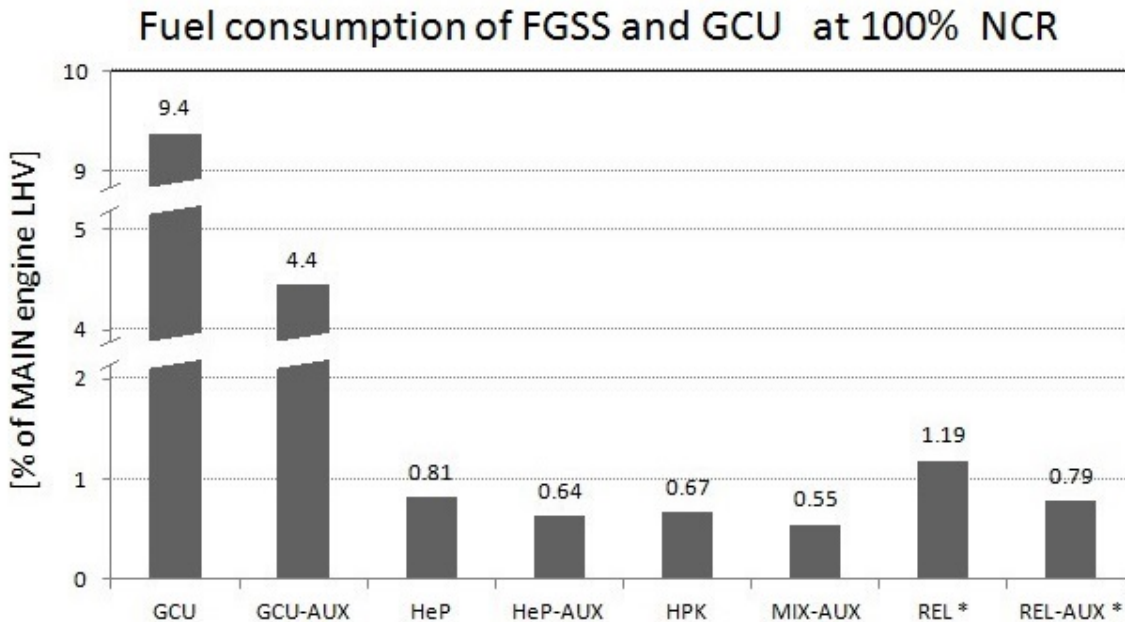


Figure 4.34: Overall FGSS primary energy consumption, including flared gas in GCU, expressed as percentage of main engine thermal power at 100%NCR. (\*Reliquefaction estimated from literature)

The flaring option GCU, and its improved version GCU-AUX, require the consumption of a considerable quantity of fuel, most of which is flared. If 4.4% of the main engine fuel consumption was to be directed to GCU the efficiency gain of implementing a slow 2-stroke gas injected engine would be greatly reduced, therefore this option is considered unacceptable. All the other processes examined offer a substantial improvement from the GCU scenarios, giving a FGSS consumption mostly below 1% of the main engine's.

As expected, since the specific compression work for compressing the BOG to the Auxiliary engine feed pressure of 6 bar is relatively low, the "-AUX" versions of the processes (i.e. GCU-AUX, HeP-AUX and REL-AUX) give a better performance than the corresponding versions GCU, HeP and REL. In general one can deduce that the first choice for BOG handling should be to feed it to the AUX engine whenever possible, other solutions should only regard the excess BOG.

The reliquefaction processes have not been simulated and their energy consumption is estimated using a specific reliquefaction work of 0.5 kWh/kg, this yields a poorer performance than the alternative processes. A more detailed comparison between the heat pump process HeP and two commercial Reliquefaction processes available for the LNG Carrier segment is illustrated in Figure 4.35.

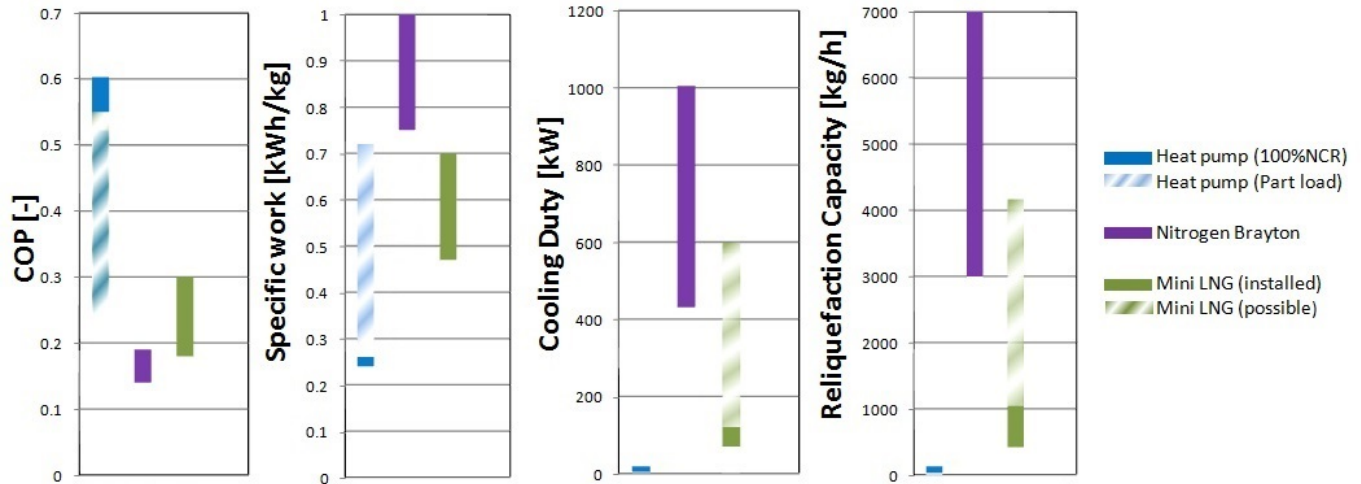


Figure 4.35: Comparison of the heat pump performance and capacity with commercially available liquefaction processes for LNGC [10, 18, 29], COP and specific work are related to each other through the evaporation enthalpy of the BOG, so are cooling duty and reliquefaction capacity

The two types of reliquefaction cycles reported are designed for LNG Carriers, to supply a capacity that is 10 to 100 times larger than the heat pump refrigeration duty. The better performance of the heat pump is due to the full integration of the cycle with the FGSS, allowing heat discharge below ambient temperature and cold compression. In conclusion the heat pump process is more efficient and seems more indicated for LNG fuelled ships, on the other hand it has the disadvantage that it can not operate when the main engine is off, this would not constitute a problem for a reliquefaction process similar to the two reported above.

The three most efficient solutions at 100%NCR are the MIX-AUX process, or "Terminal type", followed by the HeP-AUX process and the high pressure compression HPK process, the FGSS consumption for this three processes is comparable, with some advantage for the MIX-AUX process.

Since the overall energy consumption is similar for the three processes, other factors should be taken into account for a more complete assessment, some of these are the plant cost and complexity, and its turndown capability.

As already stated modeling the Off-Design operation of the process is not in the scope of this work, however running the Design model at reduced Main engine

fuel flow proved useful to define the Design features of the heat pump model, such as refrigerant compressor maximum high pressure and heat exchangers UA value. Similarly when it comes to evaluating the performance of different BOG handling processes, the part load of the main engine should be taken into account, even in the absence of an accurate Off-Design model of each process. For this purpose the Design model of some of the processes detailed above was run at reduced Main engine fuel flow, the results of this study are shown in Figure 4.36.

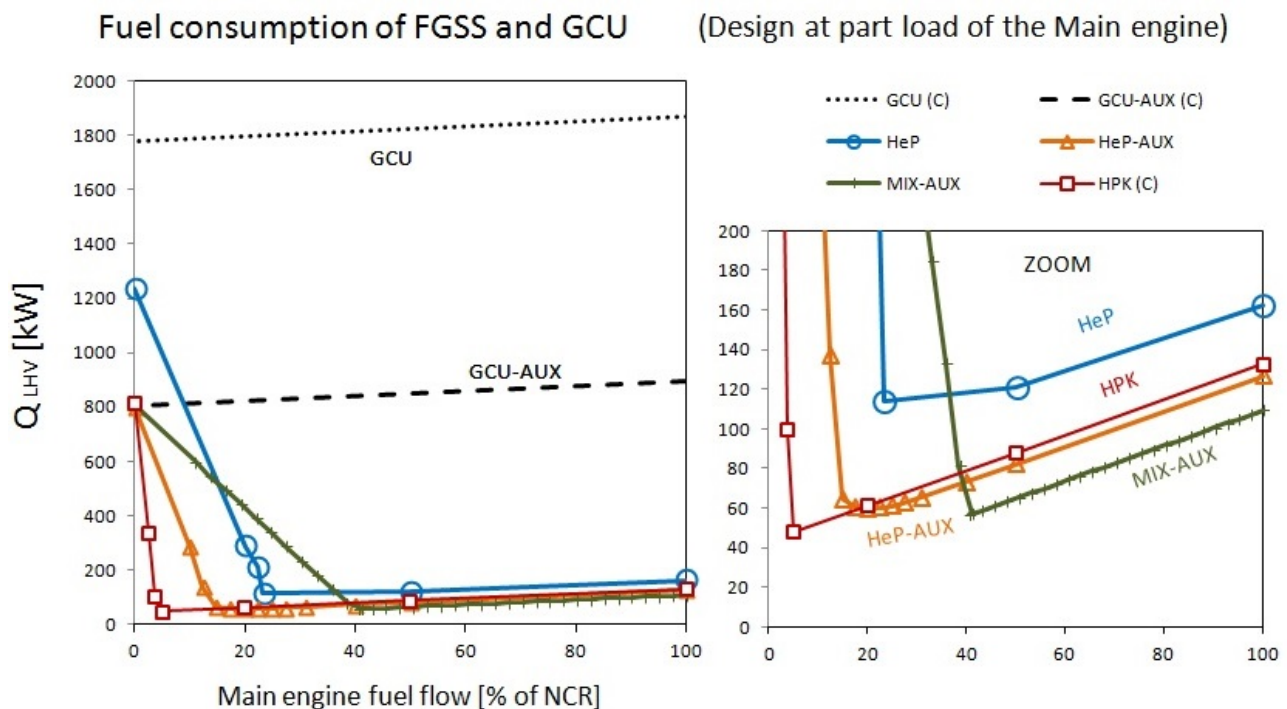


Figure 4.36: Overall FGSS primary energy consumption of different processes, calculated by the Design model with different values of the Main engine fuel flowrate.

The first observation is that for each of the four simulated processes there exist a value of the main engine fuel flowrate below which the system fails to handle all of the BOG, and starts sending part of it to the GCUs. Stepping down in fuel flow, this "crisis" aggravates until the Main engine consumption is zero and all the excess BOG is burnt in GCUs. The onset of this crisis, which corresponds to the limit of "no-flaring" operation, is different for each process. In particular the HPK process is practically immune from this problem, because it

occurs at such a low fuel flow that is below the minimum limit for gas injection mode.

The MIX-AUX process, which has the highest efficiency at full load, experiences the limit at the highest fuel flowrate of about 40%, this is possibly the only disadvantage of this process, which is by far the simplest of all.

This result for the MIX-AUX process refers to the specified constraints of 5°C required subcooling at HP Pump suction and 6.3 bar Recondenser pressure, which both limit the amount of BOG that can be condensed in the subcooled LNG stream.

The occurrence of the no-flaring limit for the different processes also depends on the boundary conditions of the FGSS, i.e. the relative weight of the heat leak, the HP fuel consumption and the LP fuel consumption. For a qualitative representation two dimensionless variables are defined

$$X = \frac{\dot{m}_{\text{BOG, evap}}}{\dot{m}_{\text{Main}}} \sim \frac{\dot{Q}_{\text{leak}}}{P_{\text{Main}}} \quad (4.3)$$

$$Y = \frac{\dot{m}_{\text{Aux}}}{\dot{m}_{\text{Main}}} \sim \frac{P_{\text{Aux}}}{P_{\text{main}}} \quad (4.4)$$

the ratio between the two variables X and Y equals the ratio between the BOG evaporated in the tank and the LP fuel consumption of the Auxiliary engine.

$$\frac{Y}{X} = \frac{\dot{m}_{\text{BOG, evap}}}{\dot{m}_{\text{Aux}}} \sim \frac{\dot{Q}_{\text{leak}}}{P_{\text{Aux}}} \quad (4.5)$$

The boundary conditions for the simulation are plotted in the X-Y plane in figure 4.37, where the blue circle represents the Design conditions of the ship tank and engines at 100% of Main engine NCR.

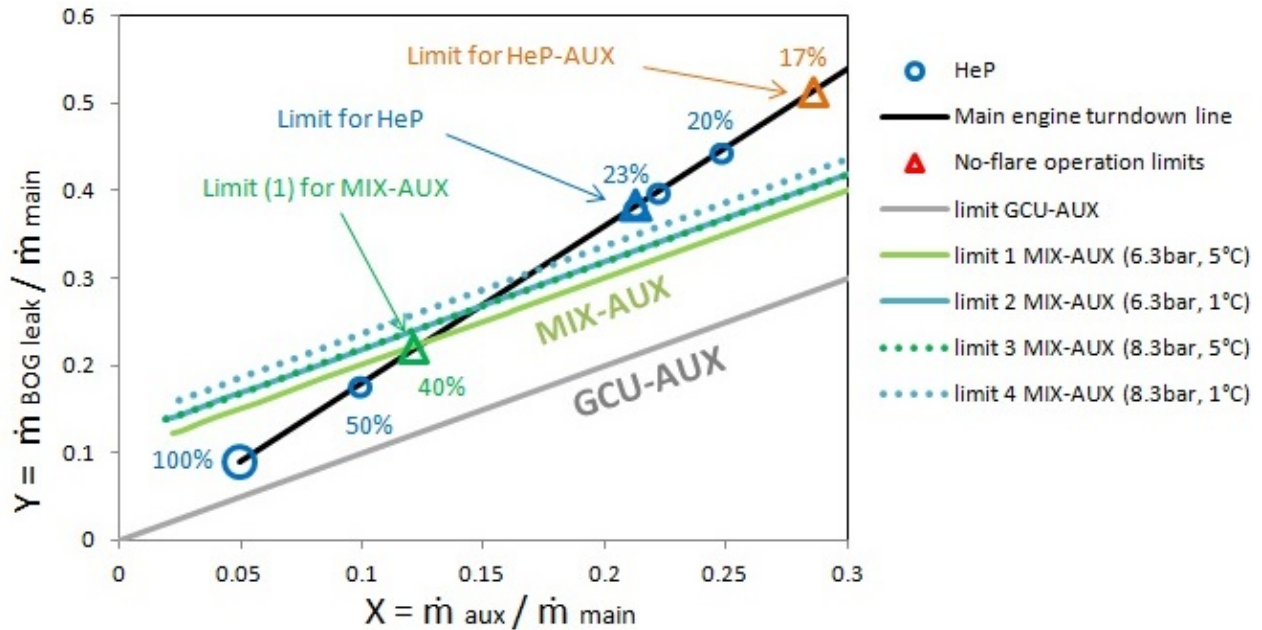


Figure 4.37: Boundary conditions for the process and limits for no-flaring operation, in a dimensionless plane

The main engine part load is represented by the black line, intersecting the origin of the axes and the 100%NCR point, supposing the AUX load and the heat leak constant.

On the grey bisector the AUX fuel consumption equals the BOG evaporation rate, this constitutes the no-flaring limit for the GCU-AUX process, any ship whose design point falls below this line will not require any additional BOG handling method except feeding it to the AUX engine.

The triangles mark the limits for the MIX-AUX, the HeP-AUX and the HeP process. The locus of the points where the limit of the MIX-AUX process occurs is the green line "limit 1 MIX-AUX" which refers to 5°C subcooling at HP Pump suction and 6.3 bar pressure in the recomdenser. If a lower subcooling and a higher pressure are allowed the no-flaring operation range can be extended, as shown by the other lines.

If a different design was chosen, for example a larger ship, with a more powerful Main engine and correspondently larger tank, but the same AUX engine



load, the design point would move to the left, and the steeper turndown line would cross the MIX-AUX limits at a higher percentage of the Main engine load. In other words the estimate of the Auxiliary engine's normal load can be a pivotal factor for choosing the most suitable BOG handling process.



# Chapter 5

## Equipment selection

### 5.1 LNG pumps

Cryogenic pumps for LNG applications are available as standard products in the market, for different applications in the various steps of the LNG chain, LNG pumps for marine applications include submersible pumps for marine tanks and HP pumps for fuel supply to HP engines.

#### 5.1.1 LNG High Pressure pump

When it comes to the selection of the HP pump, centrifugal pumps are not considered an option given the high pressure required by the ME-GI engines. Reciprocating HP cryogenic piston pumps are available on the market, designed for applications in fuelling stations for Compressed Natural Gas (CNG) vehicles, or specifically for Fuel Gas Supply System with ME-GI engines (eg. by Cryostar, Vanzetti...). As highlighted by the sensitivity analysis in the figure [C.18](#) of the appendix, the efficiency of the LNG HP pump is extremely determinant for the overall performance of the heat pump due to the pinch in the HPFHX (an increase in pump efficiency of 1% yields to a gain in the system's COP of about 2%). More in general the overall temperature rise across the pump related to the pump efficiency or to heat leak through the pump body, should be minimized in order to have a HP fluid as cold as possible in the HPFHX. These character-

istics, that would not be of particular importance in the equipment selection of a standard FGSS, deserve full consideration for the process described in this thesis and should be taken into account in the pump selection process.

### 5.1.2 LNG Low Pressure pump

For the selection of the low pressure pump, a wide number of products are available on the market. For FGSS in marine application LP submersible and non-submersible pumps are available.

Non-submersible pumps could be used if the position of the pump guarantees the NPSH required. For type-C tanks it is possible to position the pump at a low elevation next to the tank. For other types of tanks the position of the tank in the hull structure will favour the implementation of a submersible pump.

Technology for submersible pumps is well developed and models of submersible pump with submerged electric motor are available for a wide range of head and flowrate and for different applications [70, p.22]. Among other applications, submersible pumps are being manufactured specifically for extraction of LNG from the fuel tank and delivery to HP Pump and Auxiliary engines, EBARA produces submersible centrifugal LNG fuel pumps for non-LNGC ships' Fuel Gas Supply System with ME-GI engines [71, p.22].

Cryogenic pumps can have a minimum flowrate specification to ensure that the heat leak in the pump body and in the piping is not sufficient to induce cavitation in the impeller [54], for this reason and for simplicity the present design prescribes that the LP pump is used to feed both the Fuel Supply system and the Tank Reflux system, so that the flow is maintained also when the fuel supply is reduced. As a more efficient alternative to this design a dedicated pump could have been assigned to the LNG recirculation in the TRC.

On LNG Carriers dedicated LNG spray pumps are installed to distribute LNG to the spray ring [72, p.184] to control the tank atmosphere temperature, and occasionally to send LNG to forcing vaporizers. Typically spray pumps for LNGC

are 2 stage centrifugal pumps with a capacity of 40 to 50 m<sup>3</sup>/h [3, p.152], the efficiency for these machines is in the range 50 to 60% [3, p.144].

## 5.2 Refrigerant compressor

### 5.2.1 Requirements

One important feature, that differentiates this heat pump process from other reliquefaction cycles, is that the heat exits the heat pump cycle at low sub-ambient temperatures and is discharged to a process stream instead of the environment. In particular, during normal operation, the refrigerant compressor is placed after the recuperator REC and handles cold Nitrogen gas with suction temperature in the range -135 to -145°C. Most construction materials and metals are not applicable in this conditions, because of the degradation of mechanical properties at low temperatures. For example most unalloyed carbon steels become brittle at temperatures higher than -50°C [73]. The use of lubricant fluids is also restricted as they would freeze at low temperature.

For these reasons, the cold suction constrains dramatically the selection of the compressor, making it one of the most delicate step in the design of the system.

Figure 5.1 illustrates the operation conditions and specifications for the refrigerant compressor as simulated by the design model of the HeP and the HeP-AUX processes for the different main engine load scenarios, in a compressor operation map with mass flowrate in the horizontal axis and pressure ratio on the vertical axis. The results for each of the cases presented in the Chapter 4.5 are plotted together with the Refrigeration duty contour lines from the performance maps for each scenario. The bottom part of the graph in the figure shows the actual volume flowrate at suction condition which is a more adequate property for selecting a compressor.

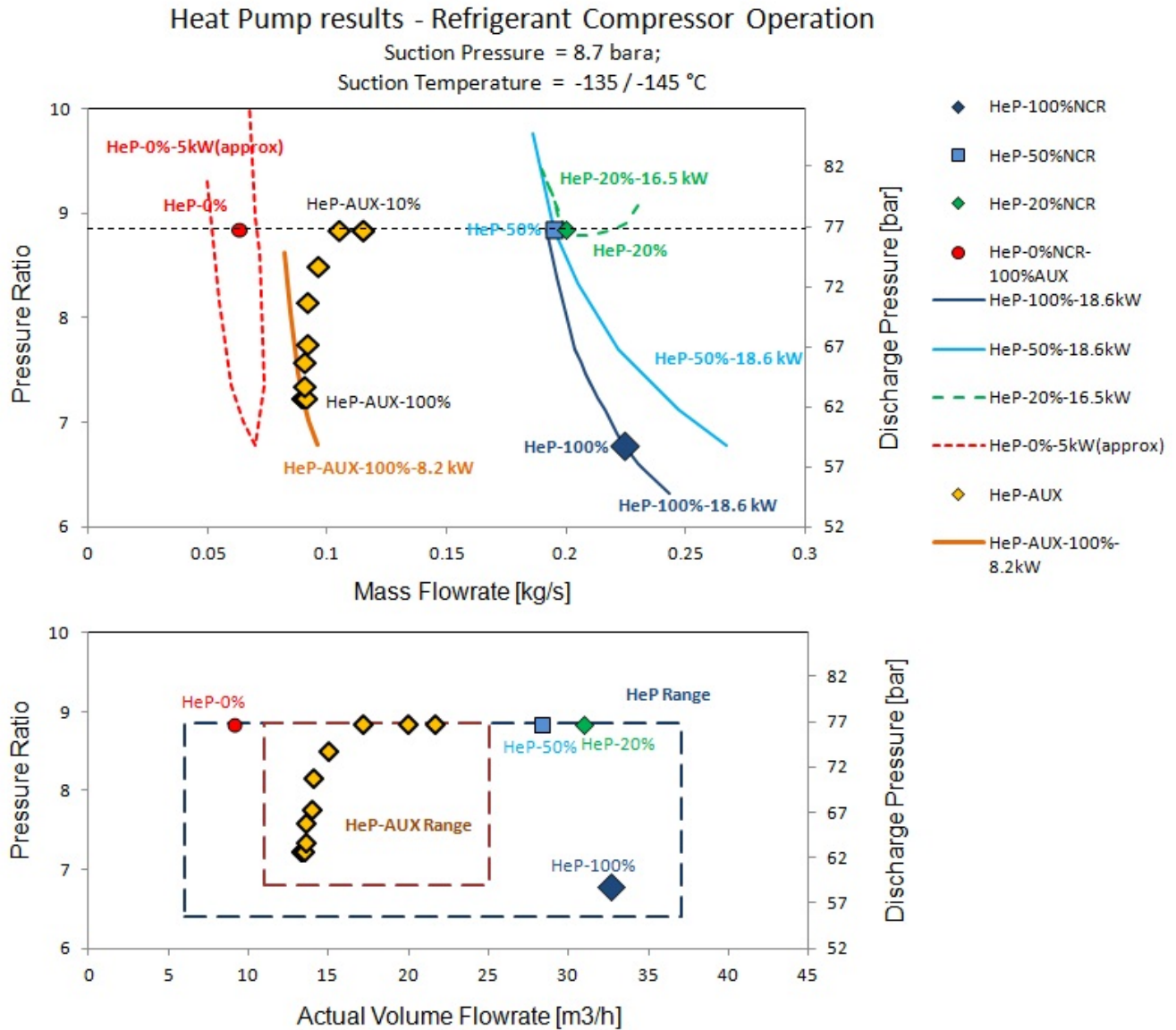


Figure 5.1: Operation range and specifications for the Refrigerant Compressor, in the HeP and HeP-AUX processes

The Figure contains all the relevant information to select a refrigerant compressors for the two scenarios, the squares indicate a possible specified range of operation in terms of pressure ratio and actual volume flowrate. The pressure rating of the compressor is the specified value of 77 bar, chosen higher than the optimum value at 100%NCR to allow operation at part load of the main engine. The HeP process demands a considerable turndown capability to the compressor in order to operate in the HeP-0%NCR-100%AUX scenario, the HeP-AUX

process does not have this problem because it can not work when the Main engine is off, therefore the operation range is more compact.

### 5.2.2 Compressor alternatives

The following types of machine have been considered in this study as possible options for the refrigerant compressor:

- Reciprocating;
- Screw;
- Centrifugal.

Table 5.1 compares three types of compressors for standard applications (non cryogenic suction) with respect to operational range. It appears that both reciprocating and screw machines exist in a oil-free configuration, but they cover a smaller range than the standard lubricated machines.

Table 5.1: Comparison table of three types of compressors [37]

Compressor Type		Reciprocating		Screw		Centrifugal
		Lube	Non-lube	Oil Flooded	Oil Free	
Pressure	Maximum Discharge Pressure	4500psiG (300barG)	1500psiG (100barG)	1500psiG (100barG)	600psiG (40barG)	3,000psiG (200barG)
	Maximum Pressure Ratio by Single Stage	3 : 1	3 : 1	> 50 : 1	4 : 1 ~7 : 1	1.5 : 1 ~ 3 : 1
Flow rate	Maximum Actual Inlet Volume	8800 ACFM (15000 m3/h)	8800 ACFM (15000 m3/h)	15000 ACFM (25000 m3/h)	41000 ACFM (70000 m3/h)	240000 ACFM+ (400000 m3/h+)
	Turndown accomplished by:	Suction valve unloaders (step and stepless) Clearance pockets Bypass	Suction valve unloaders (step and stepless) Clearance pockets Bypass	Slide valve (15-100%) step less Bypass	(None) Bypass	Inlet guide vane Speed control (70-100%) Bypass
	Polymer gas	Difficult	Difficult	Difficult	Possible	Difficult
	Dirty Gas	Possible	Difficult	Possible	Possible	Difficult
	MW Change	Possible	Possible	Possible	Possible	Difficult

(\*1) Two stage tandem arrangement maybe adopted in actual high pressure ratio application due to better efficiency.

Figure 5.2 can be used to match the operation range of the refrigerant compressor with those of standard industrial compressor products. Other cryogenic

compressors for LNG processes are qualitatively represented on the same diagram for comparison. The heat pump refrigerant compressors operates with a particularly low flowrate, that is outside the range of dynamic compressors and can be covered only by volumetric machines.

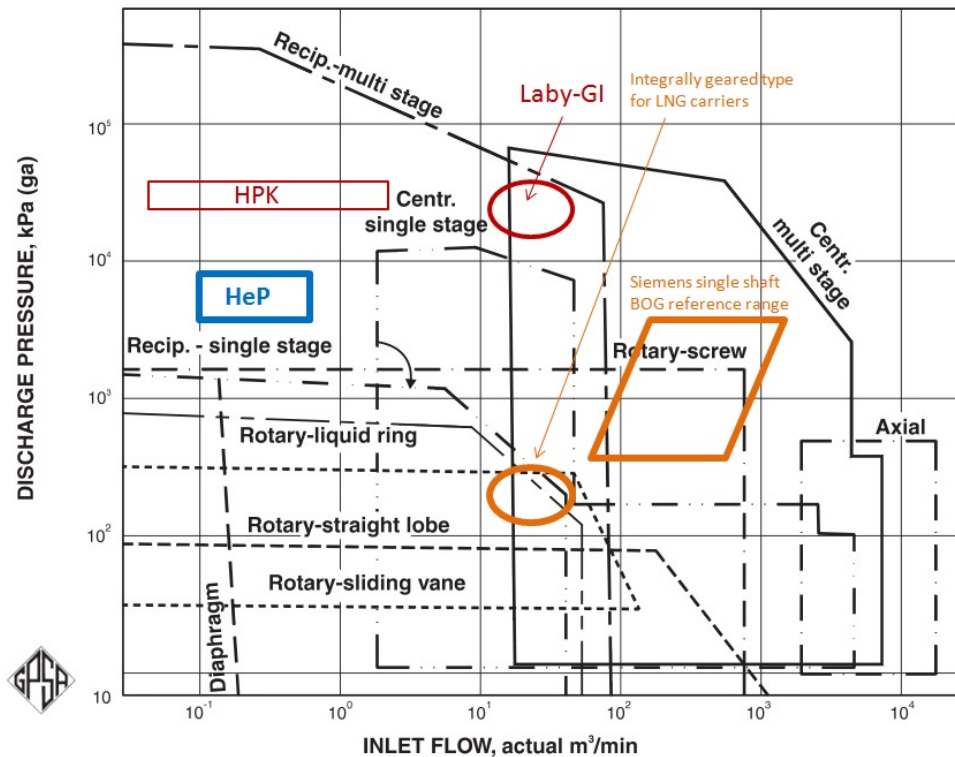


Figure 5.2: Compressor coverage chart [30, p.13-3] integrated with examples of operation ranges for BOG centrifugal compressors in LNG terminals [31] and LNG carriers. The blue rectangle indicates the heat pump specifications.

### Reciprocating compressors

Oil-free Labyrinth compressors are built for LNG BOG applications with cryogenic suction temperature as low as  $-160^{\circ}\text{C}$ , mainly for LNG terminals and storage facilities or LNG carriers applications.

Burckhardt Compression produces BOG compressors with a oil-free contact-free labyrinth sealing system, applied between the piston and cylinder walls and between the piston rod and the piston rod gland separating the oil free and lubricated areas [74]. Other manufacturers (of which SIAD, Kobelco, Dresser-Rand, Howden, IHI) offer more standard solutions with oil-free sealings with



contact between the sliding parts (eg. piston rings, or sliders in PTFE or alloys [75]) and the cylinder body.

The reciprocating compressor appears particularly suitable for the heat pump because of the following features:

- relatively low flowrate or swept volume (Figure 5.2);
- high compression ratio, with multiple stages (Figure 5.2);
- large turndown capability (reduction of flowrate) for part load operation (eg. with Variable Frequency Drive, suction valve unloaders [76] or bypass systems);
- possible reduction in compression ratio [75];

In other words besides being available in the required operating range, reciprocating machines offer good performance at part load operation (lower swept volume or lower pressure ratio than for design) [75]. When the pressure ratio deviates from the design value some reduction in efficiency is expected, this effect should be included in a complete Off-Design model of the heat pump process.

A qualitative idea of how the efficiency can vary with the discharge pressure and with the number of stages of an ordinary reciprocating compressor can be provided by Figure 5.3. A optimum stage compression ratio exists and the efficiency drops when the compression ratio deviates from this value, when more stages are added in series the optimum compression ratio is increased and the efficiency profile flattens out. However it is likely that for a compressor operating below ambient temperature, in which the cylinders are not cooled, the efficiency profile could be quite different.

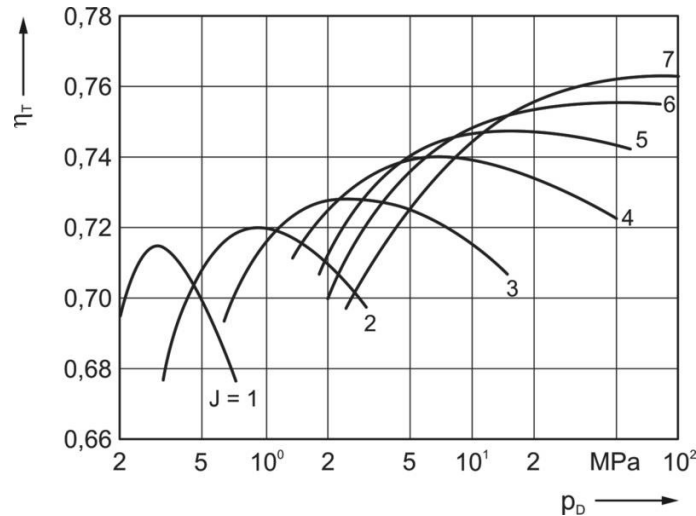


Figure 5.3: Example of isothermal efficiency profile as a function of discharge pressure and number of stages, for an ordinary reciprocating compressor with cooled stages [32]

The effect of volume flow on the compression efficiency might be even more difficult to model, because it depends primarily on the type of capacity control system that is adopted and should also take into account the different impact of the charge heating on the volumetric efficiency [77]. In other words an accurate Off-Design model of a reciprocating compressor, would at least require a specific correlation for the volumetric efficiency for cryogenic service, which goes beyond the scope of this study.

In general for a cold-suction oil-free compressor the efficiency is expected to be lower than for standard lubricated compressors, due to the complications in the design and the clearance volumetric losses, especially for labyrinth compressors [76]. The efficiency of a Burckhardt Labyrinth compressor has been estimated from the specifications for one particular compressor package in Table 5.2, using a isentropic compression model.

Table 5.2: Specifications for LNG BOG Oil-free Labyrinth compressor package from Burckhardt, at 0.99 bar and  $-142^{\circ}\text{C}$  suction, gas composition 11 mole%  $\text{N}_2$ , 89 mole%  $\text{CH}_4$  at 100% and 50% capacity [33]

**Specifications for Burckhardt 2K158-2D\_1.**

Discharge pressure bara	Inlet volume flow m <sup>3</sup> /h	Mass flow 100% kg/h	Shaft power at 100% kW	Mass flow 50% kg/h
22.22	771	1238	179	619
19.19	798	1282	170	641
18 1)	810	1301	159	650
10.29	893	1434	132	717

1) Estimated.

Figure 5.4 shows that this compressor package operates with a polytropic efficiency of about 69%, it is assumed that a similar value of the polytropic efficiency can be expected if a Burchkardt Oil-free Labyrinth BOG compressor is used for the heat pump described in the present thesis.

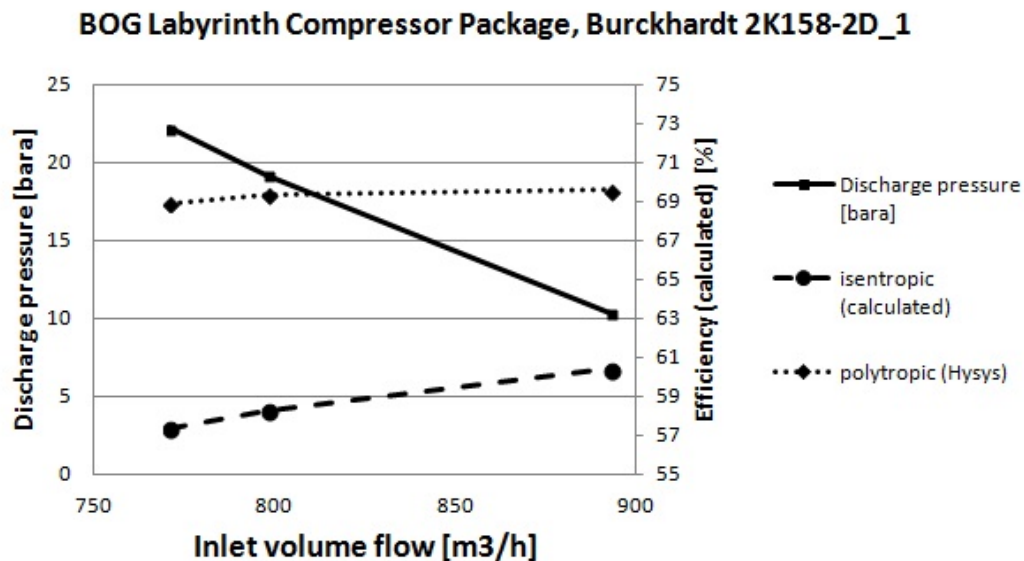


Figure 5.4: Efficiency of a BOG Oil-free Labyrinth compressor package [33]

Since the normal value input in the design model is 75% (Table 4.6), a compressor efficiency of 69% yields to a moderate degradation of the system performance, according to Figure C.16 the compressor work is expected to increase of about 12% for the normal operation scenario.

With respect to the low suction temperature, the heat pump refrigerant compressor is similar to commercially available machines in the LNG BOG compressor market, which, together with Ethylene BOG, represents the largest market for cold-suction compressors. This similarity is desirable for economic reasons since the adjustment of an existing compressor type or package, would require a lower investment cost than a fully tailored solution.

However there are some features that differentiate the heat pump refrigerant compressor from the BOG compressors, in particular the suction pressure (8.7 bar) and the maximum allowable pressure. In fact most LNG BOG compressors are designed for atmospheric suction pressure since they receive BOG from large atmospheric tanks, this means that the suction casing is designed for atmospheric pressure and lower density than specified here. At the same time, if a BOG compressor with a given pressure ratio is fed a gas at higher pressure, the outlet pressure will be many times higher than for atmospheric suction, and this might conflict with the pressure rating of the compressor structure. As an example one can consider a compressor with atmospheric suction and compressor ratio assumed constant and equal to 9: if gas at 8.7 bar is fed to the same machine it will be compressed to about 80 bar with a similar work input. The implication is that if the compressor body is designed for a discharge pressure of 9 bar, it would most likely not be qualified to work at 80 bar without structural modifications.

In chapter [4.7.1](#) the possibility of heating the compressor suction with the first stage discharge (Intercooling) has been discussed. The motivation for this modification, that complicates the process and reduces the efficiency, is to reduce the investment cost of the refrigerant compressor. This cost is expected to increase with decreasing suction temperature, due to the enhanced material requirements for the cold parts, in particular the cost function should have

steps in correspondence of the temperature where material upgrade is necessary. Table 5.3 reports an example of a material selection list for reciprocating compressor components according to the specified suction temperature.

T suction [C]		-160°C	-100°C	-40°C	-20°C
Piston rods, liners, valves, packing cases	material	Stainless Steel 17-4PH / AISI630 / 1.4542 / X5CrNiCuNb16-4	Alloy Steel AIS4340 / 1.6547 / BS835M30 / 30NiCrMo16	X30Cr13 Alloy steel 13% Chrome (1.4028 – Z33C13 –AISI420)	
	treatment	H1150M heat treatment + hardness treatment or coating	heat treated at 26-32 HRC + hardness treatment or coating.	heat treated to 850-1000 N/mm <sup>2</sup> + hardness treatment or coating	
Cylinders	casting material	Grey cast iron GG25 (ASTM A48gr30 – EN-GJL-250) / GG30 / GGGNi35 (Ni-Resist nodular cast Iron) (ASTM A436gr2B) / ASTM A351cf8			ordinary
Piston rings, wear bands, seal elements	material	Polymer alloy / Filled PTFE			

Table 5.3: Example of material selection guidelines for reciprocating compressor parts depending on suction temperature, from a compressor component manufacturer

The table evidences three temperature levels at which the cost is expected to step up, the first is at -20°C due to the adoption of special casting material for the cylinders, the others occur at about -40°C and -100°C due to upgrade of material specifications for piston rods, liners, valves and packings. To assess the viability of the intercooling option the impact of the suction temperature on the cost of the machine should be quantitatively estimated.

#### Screw compressors

Screw compressors are also available with an oil-free design, where a clearance between the two screws guarantees that there is no contact between the moving parts [37]. Even though the manufacturers offer screw compressor solution that can replace reciprocating compressors in a number of applications [37], no information has been found regarding use of screw compressors with cold suction temperatures. However if this kind of machine was made available it would certainly be an interesting alternative to the reciprocating option.

### Centrifugal compressors

Centrifugal compressors are used for LNG BOG handling in LNG terminals and LNG carriers, they have also been developed for low temperature cryogenics Helium applications [78], [79, p.174].

Since in any kind of centrifugal compressor the clearance between the impeller and the casing is not lubricated the use of these machines for cold-suction applications poses less challenges than other types of compressors do. In the Low Duty BOG compressor design for LNG carriers the lubricated shaft bearings are located in the warm gearbox separated from the cold impeller channels, pressurized seal gas (eg. Nitrogen) is injected in the labyrinth sealings between the bearings and the compressor rotor to avoid any oil slip into the impeller and gas penetration in the gearbox [3].

There are a number of reasons why the centrifugal compressors are considered not suitable for the heat pump application:

- they are generally designed for large volume flowrate and low compression ratio (Figure 5.2);
- they have poor turndown capability, usually work around 80-100% of capacity [78, p.215][76];
- they require stable suction temperature and density to keep within the surge limits [76]

### 5.3 BOG compressor

As discussed the BOG compressor allows to send as much BOG as possible to the Auxiliary engine offering the most immediate and efficient solution to the BOG handling problem (HeP-AUX case). When it comes to component selection the same considerations that were outlined in the previous section are still valid, with the advantage that the compressor operates in the range 1 to 6.3 bar, as

most commercial LNG BOG packages. Like for the refrigerant compressors it can be concluded that a reciprocating compressor is probably the best option for BOG compression.

## 5.4 Heat exchangers

The heat pump process (HeP) is constituted by four heat exchangers belonging to the nitrogen refrigerant cycle, namely HPFHX, LPFHX, REC and TRC (the LPFHX is not present in the HeP-AUX configuration) and two belonging to the Fuel Gas Supply System (High Pressure Vaporizer "HPV" and Low Pressure Vaporizer "LPV").

The two vaporizers (HPV and LPV) need to be sized regardless of the heat pump operation, as they would be in service also when the heat pump is off. Moreover they are standard process equipment produced for ME-GI systems for which specifications already exist. For these reasons the requirements for the vaporizers have not been covered henceforward.

Regarding the four heat pump heat exchangers the requirements regarding flowrate and pressure rating can be extracted from the "Process equipment mass and energy balance" Tables for each of the design model scenarios. From the simulations presented in this thesis, some suggestions can be made regarding the types of heat exchangers to be used, this would set the basis for further detailed calculations and provide accurate inputs to a future Off-Design model.

The heat exchanger types taken into considerations in this chapter are Shell&Tube heat exchangers (S&T) and Plate (Plate&Frame) heat exchangers. The former are considered a default choice since they are available in many different configurations and built for a wide range of operating parameters, S&T heat exchangers can also support high pressure on the shell and especially the tube side and high differential pressure between the two sides [80]. Plate heat exchangers are

more compact and cheaper than S&T but can be used in a more limited range of applications [81], in particular they are not designed for high pressure and do not support high differential pressure between the two sides that would bend the plates. Copper brazed plate heat exchangers are used in the Mini LNG reliquefaction process by Sintef at cryogenic temperatures and with differential pressures up to 17 bar between the hot and cold side. This application proves that these components can work also with multicomponent mixtures undergoing phase change.

Plate-Fin heat exchangers are even more compact than Plate&Frame but have not been taken into consideration because they are more complex and delicate and require slow thermal transients due to the poor mechanical resistance to thermal stress. Considering the type of fluids and the pressures in the heat pump process a possible set of choices for the heat exchangers could be:

- HPFHX: Shell&Tube  
due to the relatively high pressure on the LNG side (300 bar) and the differential pressure;
- LPFHX: Shell&Tube  
due to the relatively high pressure on the refrigerant side (up to 77 bar) and the differential pressure. It should be noted that if the refrigerant is on the tube side the evaporating LNG mixture could observe liquid enrichment on the shell side with degradation of heat transfer effectiveness. If this is considered a problem LNG should be evaporated in the tube side;
- REC: Shell&Tube  
same considerations as for the LPFHX, in this case the HP refrigerant should flow in the tube side so that the shell is not exposed to high pressure;
- TRC evaporator: Plate  
since it is allowed by the moderate pressure on both sides.



The main parameter for the heat exchanger sizing that can be extracted from the simulation results is the  $U \cdot A$  product between the heat transfer coefficient  $U$  [ $\text{kW}/(\text{m}^2 \cdot \text{K})$ ] and the heat exchange area  $A$  [ $\text{m}^2$ ]. In Figure 5.5 the  $U \cdot A$  values for each heat exchanger computed by the Design model are displayed for four different scenarios of Main engine fuel flow.

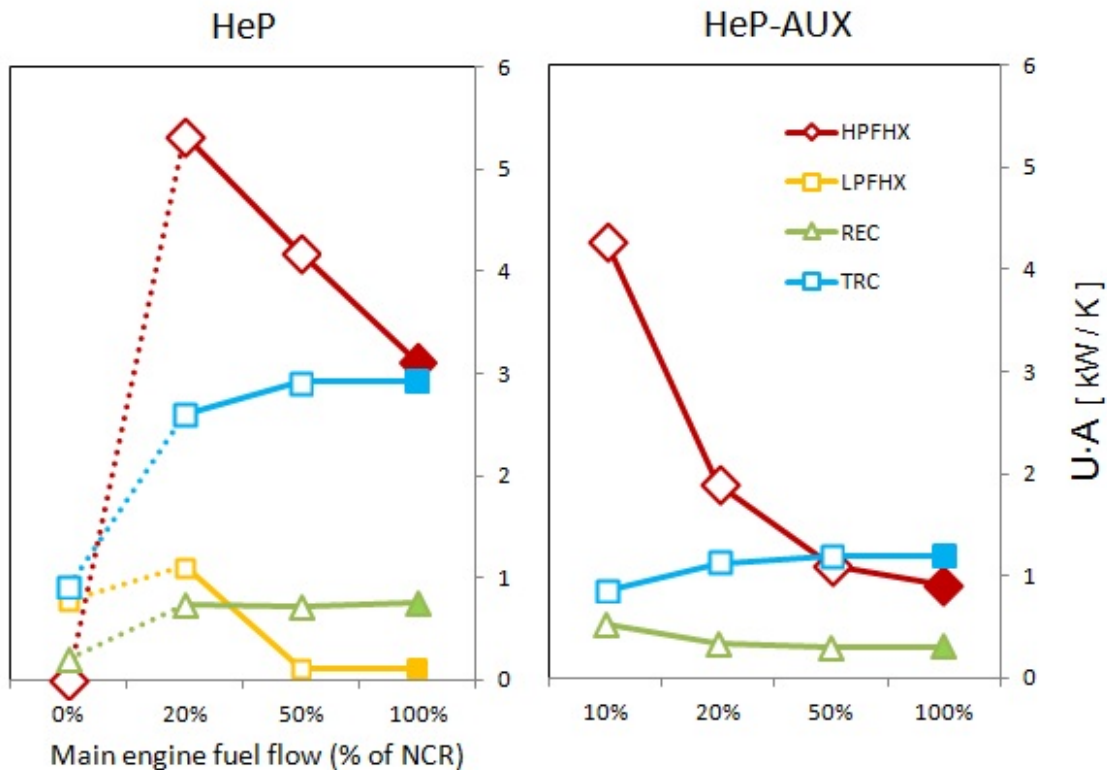


Figure 5.5: Heat Exchangers  $U \cdot A$  values, calculated by the Design Model to provide a specified MITA of  $5^\circ\text{C}$ , for the HeP and HeP-AUX processes.

The diagram indicates that, for the heat exchangers crossed by LNG fuel, the heat transfer area required to ensure the specified  $5^\circ\text{C}$  MITA increases at low main engine load. For the HPFHX this is due to the reduced flowrate on the HP LNG side, that pushes the LNG curve against the nitrogen curve, causing an internal pinch point and lowering the LMTD of the heat exchanger. This effect is even more relevant for the LPFHX in the HeP process, since the heat transferred by this component in the HeP-20%NCR case is many times larger than for the normal operation scenario HeP-100%NCR.

Based on this analysis the design value the heat transfer area of the HPFHX and LPFHX should be close to the value estimated by the part load scenarios, rather than the normal operation scenario. For example for the HPFHX a UA value of 5-6 kW/K could be an appropriate specification for the component selection and for accurate Off-Design modeling of the process.

# Chapter 6

## Conclusion

A heat pump process has been designed and optimized, for the purpose of extracting heat from an LNG marine fuel tank and thus control the BOG production. Two layouts of the heat pump process, indicated with "HeP" and "HeP-AUX", have been simulated with HYSYS® and compared with other options for BOG handling described in the literature.

The main characteristic features of the system, that differentiate it from standard reliquefaction cycles for LNG Carriers, are the cold compressor suction, the absence of heat discharge to the environment and the complete heat integration with the Fuel Gas Supply System. These features make the heat pump more efficient than reliquefaction cycles in the given Design scenario. However, the reliquefaction is the only process among those considered that ensures BOG control when the Main engine is off.

The simulation results show that the most efficient solutions are the heat pump process coupled with a BOG compressor for Auxiliary engine feed (HeP-AUX), the "Terminal type" or Recondenser process (MIX-AUX) and the High Pressure Compression of the BOG (HPK).

The MIX-AUX process gives the lowest energy consumptions but fails to recondense all BOG when the Main engine load is low. The HeP-AUX and the HPK

process have a similar energy consumption, but the HPK ensures that the BOG is used in all of the operating range of the engine down to the minimum for gas injection. None of these three processes can operate when the main engine is off, in which case the BOG that exceeds the Auxiliary consumption is burnt in Gas Combustion Units (GCU). Table 6.1 summarizes the positive and negative aspects of these three alternatives regarding efficiency and plant complexity.

Table 6.1: Pros and cons of the three best options for BOG handling

	<b>HeP-AUX</b>	<b>MIX-AUX</b>	<b>HPK</b>
Energy consumption (100%NCR)	good	excellent	good
Main engine turndown tolerance (based on Design model simulations)	good	fair	excellent
BOG handling in Idle/Harbour scenario	GCU	GCU	GCU
Number of additional components (compared to GCU scenario)	5	2	1
Special components	Refrigerant compressor	Recondenser	HPK: 5 stages reciprocating
"Critical" HX	HPFHX, REC	-	-
Overall plant complexity	high	low	medium

It has been assumed that in the HPK scenario a five stages reciprocating machine would be needed, similar to the Laby-GI compressor for LNG Carrier service, redesigned for the significantly lower capacity. This is the only non conventional process components of the HPK layout, that moderately increases the overall plant complexity.

The MIX-AUX process is by far the simplest of the three, the only special component required is the Recondenser which is a gas-liquid contactor operating at a moderate pressure.

The HeP-AUX process on the contrary counts a higher number of units, of which one Nitrogen two stage reciprocating compressor with moderately high discharge

pressure (77 bar) and two heat exchangers with high differential pressure, making this process the most complex among the three.

Given its simplicity and high efficiency, the MIX-AUX process is probably the most suitable for the given design specification.

It is not excluded that the heat pump process could compete with the MIX-AUX in a different design scenario, where the relative weight of the AUX engine consumption is lower and the MIX-AUX process flexibility at part load is reduced.

# Appendix A.0 ME-GI engines

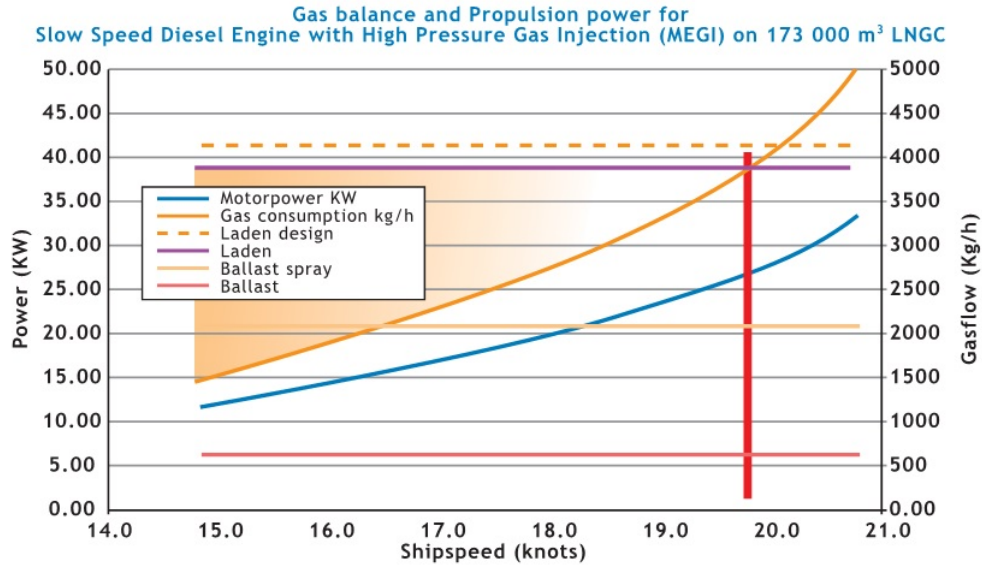


Figure A.1: LNG Carrier estimated BOG evaporation and consumption rate as a function of ship speed [34, p.5]

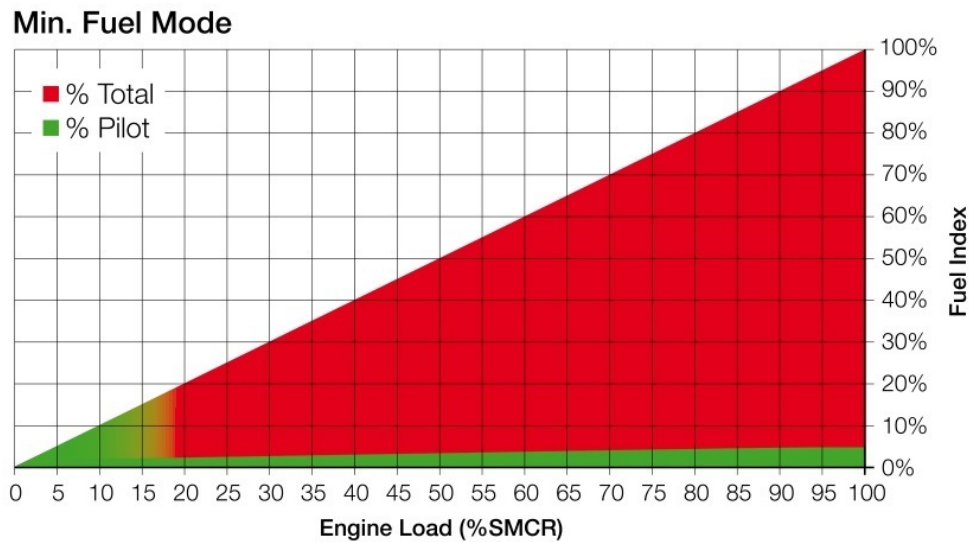


Figure A.2: Quantity of pilot fuel at varying load of the ME-GI engine at Minimum Fuel Mode [19]

## MAN B&W Low Speed Propulsion Engines

### Engine Type Designation

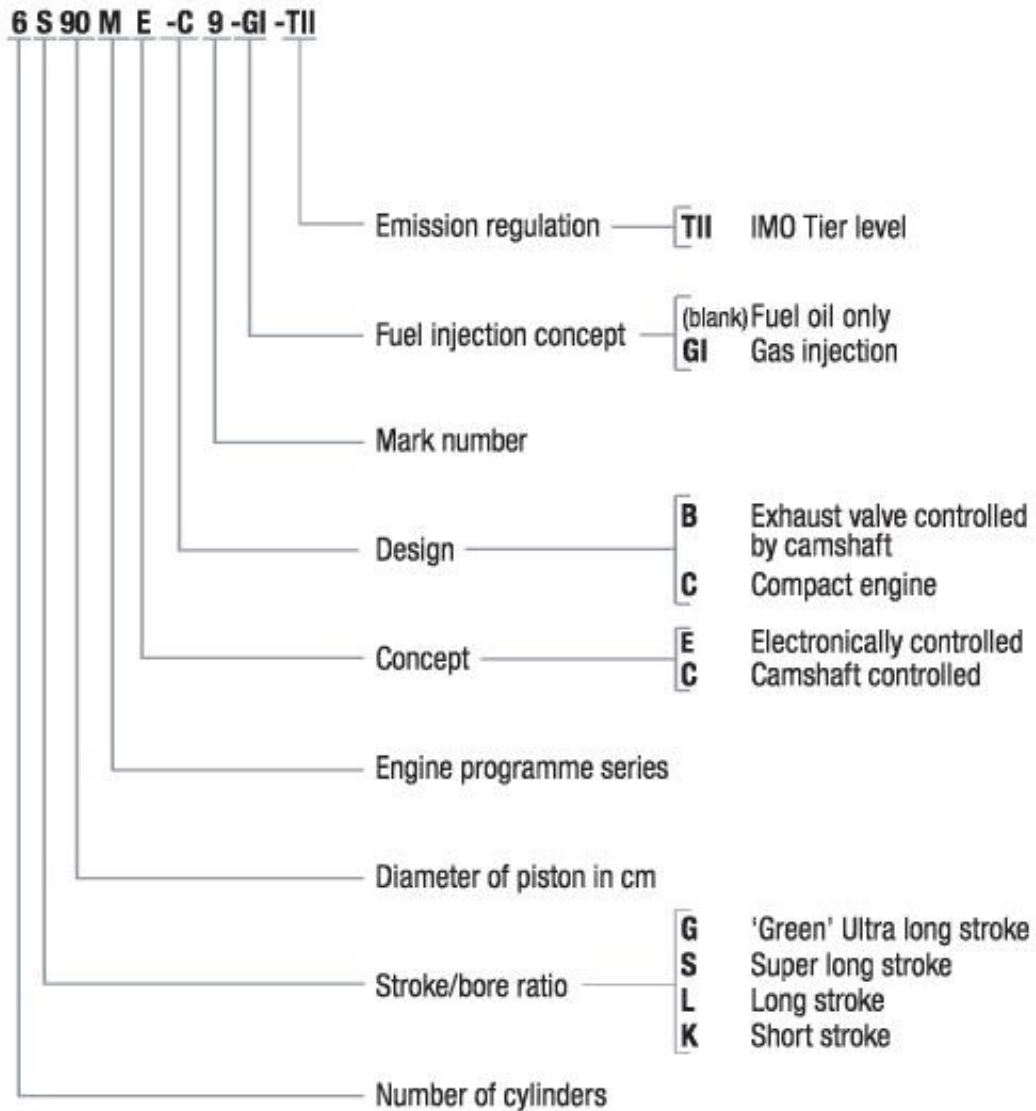
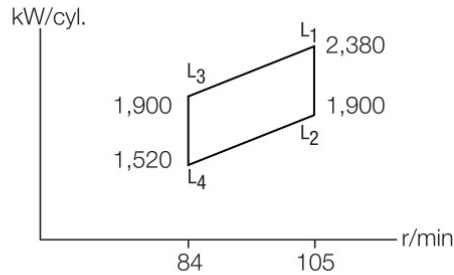


Figure A.3: Nomenclature for MAN engines [35, p.18]

**MAN B&W S60ME-C8-GI**

Cyl.	L <sub>1</sub> kW	Stroke: 2,400 mm
5	11,900	
6	14,280	
7	16,660	
8	19,040	



**SFOC gas engines [g/kWh]**

L<sub>1</sub>/L<sub>3</sub> MEP: 20.0 bar – L<sub>2</sub>/L<sub>4</sub> MEP: 16.0 bar

		50%	75%	100%
Gas and pilot fuel (42,700 kJ/kg)	L <sub>1</sub>	164.5	162.0	168.0
	L <sub>2</sub>	160.5	156.0	162.0
	L <sub>3</sub>	164.5	162.5	168.0
	L <sub>4</sub>	160.5	156.5	162.0
Liquid fuel only (42,700 kJ/kg)	L <sub>1</sub> / L <sub>3</sub>	167.5	165.0	169.0
	L <sub>2</sub> / L <sub>4</sub>	163.5	159.0	163.0

Specific gas consumption consists of 3% pilot liquid fuel and gas fuel.

Gas fuel LCV (50,000 kJ/kg) is converted to diesel fuel LCV (42,700 kJ/kg) for comparison with diesel engine

**Distributed fuel data [g/kWh]**

		50%	75%	100%
Gas fuel (50,000 kJ/kg)	L <sub>1</sub>	133.7	133.1	139.2
	L <sub>2</sub>	128.5	126.7	133.0
	L <sub>3</sub>	133.7	133.6	139.2
	L <sub>4</sub>	128.5	127.1	133.0
Pilot fuel (42,700 kJ/kg)	L <sub>1</sub> / L <sub>3</sub>	8.0	6.1	5.0
	L <sub>2</sub> / L <sub>4</sub>	10.0	7.6	6.3

**Specifications**

Dimensions:		A	B	C	H <sub>1</sub>	H <sub>2</sub>	H <sub>3</sub>
	mm	1,020	3,770	1,300	10,825	10,000	9,775
Cylinders:		5	6	7	8		
L <sub>min</sub>	mm	6,439	7,459	8,479	9,499		
Dry mass	t	308	350	393	452		

Figure A.4: ME-GI Engine datasheet for the design case selection [35, p.53]



# Appendix B.0 Ships Operational Profiles

## B.1 Main engine

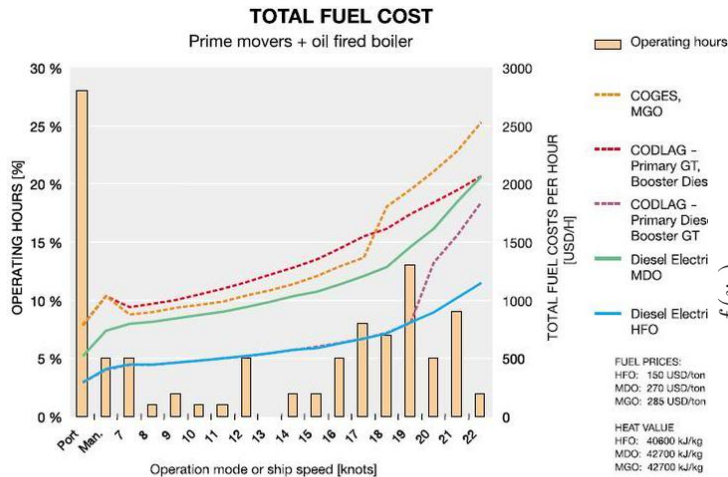


Fig. 4 Fuel cost at different speeds for a Panamax-max vessel.

Figure B.1: (Operation profile of a Panamax-max vessel)

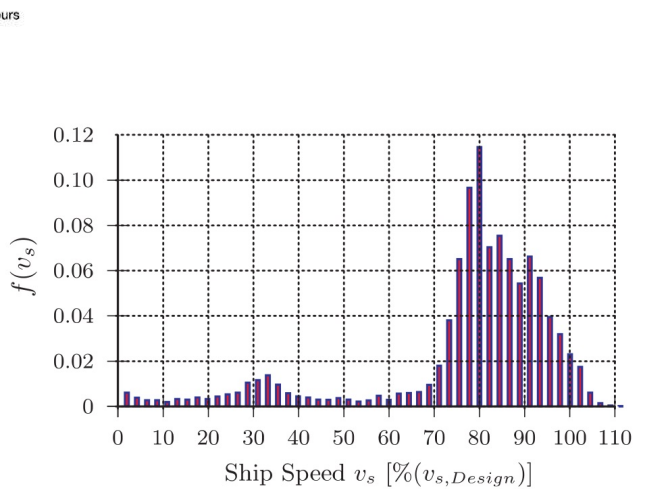


Figure B.2: Operation profile of a North Sea ferry, [36]

Table B.1: Measurement of power consumption of a chemical tanker vessel during the analysed navigation conditions [38]

Operation Scenario	Speed [kn]	Mechanical	Electrical	Thermal	% time [%]
		Power [KW]	Power [KW]	Power [KW]	
Navigation-full load	15	7363	752	6949	41,4
Navigation-full load	12	4400	752	6844	2,8
Navigation-full load	9	2200	752	6759	1,0
Navigation-ballast trip	15	6000	752	694	41,4
Navigation-ballast trip	12	3500	752	603	2,8
Navigation-ballast trip	9	1930	752	541	1,0
Manoeuvring full load		2018	1782	4645	0,3
Manoeuvring ballast		1930	1782	386	0,1
Waiting full load		0	489	6654	1,5
Waiting ballast		0	489	447	2,7
Harbour cargo handling (Harbour)		0	2123	4838	4,7
		0	470	331	0,4

Table B.2: Operation profile of the vessel with respect to main and auxiliary engines load, calculated from table B.1

Aux Engine							
5	80-105%	5	0,4				
	40-80%						
95	20-40%	5	2	6	41	41	
	0-20%						
	0%						
	% Installed Power	0%	0-30%	30-60%	60-80%	80-100%	Main Engine
% Time		9	2	6	41	41	

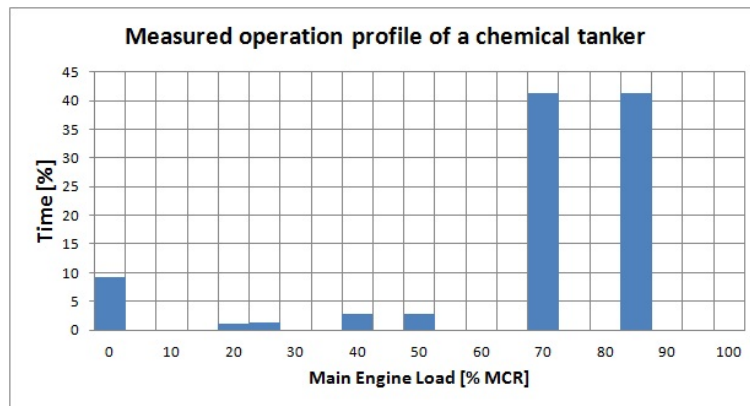


Figure B.3: Main engine operation profile of the vessel, from Table B.1

## B.2 Auxiliary engines

Table B.3: Auxiliary engine load in relation to the value at normal operation and as a fraction of the installed capacity, extracted from Table B.4

Ship Regime	Total Load [kW]	Fraction of Normal Power	Fraction of Installed Power
Normal Seagoing	538.5	100%	16%
Normal + Rep. Cont. Keep	645.4	120%	19%
Leaving Port with Thruster	2820.1	524%	83%
Leaving Port + Alpha	2946.1	547%	87%
Cargo Handling	1157.1	215%	34%
Rest In port	395.0	73%	12%
Emergency Service	72.1	13%	2%

ANTICIPATED ELECTRIC POWER CONSUMPTION TABLE

TS1533 DATE 2005/10/11

EL. & CONT. ENG. DEPT CHECKED BY

M: SC: AC: CE: HULL GROUP: MACH GROUP:

OWNER : GRIEG CLASS : INV-EO

KIND : 45 OPEN HATCH BC RULE : SOLAS2000, MARPOL, USCG(FV), PANAMA

DEADWEIGHT : 45,000 TON

PRINCIPAL DIMENSIONS : LPP 187 M X B 31 M X D 19 M - DFT 12 M

MAIN ENGINE : 6560MC 10,520 KW(MCR) 96.0 RPM X 1 SET

REMARKS : DIESEL GENERATOR : 1300 KW ( 1625 KVA ) 720 RPM X 2 SETS  
 DIESEL GENERATOR : 720 KW ( 900 KVA ) 720.0 RPM X 1 SET  
 EMERG. GENERATOR : 80 KW ( 100 KVA ) 1800 RPM X 1 SET

(A) TOTAL ELECTRIC POWER BALANCE CALCULATION

ITEM	NORMAL SEAGOING	NORMAL + REF. CONT. KEEP	LEAVING PORT WITH JARHUSTER	LEAVING PORT + ALPHA	CARGO HANDLING	REST IN PORT	EMERGENCY SERVICE
HULL CONTINUOUS LOAD (KW)	127.5	234.4	2278.3	2404.3	681.8	88.3	49.5
HULL PART INTERMITTENT LOAD (KW)	74.4	74.4	74.4	74.4	74.4	74.4	0.0
MACHINERY CONTINUOUS LOAD (KW)	320.5	320.5	455.8	455.8	329.4	190.5	0.0
MACHINERY PART INTERMITTENT LOAD (KW)	34.8	34.8	9.8	9.8	105.2	100.2	0.0
ELECTRICAL CONTINUOUS LOAD (KW)	54.1	54.1	57.9	57.9	86.0	58.0	22.6
ELECTRICAL PART INTERMITTENT LOAD (KW)	0.0	0.0	0.0	0.0	0.0	0.0	0.0
1) TOTAL CONTINUOUS LOAD (KW)	502.1	609.0	2792.0	2918.0	1097.2	336.8	72.1
2) INTERMITTENT LOAD (KW)	109.2	109.2	84.2	84.2	179.6	174.6	0.0
3) 2)/DIVERSITY FACTOR (3.0) (KW)	36.4	36.4	28.1	28.1	59.9	58.2	0.0
4) TOTAL LOAD 1) + 3) (KW)	538.5	645.4	2820.0	2946.0	1157.1	395.0	72.1
5) WORKING GENERATORS (KW X NO.)	DG 720 KW X 1	DG 720 KW X 1	DG 1300 KW X 2 DG 720 KW X 1	DG 1300 KW X 2 DG 720 KW X 1	DG 1300 KW X 2 DG 720 KW X 1	DG 720 KW X 1	EG 80 KW X 1
6) AVAILABLE GENERATOR CAPACITY	720.0 KW	720.0 KW	3320.0 KW	3320.0 KW	2600.0 KW	720.0 KW	60.0 KW
7) 4) / 6)	F 74.8 %	89.6 %	84.9 %	85.7 %	44.5 %	54.9 %	90.1 %

Figure B.4: Anticipated electric power consumption table for a vessel of a similar size than the design case [7]

# Appendix C.0 Simulation results

## C.1 Tank energy balance and cooling duty calculations

When simulation results are presented the refrigeration duty is calculated on the basis of an energy balance on the LNG fuel tank.

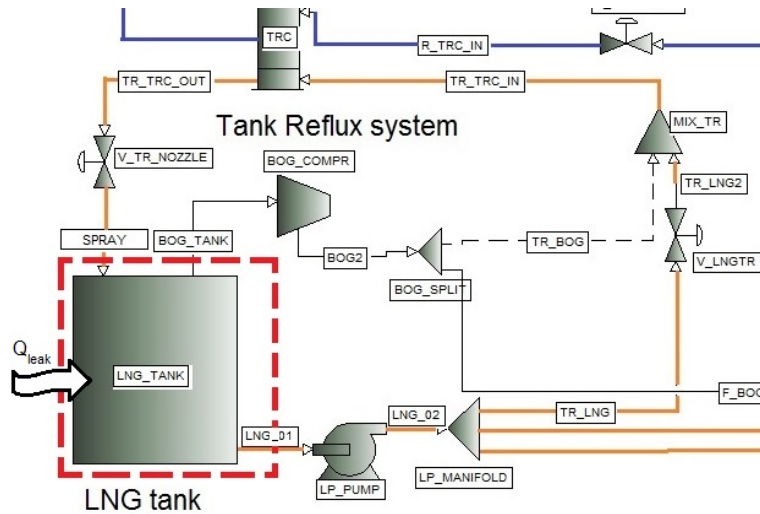


Figure C.1: Energy balance control volume

Energy balance of the LNG fuel tank, including BOG extraction

$$\frac{dE}{dt} = \dot{Q}_{leak} - \dot{m}_{LPP} \cdot h_{LNG} + \dot{m}_{TR} \cdot h_{Spray} - \dot{m}_{BOG} \cdot h_{BOG} \quad (C.1)$$

Energy balance of the LNG fuel tank, excluding BOG extraction

$$\frac{dE}{dt} = \dot{Q}_{leak} - \dot{m}_{LPP} \cdot h_{LNG} + \dot{m}_{TR} \cdot h_{Spray} \quad (C.2)$$

Energy balance of the LNG fuel tank, LP pump term is split

$$\frac{dE}{dt} = \dot{Q}_{leak} - \dot{m}_{fuel} \cdot h_{LNG} - \dot{m}_{TR} \cdot (h_{LNG} - h_{Spray}) \quad (C.3)$$

Refrigeration duty is calculated from the enthalpy increase of the Tank Reflux

stream, the contribution of the fuel to the energy balance is neglected

$$\dot{Q}_{Ref} = \dot{m}_{TR} \cdot (h_{LNG} - h_{Spray}) = \dot{m}_{TR} \cdot (\Delta h_{TRC} - \Delta h_{LPP}) \quad (C.4)$$

## C.2 Case studies

### C.2.1 Case HeP - 100 % NCR

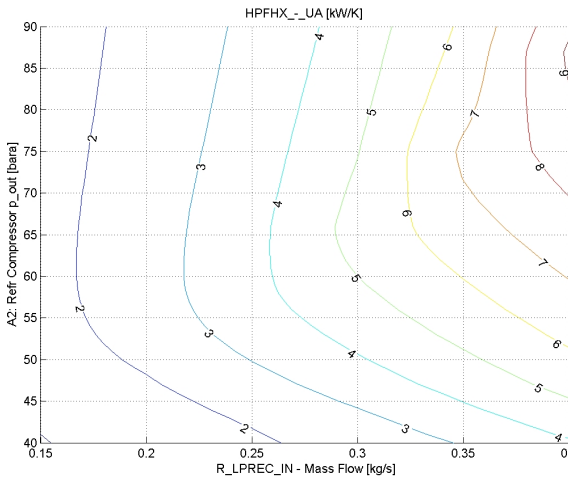


Figure C.2: HPFHX: UA

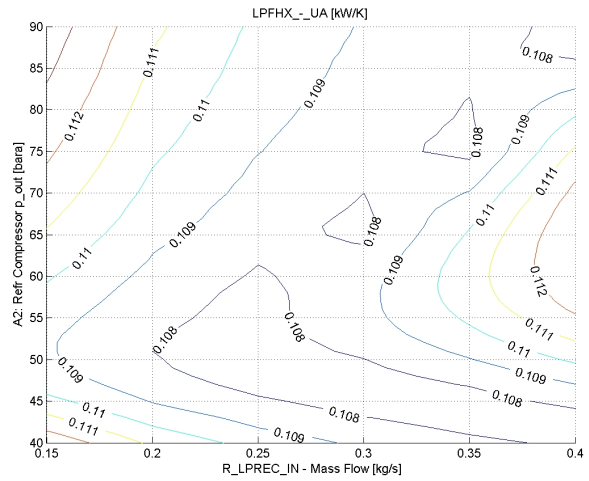


Figure C.3: LPFHX: UA

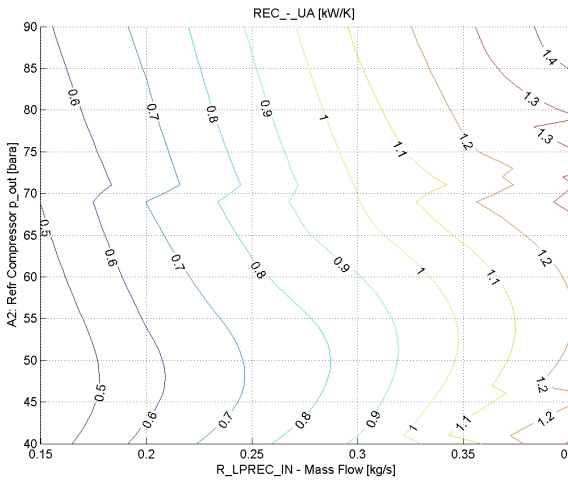


Figure C.4: REC: UA

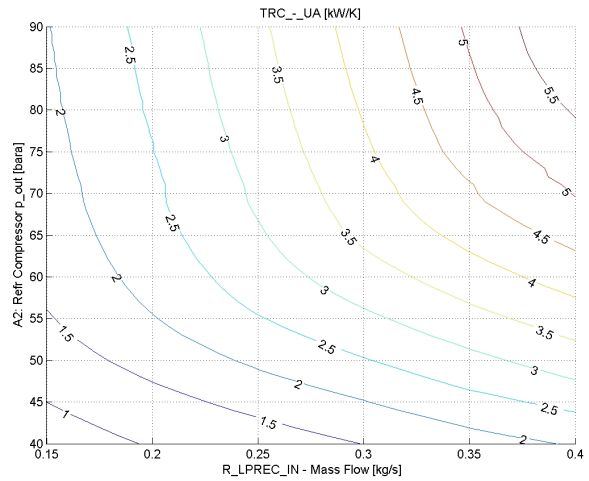


Figure C.5: TRC: UA

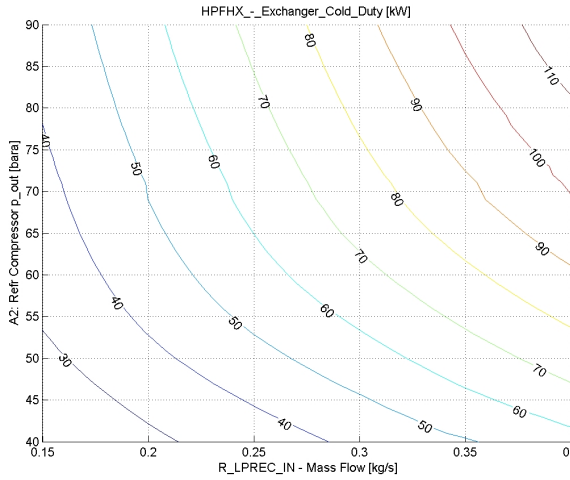


Figure C.6: HPFHX: Duty

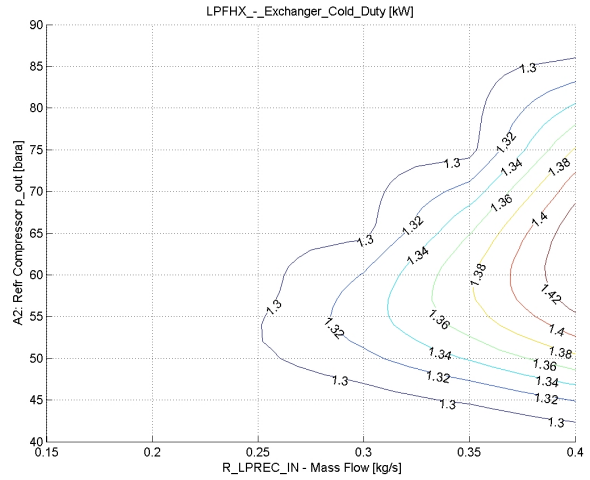


Figure C.7: LPFHX: Duty

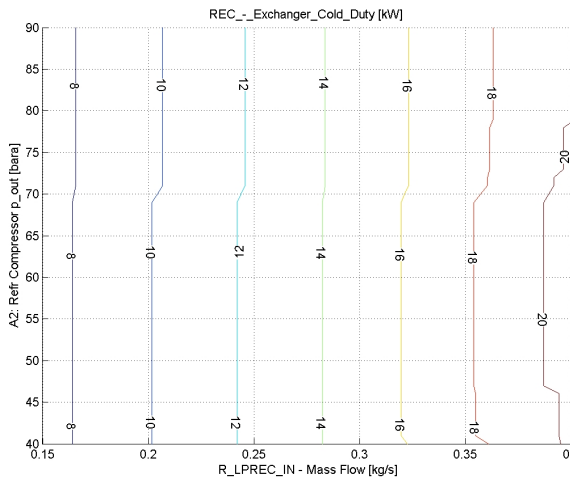


Figure C.8: REC: Duty

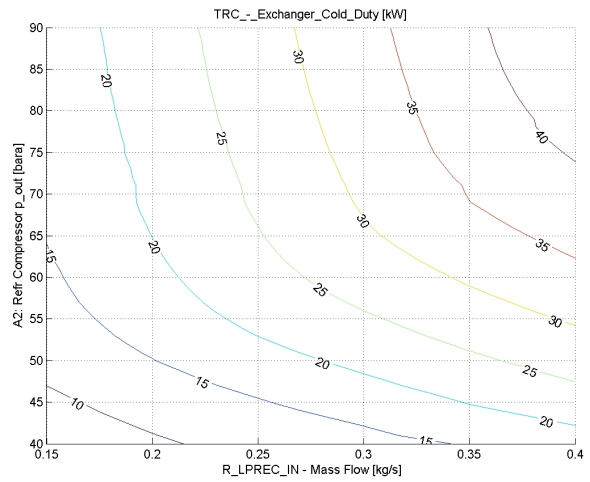


Figure C.9: TRC: Duty

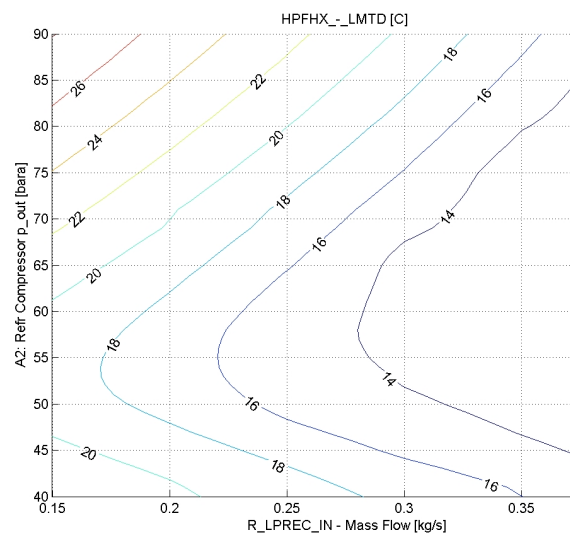


Figure C.10: HPFHX: LMTD

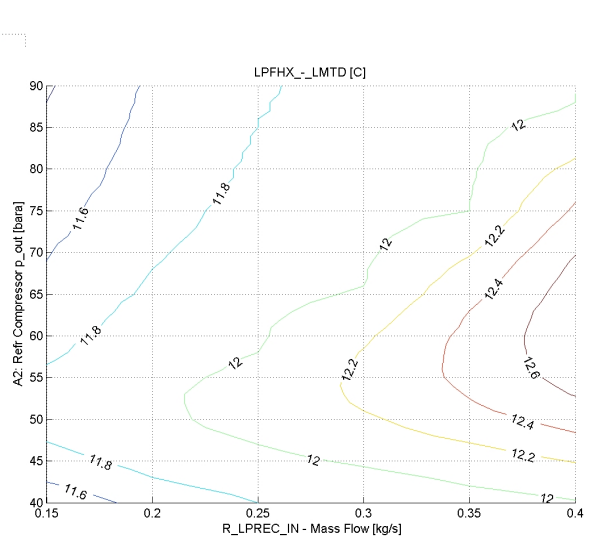


Figure C.11: LPFHX: LMTD

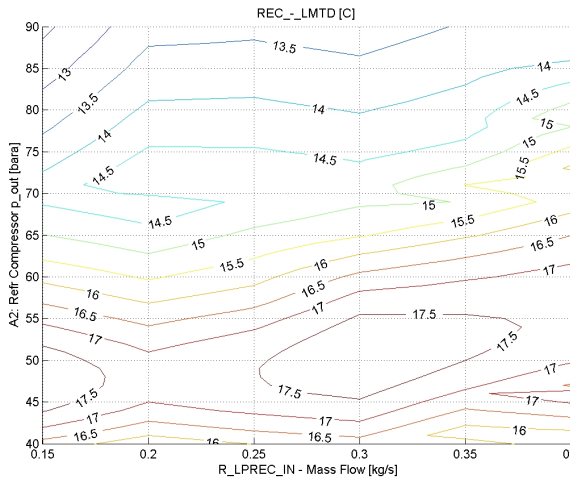


Figure C.12: REC: LMTD

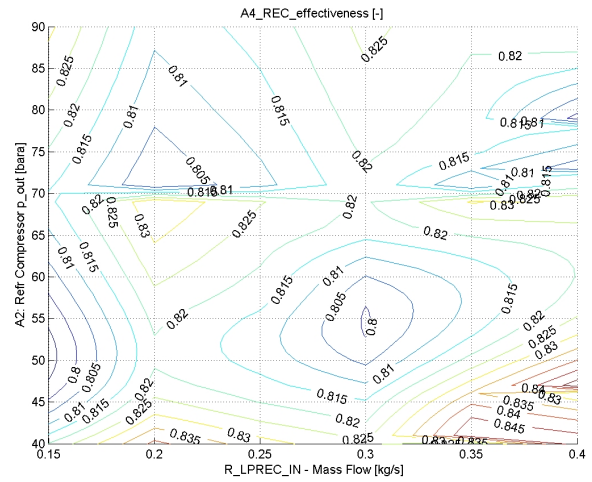


Figure C.13: REC: Effectiveness

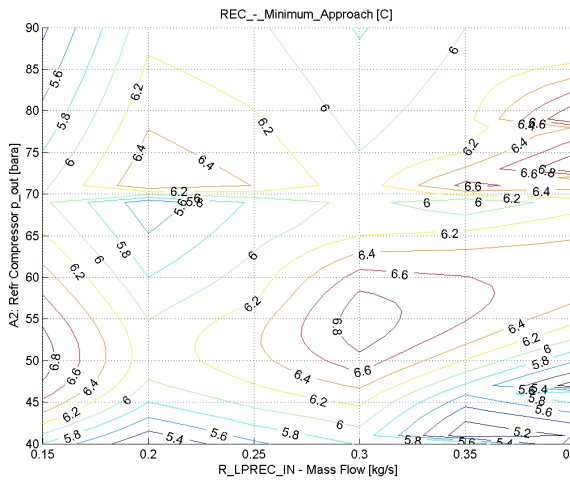


Figure C.14: REC: MITA

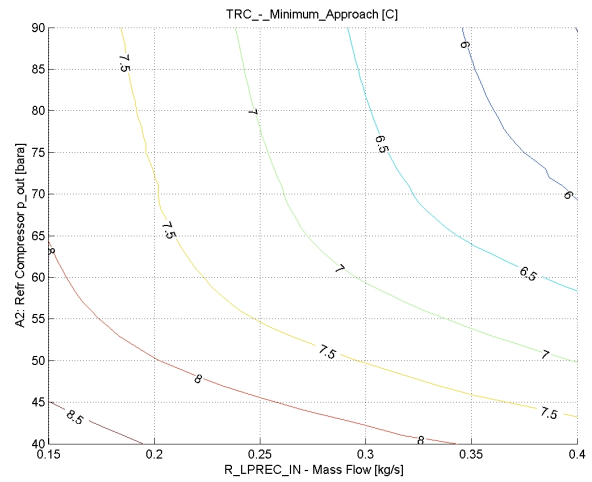


Figure C.15: TRC: MITA

### C.3 Sensitivity Analyses

#### C.3.1 Case HeP - 100 % NCR

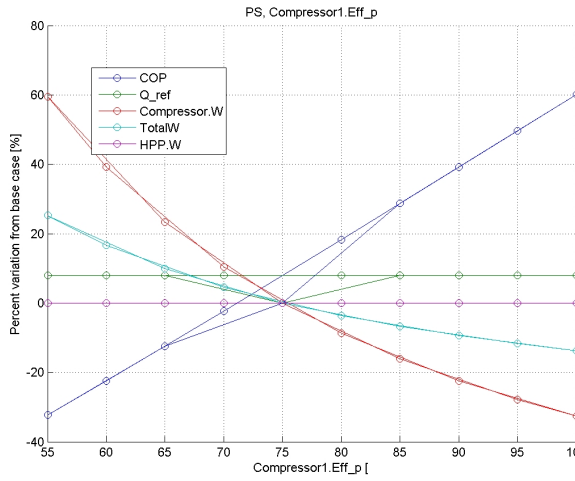


Figure C.16: Refrigerant Compressor polytropic efficiency

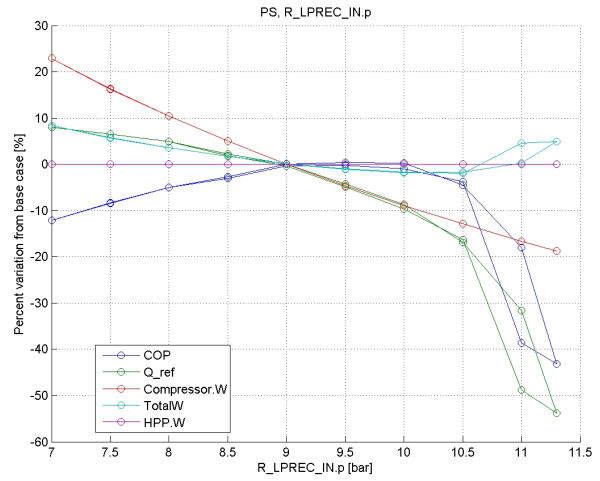


Figure C.17: Evaporation pressure (R-LPREC-IN)

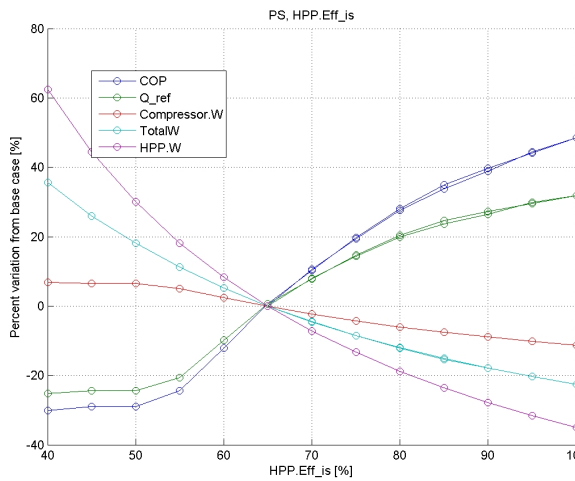


Figure C.18: HP Pump efficiency

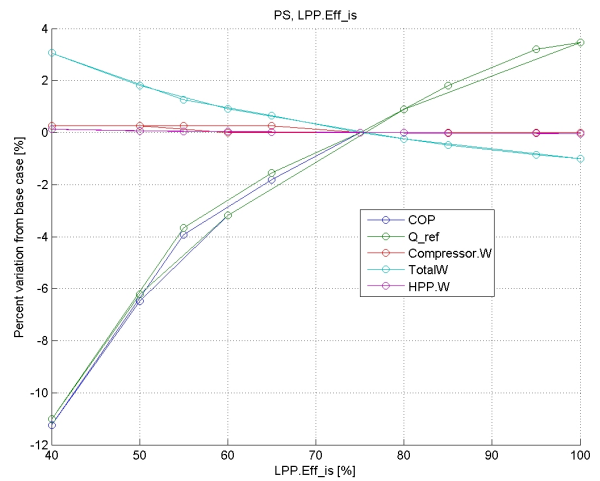


Figure C.19: LP Pump efficiency



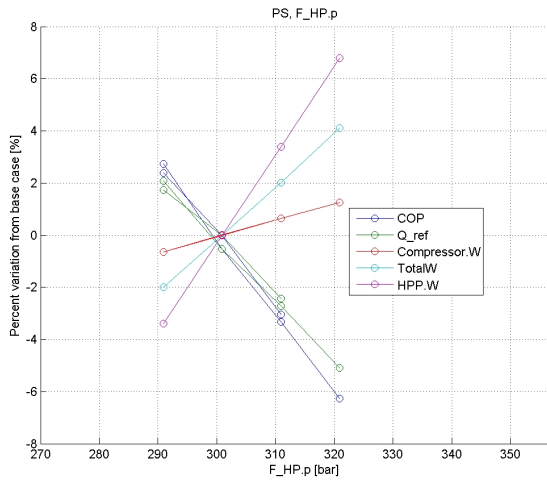


Figure C.20: HP Fuel pressure

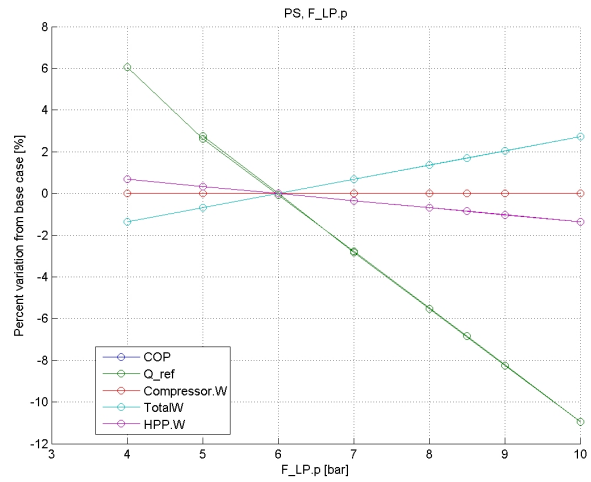


Figure C.21: LP Fuel pressure

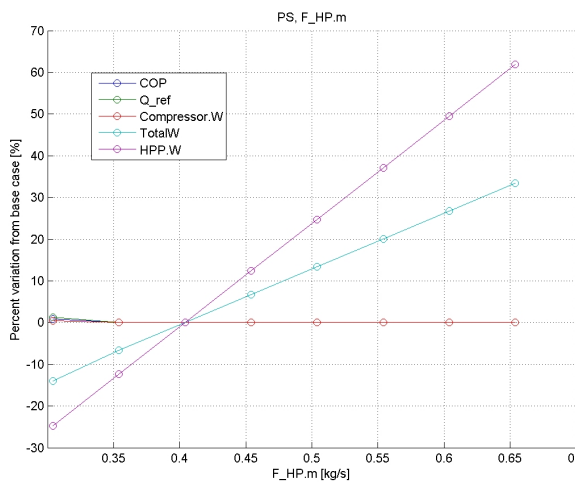


Figure C.22: HP Fuel flowrate

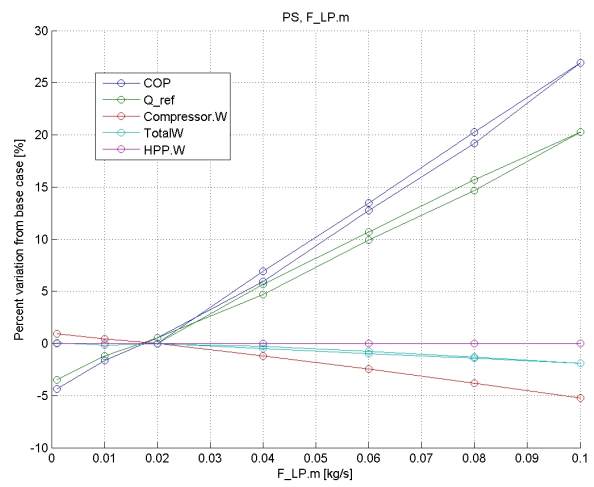


Figure C.23: LP Fuel flowrate

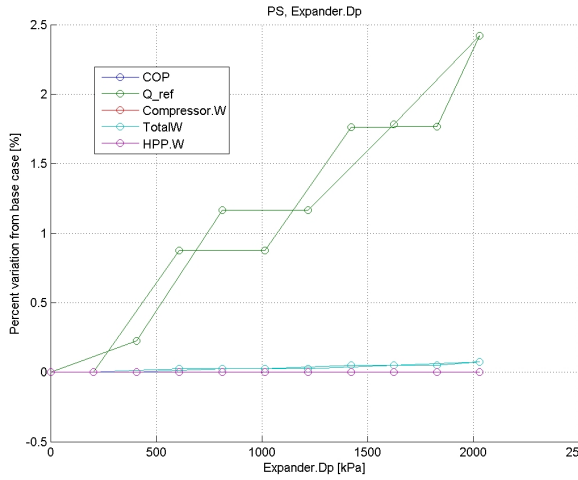


Figure C.24: Expander pressure difference (efficiency=60%)

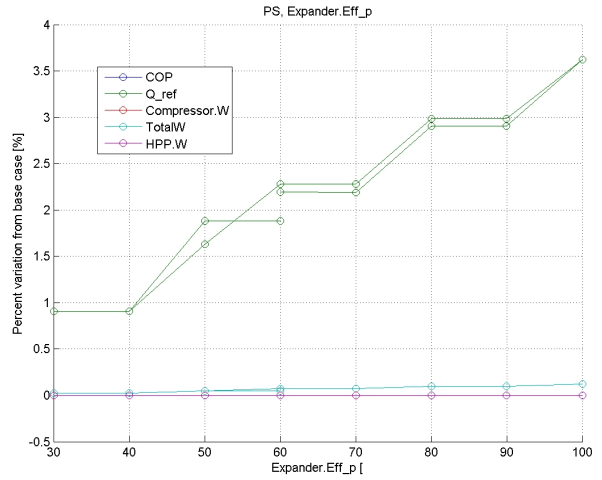


Figure C.25: Expander efficiency (Expander pressure drop=2030kPa)

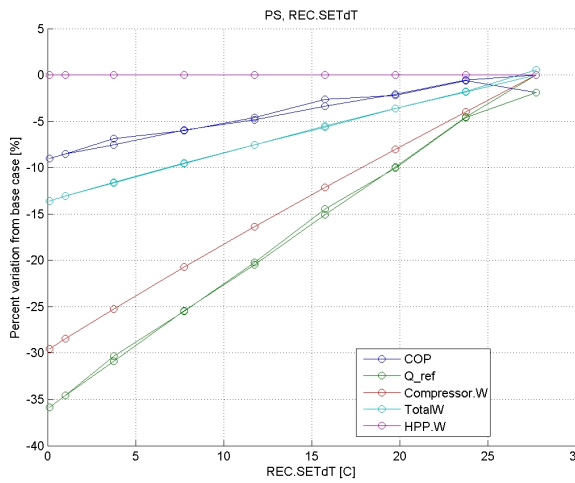


Figure C.26: REC Temperature increase on the LP side

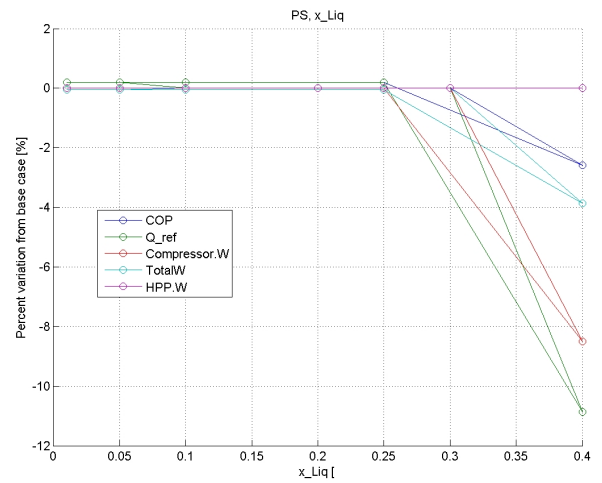


Figure C.27: TRC evaporator outlet liquid fraction

# Appendix D.0 Acronyms

AUX Auxiliary Engine

bara bar absolute

BOG Boil Off Gas

BOGK Boil Off Gas Compressor

COP Coefficient Of Performance

ECA Emission Control Area

FGSS Fuel Gas Supply System

GCU Gas Combustion Unit

HeP Heat Pump

HeP-AUX Heat Pump with BOG Auxiliary engine feed

HFO Heavy Fuel Oil

HP High Pressure

HPFHX High Pressure Fuel Heat Exchanger

HPK High Pressure Compressor

HPP High Pressure Pump

HX Heat Exchanger

IC InterCooler

IMO International Maritime Organization

LNG Liquefied Natural Gas

LNGC LNG Carrier

LP Low Pressure

LPFHX Low Pressure Fuel Heat Exchanger

LPP Low Pressure Pump

MCR Maximum Continuous Rating

MDO Marine Diesel Oil

ME-GI MAN Electronically controlled Gas Injected engines

MITA Minimum Internal Temperature Difference

MIX-AUX Terminal type process

NCR Normal Continuous Rating = continuous service rating (S)

NMCR Nominal Maximum Continuous Rating (L1)

PFD Process Flow Diagram

REC RECuperator

REFK Refrigerant Compressor

SFOC Specific Fuel Oil Consumption

SMCR Selected Maximum Continuous Rating (M)

TRC Tank Reflux Cooler

# Bibliography

- [1] Jerzy Herdzyk. Lng as a marine fuel, possibilities and problems. *Journal of KONES Powertrain and Transport*, 18(2), 2011.
- [2] DuPont. What is your imo annex vi sulphur compliance plan. <http://www.dupont.com/>, 2015.
- [3] Witherby. LNG Shipping Knowledge. Witherby Seamanship International Ltd, 2011.
- [4] Vilmar Aesoy, Per Magne Einang, Dag Stenersen, Erik Hennie, and Ingebrigt Valberg. Lng-fuelled engines and fuel systems for medium-speed engines in maritime applications. *JSAE*, 2011.
- [5] TGE. Efficient, low cost lng bog handling by integration of cascade liquefaction and laby-gi fuel gas compressor for me-gi propulsion system. In *Gastech*, May 2009. Abu Dhabi.
- [6] R P Sinha and Wan Mohd Norsani Wan Nik. Investigation of propulsion system for large lng ships. In *1st International Conference on Mechanical Engineering Research 2011*, 2011.
- [7] Dag Stenersen. Master thesis supervision. personal communication, 2014.
- [8] Denis Griffiths. *Marine low speed diesel engines*. Institute of Marine Engineers, Science and Technology, 2006.
- [9] Wartsila. *Wartsila 2-stroke low pressure dual-fuel engines*. Wartsila Ship Power Business White Paper, 2013.
- [10] J. Romero Gomez, M. Romero Gomez, R. Ferreiro Garcia, and A. De Miguel Catoira. On board lng reliquefaction technology: a comparative study. *Polish Maritime Research*, 21:77–88, 2014.

- [11] Addy Majewski. Dieselnets technology guide, 2006.
- [12] Vilmar Aesoy and Dag Stenersen. Low emission lng fuelled ships for environmental friendly operations in arctic areas. In Proceedings of the ASME 2013 32nd International Conference on Ocean, Offshore and Arctic Engineering, OMAE2013-11644, June 2013.
- [13] Samsung. Gas fuelled ship, december 2010. presentation for DNV.
- [14] MAN. 45000 m3 lng tanker engine application. Technical report, MAN Diesel Turbo, january 2013. rev0.
- [15] MAN. Lng carrier propulsion by me engines and reliquefaction, 0.
- [16] Hamworthy. Lng systems for marine application, lng reliquefaction and lng regasification, 2014.
- [17] Cryostar. The cryostar magazine, special report reliquefaction system ecorel, 2007.
- [18] Geir Skaugen. Liquefaction of natural gas. how can fundamental rd help the industry? case studies from gts. In 6th Annual LNG TECH Global Summit. SINTEF Energy Research, 2011.
- [19] MAN. Me-gi dual fuel, a technical, operational and cost-effective solution for ships fuelled by gas. Copenhagen, Denmark, 0.
- [20] MAN. Lng carriers with me-gi engine and high pressure gas supply system, 2007.
- [21] Hyundai. Hhi-fgss for me-gi engine (for proposal). Technical report, Hyundai Heavy Industries Co., Ltd, Engine & Machinery Division, May 2012.
- [22] H C Jung. Gas fuelled container ship (evaluation of economic analysis), 2015.

- [23] Eirik Melaaen. Fuel gas handling system and bog reliquefaction for lng carrier. In Two stroke debut of dual fuel engine. Wartsila, 2013.
- [24] Jorn Magnus Jonas. A plant comprising a tank for storing of liquid natural gas (lng) as marine fuel, 2011.
- [25] Gerd-Michael Wursig. Lng fuel tank, benefits and challenges. Tekna presentation, June 2013. DNV.
- [26] Bjorn Munko. Economic design of small scale lng tankers and terminals. LNG Conference Offshore Center, Denmark, 2007.
- [27] Mario Miana, Regina Legorburo, David Diez, and Young Ho Hwang. Calculation of boil-off rate of liquefied natural gas in mark iii tanks of ship carriers by numerical analysis. Applied Thermal Engineering, 2015. Accepted manuscript.
- [28] Jostein Pettersen, Even Solbraa, and Olav Boland. TEP 4185 Natural Gas Technology Compendium. NTNU Department of Process and Energy Engineering, 2013.
- [29] Petter Neksa. Master thesis supervision. personal communication, 2014.
- [30] GPSA Gas Processors Suppliers Association. Engineering Data Book. GPSA, 2004.
- [31] Sven Erik Brink. Single shaft turbocompressors for bog recovery in lng terminals. Siemens AG Energy, 2010.
- [32] EFRC. European forum of reciprocating compressors, <http://www.recip.org>, 2014.
- [33] Andreas Norberg. Master thesis supervision. personal communication, 2014.
- [34] Cryostar. The cryostar magazine, 2008.

- [35] MAN. Marine Engine IMO Tier II Programme 2014. MAN Diesel Turbo, 2014.
- [36] Lars Greitsch, Georg Eljardt, and Stefan Krueger. Operating conditions aligned ship design and evaluation. In First International Symposium on Marine Propulsors, Trondheim. Hamburg University of Technology (TUHH), June 2009.
- [37] Ohama, Kurioka, Tanaka, and Koga. Process gas applications where api 619 screw compressors replaced reciprocating and centrifugal compressors. In Proceedings of the 35th turbomachinery symposium, September 2006.
- [38] Fabio Burel, Rodolfo Taccani, and Nicola Zulian. Improving sustainability of maritime transport through utilization of liquefied natural gas (lng) for propulsion. *Energy*, 57:412–420, August 2013.
- [39] Pierre Sames. Costs and benefits of lng as a ship fuel for container vessels. Technical report, Germanischer Lloyd, 2011.
- [40] Meike Baumgart. Lng-fueled vessels in the norwegian short-sea market. Master's thesis, Norges Handelshoyskole, 2010.
- [41] Richard Gilmore, Stavros Hatzigrigoris, Steve Mavrakis, Andreas Spertos, and Antonis Vordonis. Lng carrier alternative propulsion systems. Technical report, SNAME GREEK SECTION, February 2005.
- [42] John Heywood. *Internal Combustion Engine Fundamentals*. 1988.
- [43] JungHan Lee, Jin Yeol Yu, John Linwood, and Martin Fux. New generation lngc with 2 stroke gas engine and innovative re-liquefaction system. In Gastech Conference and Exhibition. DSME, Burckhardt Compression, October 2012.
- [44] Per Magne Einang. The norwegian lng ferry. In *Natural Gas Vehicle*, 2000.



- [45] George Teriakidis. Lng as fuel - recent development. Technical report, DNVGL, february 2014.
- [46] Mogens Schroder Bech. North european lng infrastructure project - baseline report. Technical report, Danish Maritime Authority, october 2011.
- [47] Lars Petter Blikom. The only thing that matters is cost of fuel, November 2011.
- [48] Gerd-Michael Wursig. Lng for ships - the key elements. DNV Presentation, June 2014. Ref: PriceWaterhouseCoopers and US Energy Information Administration.
- [49] Jeong Hwan Kim and Joong Hyo Choi. Structural development of lng fueled large container ship. In ASME 2013 32nd International Conference on Ocean, Offshore and Arctic Engineering, June 2013.
- [50] P. Neksa, E. Brendenga, M. Dreschera, and B. Norberg. Development and analysis of a natural gas reliquefaction plant for small gas carriers. *Journal of Natural Gas Science and Engineering*, 2:143–149, 2010.
- [51] IM Skaugen. Small scale lng - multigas carriers, 0.
- [52] Lars Juliussen, Michael Kryger, and Anders Andreasen. Man b&w me-gi engines. recent research and results. In *Proceedings of the International Symposium on Marine Engineering (ISME)*, volume ISME585. MAN Diesel & Turbo, 2011.
- [53] Chansaem Park, Kiwook Song, Sangho Lee, Youngsub Lim, and Chonghun Han. Retrofit design of a boil-off gas handling process in liquefied natural gas receiving terminals. *Energy*, 44:69–78, 2012.
- [54] Jorn Magnus Jonas. Master thesis supervision. personal communication, 2014.

- [55] MAN. Basic principles of ship propulsion, 2004.
- [56] Maritime Connector. Ship sizes, 2007.
- [57] MAN. MAN B&W 98-50 ME/ME-C-TII Type Engines Engine Selection Guide. MAN Diesel Turbo, 1 edition, June 2010.
- [58] Christos Frangopoulos George Dimopoulos. A dynamic model for liquefied natural gas evaporation during marine transportation. *International Journal of Thermodynamics*, 11(3):123–131, September 2008.
- [59] Aspen. Aspen HYSYS V8.3 User Guide. Aspen Technology, Inc., August 2013.
- [60] Eric C. Carlson. Don't gamble with physical properties for simulations. *Chemical Engineering Progress*, 1996. Aspen Technology, Inc.
- [61] Gadhiraaju Venkatarathnam. *Cryogenic Mixed Refrigerant Processes*. Springer, 2008.
- [62] S. Mokhatab, J. Y. Mak, J. V. Valappil, and D. A. Wood. *Handbook of LNG*. Boston Gulf Professional Publishing, 2014. Chapter 1 - LNG Fundamentals.
- [63] Abdullah Alabdulkarema, Amir Mortazavia, Yunho Hwanga, Reinhard Radermachera, and Peter Rogers. Optimization of propane pre-cooled mixed refrigerant lng plant. *Applied Thermal Engineering*, 2011.
- [64] Martin Heller, Peter Ernst, and Sulzer Roteq. *Compressors for the lowest temperatures*. Technical report, Burckhardt, 1998.
- [65] Chris Keogh. Reliability and performance. looks at the operational experience with reciprocating boil off compressors that are used at an lng storage plant in western france. *LNG Industry*, 2008.
- [66] J Sarkar, Souvik Bhattacharyya, and M Ram Gopal. Optimization of a transcritical co<sub>2</sub> heat pump cycle for simultaneous cooling and heating applications. *International Journal of Refrigeration*, 2004.

- [67] F Kauf. Determination of the optimum high pressure for transcritical co<sub>2</sub> refrigeration cycles. *International Journal of Thermal Sciences*, 38, 1999.
- [68] S M Liao, T S Zhao, and A Jakobsen. A correlation of optimal heat rejection pressures in transcritical carbon dioxide cycles. *Applied Thermal Engineering*, 20, 2000.
- [69] D M Robinson and E A Groll. Efficiencies of transcritical co<sub>2</sub> cycles with and without an expansion turbine. *International Journal of Refrigeration*, 21, 1998.
- [70] Rush and Hall. Tutorial on cryogenic submerged electric motor pumps. In *Proceedings of the 18th International Pump Users Symposium*. EBARA International Corporation, 2001.
- [71] Jeff Gumbrell. Application and adaptation of traditional lng pump technology for the growing small-scale lng market. In *8th annual LNG Tech global summit*. EBARA, 2013.
- [72] Coyle and Patel. Processes and pump services in the lng industry. In *Proceedings of the Twenty-second International Pump User Symposium*. KBR, 2005.
- [73] Peter Ernst. The lng bog labyrinth-piston compressor with flexible capacity control. In *Gastech Houston*. Sulzer-Burckhardt, 2000.
- [74] Burckhardt. Laby compressors - contactless labyrinth sealing for highest availability, 2014.
- [75] Mario Imberti. Personal communication. reference person in SIAD, 2014.
- [76] Nakoi Akamo. Process critical compressors. LNG Industry, 2008. Kobe Steel Ltd.

- [77] Syed Mubarak. Apply new guidelines to select compressors for low-temperature service. *Hydrocarbon Processing*, 2012.
- [78] L Tavian. Large cryogenic systems at 1.8 k. In *European Particle Accelerator Conference*, 2000.
- [79] Klaus D. Timmerhaus and Richard Reed. *Cryogenic Engineering: Fifty Years of Progress*. Springer, 2006.
- [80] Warren D. Seider, J.D. Seader, and Daniel R. Lewin. *Product and Process Design Principles: Synthesis, Analysis, and Evaluation*. Wiley, 2004.
- [81] V. Mulyandasari A. L. Ling. Heat exchanger selection and sizing (engineering design guideine). Technical report, KLM Technology Group, 2010.